IMMUNE REGULATION AND EVASION OF ACUTE RESPIRATORY VIRUS INFECTION

By

Meredith C. Rogers

Dissertation

Submitted to the Faculty of the

Graduate School of Vanderbilt University

In partial fulfillment of the requirements

for the degree of

DOCTOR OF PHILOSOPHY

in

Microbiology and Immunology

August 31, 2018

Nashville, Tennessee

Approved:

R. Stokes Peebles, M.D.

Terence Dermody, M.D.

Daniel Moore, M.D., Ph.D.

Ambra Pozzi, Ph.D.

John V. Williams, M.D.

To my parents,

Who taught me to approach the world with an open and curious mind.

Acknowledgements

This work was supported financially by NIH grants AI085062 from the National Institute of Allergy and Infectious Diseases, and T32GM007347 for the Vanderbilt Medical Scientist Training Program. This project used the UPMC Hillman Cancer Center and Tissue and Research Pathology/Health Sciences Tissue Bank shared resource, which is supported in part by award P30CA047904. The VMC Flow Cytometry Shared Resource is supported by the Vanderbilt Ingram Cancer Center (P30 CA68485) and the Vanderbilt Digestive Disease Research Center (DK058404). This work would not have been possible without this generous support.

There aren't enough words to say how essential the support of my mentor, John Williams, has been to fostering my graduate school development as well as my future career as a physician scientist. John welcomed me into the lab as a rotation student who had a firm interest in infectious disease but only a limited understanding of immunology. His patience and teaching helped guide me through that first year of mouse wrangling, learning techniques, optimizing assays, planning experiments, and analyzing data. With his encouragement I grew from a timid student to someone who was ready to take the reins of my project and move it past the established parameters of our lab's expertise, into new and uncharted territory.

When John broke the news that he would be moving the lab to the University of Pittsburgh, I was, reasonably, devastated at first. I had just started making real headway in my project and was gaining confidence in my own abilities. John made sure to explain

what all my options were going forward, from moving with the lab, to transferring labs, or to finishing my work at Vanderbilt under the co-mentorship of another PI. I toyed with the latter two options...for about 48 hours. But it was obvious to me that moving with John was really the only option worthy of serious consideration. From his guidance to our conversations about topics both educational and mundane, I knew that John was the only PI I wanted to work with for my graduate school years.

I immediately became the senior student—and only student, at first—of the lab once we moved. John's support during that time was essential, but so was his trust that I was capable of pursuing my projects in the directions that I thought were most interesting and most important. And even when I came to John completely convinced that an experiment wasn't going anywhere, he was able to see the light in data that I couldn't make heads or tails of. His enthusiasm for pursuing these interesting avenues has served to inspire me to pursue new ideas that have only strengthened this work. John always says that the most important contribution of a scientist, and the role that he enjoys the most, is mentoring and supporting students. If I can achieve even a fraction of his success in mentorship throughout my own career, I will consider that a stellar achievement.

While John sets the tone for the caring and energetic environment of the lab, my fellow lab members ensure that this credo is carried out. Monika Johnson, our lab manager, was the other half of our nascent Pittsburgh lab when we first moved, and has provided stimulating discussions, scientific expertise, and mental health support (both through words and chocolate) over the years. Kristina Lamens, Nazly Shafagati, and Amy Kinzler have been wonderful friends, scientific thinkers, and happy hour and goat

yoga companions. My work on Tregs was greatly improved by Kristina's and Nazly's contributions. Yu Zhang and Jiuyang Xu ("The Boys") provided stimulating scientific discussions. Additionally, my STAT2 work would not have been fully realized without Jiuyang's careful design and creation of plasmids. I will also miss Santiago Lopez's lab serenades as well as his helpful feedback on data during lab meetings.

I must also acknowledge former members of the lab, especially Sharon Tollefson, Drew Hastings, Sherry Wen, Jen Schuster, and John Erickson, who taught me techniques and scientific thinking and helped me grow over my first two years with the lab. A particular thanks to John Erickson, whose discoveries set the foundation for my work here.

My thesis committee has challenged me to think beyond the obvious in my project, and I have grown so much as a scientist with their help. My committee chair, Stokes Peebles, provided the fruitful suggestion that we look at type 2 immunity and ILC2s in the Treg project. Treg expertise from Dan Moore and my former committee member Eric Sebzda also guided this project from inception to fruition. Terry Dermody's enthusiasm for my mouse adaptation and STAT2 project encouraged me to pursue a new direction that I hadn't originally proposed for my thesis. Ambra Pozzi provided a critical eye and encouraged me to keep the big picture in mind when I got bogged down with minor details.

Science cannot be done in a vacuum. We are surrounded by a fantastic group of labs focused on both infectious disease and immunology, which fosters a community of collaboration and scientific rigor. Members of the Alcorn and Dermody labs in particular

have provided fantastic advice, reagents, and support as I progressed through this work.

This work could not have been completed without the flow cytometry, histology, and animal care resources at both Vanderbilt and the University of Pittsburgh. Additionally, I was grateful to be able to rely on the tetramer reagents supplied by Sebastian Joyce and his lab even after we had moved.

The Department of Pathology, Microbiology, and Immunology and the graduate program in Microbiology and Immunology at Vanderbilt provided a wonderful home and supportive training environment for me, both while our lab was in Nashville, and while I finished this work in Pittsburgh.

The Vanderbilt MSTP leadership, both former and current members, have been essential to my success throughout these years. When Terry Dermody called to invite me to join the MSTP back when I was a college senior, I thought carefully about the offer. Ultimately it was the people of the Vandy MSTP--both the administration and my peers--who made this the obvious best choice for my training. In particular, Terry taught me to be a more comfortable and effective speaker, writer, and scientific thinker. Additionally, Melissa Krasnove is a warm and wonderful friend, who has been a rock for me when times have been tough over the past years.

My Vanderbilt MSTP classmates have weathered the ups and downs of this journey alongside me, and I'm so excited to finally be coming out the other side with them. In particular, Lillian Juttukonda and Merla Hubler have been amazing friends ever since our MSTP orientation and are both fantastic scientists and wonderfully crazy dancers.

My boyfriend Matt has been so supportive and understanding when “I’m gonna head home in 15 minutes” turns into 2 hours later. Ever since our first conversation, he has always asked questions about my research—and is patient with me when I use him as a guinea pig for figuring out how to explain my work in more approachable ways. He is also the best cat dad I could ask for.

Finally, to my family: my brother Brandon helped plant the earliest seeds of my scientific interest, when he talked to me about how much he loved his 10th grade biology class. 2 years later, when I took the same class, I approached the material with excitement, even when it was difficult. I’m looking forward to making my niece just as excited about science in the coming years.

And to my parents, who sent me to science camp when I was little and always ask, “how are the mice doing?” when we talk now. You taught me to ask questions, to work hard, to approach problems creatively, and to always believe in myself. Even though I’m sure you have no idea how your daughter ended up studying T cells in mice, none of this would have been possible without you.

Table of Contents

Page

Acknowledgements iii
List of Figures x
List of Tables xii
Chapter I: Introduction 1
Thesis Overview 1
Burden of respiratory viruses 2
Viral causes of acute respiratory infection 3
Human metapneumovirus 3
Influenza virus 6
Innate immune response to HMPV 7
Innate immune inhibition by HMPV 10
Interference of STAT signaling by viruses 14
STAT2 as a host determinant of virus tropism 15
Adaptive immunity to respiratory viruses and cell-mediated immunopathology 18
$CD8^+$ T cell impairment in respiratory virus infection 19
$CD4^+$ Regulatory T cells 21
Treg Mouse Models 24
Tregs in respiratory virus infection 25
RSV 26
Influenza A virus (IAV) and Tregs 31
$CD8^+$ T cell exhaustion and inhibitory receptors 33
Characteristics of inhibitory receptors 34
PD-1-mediated T cell impairment in acute respiratory virus infection 36
Project Goals and Hypotheses 39
Chapter II: $CD4^+$ regulatory T cells exert differential functions during early and late stages of the immune response to respiratory viruses 41
Introduction 41
Results 42
Tregs are increased and activated in response to HMPV 42
Treg depletion leads to enhanced anti-HMPV responses during infection 44
Tregs inhibit immune control of HMPV replication while decreasing inflammation 47
Depletion and blockade of Tregs using αCD25 treatment improves anti-HMPV $CD8^+$ T cell response 49
Treg depletion early or late in HMPV infection reveals differential functions of Tregs 50
Absence of Tregs during priming phase of infection impairs migration of DCs and $CD8^+$ T cells to lymph nodes and lung 53
Early Treg depletion leads to type 2 immune skewing, while late depletion maintains type 1 response 57
Tregs have differential roles in early and late influenza virus infection 62
Neither early nor late depletion of Tregs affects the $CD8^+$ T cell memory recall response to HMPV 64

Tregs do not function additively or synergistically with PD-1 to impair $CD8^+$ T cell responses to HMPV and other respiratory viruses 65
Discussion **67**
Materials and Methods **74**
Chapter III: Genetic absence of PD-L1 does not restore $CD8^+$ T cell function during respiratory virus infection and delays virus clearance **82**
Introduction **82**
Results **84**
$PD\text{-}L1^{-/-}$ mice have impaired T cell function and virus clearance 84
$PD\text{-}L1^{-/-}$ mice upregulate multiple inhibitory receptors 86
Antibody blockade of PD-L2 does not restore T cell function in $PD\text{-}L1^{-/-}$ mice 87
Bone marrow chimeras of WT/$PD\text{-}L1^{-/-}$ mice have equal T cell function, but hematopoietic PD-L1 appears to limit inhibitory receptor expression 90
Discussion **91**
Materials and Methods **96**
Chapter IV: STAT2 limits host species specificity of human metapneumovirus **99**
Introduction **99**
Results **101**
Serial passage of HMPV in $STAT1^{-/-}$ and $STAT2^{-/-}$ mice 101
HMPV infection prohibits nuclear translocation of STAT1 and STAT2 in human cells 103
HMPV antagonizes STAT1 and STAT2 in primate but not murine cells 105
HMPV inhibition of STAT1 or STAT2 occurs independently of the other 106
Expression of hSTAT2 but not mSTAT2 promotes STAT1/2 inhibition by HMPV 108
Discussion **109**
Materials and Methods **115**
Chapter V: Summary and Future Directions **121**
Thesis Summary **121**
Future Directions **128**
Cell-specific roles of PD-1/PD-L1 128
Human polymorphisms in PD-1/PD-L1 and their role in respiratory virus infection 130
Manipulation of Tregs or inhibitory receptors during respiratory virus infection and vaccination 131
Mouse adaptation of HMPV 133
Interactions of HMPV and STAT1/2 136
Conclusions and Significance **140**
References **142**

List of Figures

Page

Figure 1-1. HMPV virion structure 5

Figure 1-2. Comparison of RSV and HMPV genomes 6

Figure 1-3. Mechanisms of HMPV evasion from innate immune recognition 11

Figure 1-4. STAT2 is less conserved than other STAT proteins 14

Figure 1-5. T cell impairment in respiratory virus infection 20

Figure 1-6. Tregs function by a variety of mechanisms 23

Figure 2-1. Tregs become increased and activated in the lungs of HMPV-infected mice 44

Figure 2-2. Treg depletion leads to an enhanced HMPV-specific $CD8^+$ T cell response 46

Figure 2-3 Treg depletion reduces virus titers but increases histopathology 48

Figure 2-4. Depletion and blockade of Tregs with αCD25 restores $CD8^+$ T cell function 50

Figure 2-5. $CD8^+$ T cells fail to mount a robust response and clear virus efficiently when Tregs are depleted before inoculation 52

Figure 2-6. Treg deficiency leads to impaired DC and $CD8^+$ T cell migration early in infection 55

Figure 2-7. Early Treg depletion leads to imbalance of Th2 cytokines, Th2 cells, and ILC2s 59

Figure 2-8. Gating strategy for ILC2s 60

Figure 2-9. ILC2 markers 61

Figure 2-10. Tregs exert differential functions in the early and late immune response to influenza infection 63

Figure 2-11. Early or late Treg depletion during primary infection does not affect memory recall response to secondary challenge..... 65

Figure 2-12. Treg depletion combined with PD-L1 blockade does not enhance $CD8^+$ T cell function more than Treg depletion alone..... 67

Figure 3-1. PD-$L1^{-/-}$ mice have an impaired $CD8^+$ T cell response to HMPV infection 85

Figure 3-2. PD-$L1^{-/-}$ mice are impaired regardless of respiratory virus infection 85

Figure 3-3. PD-$L1^{-/-}$ mice upregulate inhibitory receptors at baseline and during infection 87

Figure 3-4. PD-L2 does not compensate for PD-L1 in PD-$L1^{-/-}$ mice 89

Figure 3-5. WT/PD-L1 reciprocal bone marrow chimeras do not have more functional $CD8^+$ T cells in response to HMPV infection..... 91

Figure 4-1. Serial passage of HMPV in $STAT1^{-/-}$ and $STAT2^{-/-}$ mice 102

Figure 4-2. Nuclear localization of STAT1 and STAT2 is inhibited by HMPV 104

Figure 4-3. HMPV reduces STAT1 and STAT2 activation in primate cells, but not murine cells 106

Figure 4-4. HMPV does not require STAT1 or STAT2 to inhibit expression and phosphorylation of the other..... 107

Figure 4-5. Expression of human STAT2 promotes STAT1 and STAT2 inhibition, while murine STAT2 inhibits STAT degradation..... 109

Figure 5-1. T cell impairment in respiratory virus infection..... 122

Figure 5-2. HMPV inhibition of STAT1/2 127

List of Tables

Page
Table 1-I. STAT inhibition by paramyxoviruses 16

Table 2-I. Chemokines with a role in T cell migration 56

CHAPTER I

Introduction*

Thesis Overview

Respiratory virus infections are a significant burden on healthcare systems, yet the balance between immune protection and pathology in these infections is poorly understood. This thesis establishes the role of immunoregulatory cells and molecules, specifically Tregs and PD-L1, in the immune response to infection by human metapneumovirus (HMPV) and other respiratory viruses. The thesis also uncovers the contribution of STAT2 in host species restriction of HMPV infection. In Chapter I, I provide background information about HMPV and influenza, the innate immune response to respiratory viruses and viral innate evasion strategies, and adaptive immunity to ARI along with regulatory mechanisms that modify the adaptive immune response. In Chapter II, I describe how regulatory T cells (Tregs) respond to infection by HMPV. I further demonstrate that Tregs have an essential temporal function in respiratory virus infection and that deficiency of these cells during priming of infection reduces the $CD8^+$ T cell response via impaired cell migration. Treg deficiency early in infection also skews the immune response towards type 2 immunity in both adaptive and innate cells. In Chapter III, I report the role of the inhibitory ligand PD-L1 in PD-1-

*Some sections of this introduction are from: Rogers MC & Williams JV. 2018. *Quis Custodiet Ipsos Custodes?* Regulation of Cell-Mediated Immune Responses Following Viral Lung Infections. Reprinted with permission from the *Annual Review of Virology*, Volume 5 © 2018 by Annual Reviews, http://www.annualreviews.org/.

mediated impairment of the $CD8^+$ T cell response to respiratory virus infection. Genetic deficiency of PD-L1 does not restore function to impaired $CD8^+$ T cells, despite the fact that antibody blockade of the same molecule leads to more functional virus-specific cells in WT mice. However, in bone marrow chimera experiments, PD-L1 deficiency on hematopoietic cells appears to drive increased inhibitory receptor expression on $CD8^+$ T cells. Chapter IV establishes how HMPV's capacity to control antiviral innate immunity is specific to host species and how STAT-2 contributes to this host species restriction of HMPV infection. I summarize the thesis work in Chapter V and speculate on future directions of these projects as well as of the field.

Burden of respiratory viruses

Acute lower respiratory infections are a leading cause of death in children worldwide and a major cause of morbidity and mortality among adults (1). In high-income nations, deaths from acute respiratory illness are less common due to supportive therapies and hospital resources; nonetheless, the US spends an estimated $51.8 billion annually on treatments for acute respiratory infections, a figure that does not factor in the economic burden of lost productivity faced by patients or their caregivers (2). The most common etiologies of these infections are viruses, including respiratory syncytial virus (RSV), human metapneumovirus (HMPV), influenza virus, parainfluenzaviruses, adenovirus, rhinovirus, and others. Since licensed vaccines are not available for any respiratory virus except influenza, these infections will continue to be a strain on health care systems globally. Moreover, acute viral lower respiratory infections can lead to sequelae related to immunopathology, such as asthma,

bronchiectasis, and exacerbations of underlying lung diseases (3). A thorough understanding of the immune response to respiratory viruses, including regulation of these immune responses by Tregs and inhibitory receptors, is crucial to develop effective treatments and vaccines.

Viral causes of acute respiratory infection

Human metapneumovirus

Discovered in 2001 (4), HMPV is a leading cause of lower respiratory tract infection in pediatric and elderly populations (5-9). Serologic evidence indicates that essentially all children are infected with HMPV by the time they are 5 years old (4, 10). In the majority of children, HMPV infection resolves without incident. However, HMPV can cause bronchiolitis and pneumonia in some patients (11, 12), and some of these will require supportive inpatient care. It is not yet fully understood why some pediatric patients progress to severe disease or even death; underlying conditions such as prematurity and asthma can predispose towards severe HMPV (12, 13), but as evidenced by cases of severe disease in infants and children who are otherwise healthy (5, 13), there are many other factors that have yet to be uncovered. HMPV infection can lead to asthma exacerbations and wheezing in all age groups (13-17), similar to RSV, indicative of immune skewing towards a type 2 response by HMPV. There is also evidence that early HMPV infection can predispose towards development of asthma (18). In my Treg data in chapter 2, I present one potential driver of type 2 immune bias in HMPV and influenza infection.

Reinfection with HMPV is common: 5-15% of upper respiratory infections are due to HMPV (5, 6). Reinfection likely occurs throughout life, as adults maintain anti-HMPV antibody titers over time (19, 20). Generally, reinfection is confined to upper respiratory infections or subclinical infection (5, 13, 15). However, children and adults who are immunocompromised due to chronic conditions, immunosuppression, or advanced age can have severe HMPV reinfection (7, 16, 21, 22). The incidence of severe disease in patients who have deficient T cell immunity supports the idea that a robust adaptive immune response is essential for fighting HMPV infection. As I show in this thesis work, careful balance of proinflammatory and suppressive signals are crucial for control of HMPV infection.

Human metapneumovirus genome

HMPV is an enveloped, negative-sense, single-stranded RNA virus in the Pneumoviridae family, which includes its closest human disease-causing relative, RSV (23). Based on genetic diversity, HMPV can be divided into 4 genotypes: A1, A2, B1, and B2, which circulate simultaneously in the human population (5, 6, 24, 25). HMPV produces 9 viral proteins from 8 genes (26). The HMPV surface proteins include the F fusion protein, which is required for virus entry (27), the G protein, which is glycosylated and has been proposed as an attachment protein (26, 28), and the small hydrophobic SH protein. The HMPV M matrix protein provides structure to the virion membrane and proteins contained within the envelope (29). Inside the virion, the HMPV genome is encapsidated by the N nucleoprotein. Also in the virion interior are the P phosphoprotein, two ORFs of the M2 protein (M2-1 and M2-2), and the L polymerase,

all of which have roles in viral transcription and replication (**Figure 1-1**) (30-32). Viruses with small genomes often encode polyfunctional proteins that carry out the many varied functions that a virus requires to successfully infect and replicate inside a cell (33), and thus even proteins with well-defined functions could have a secondary role in antagonism of host proteins.

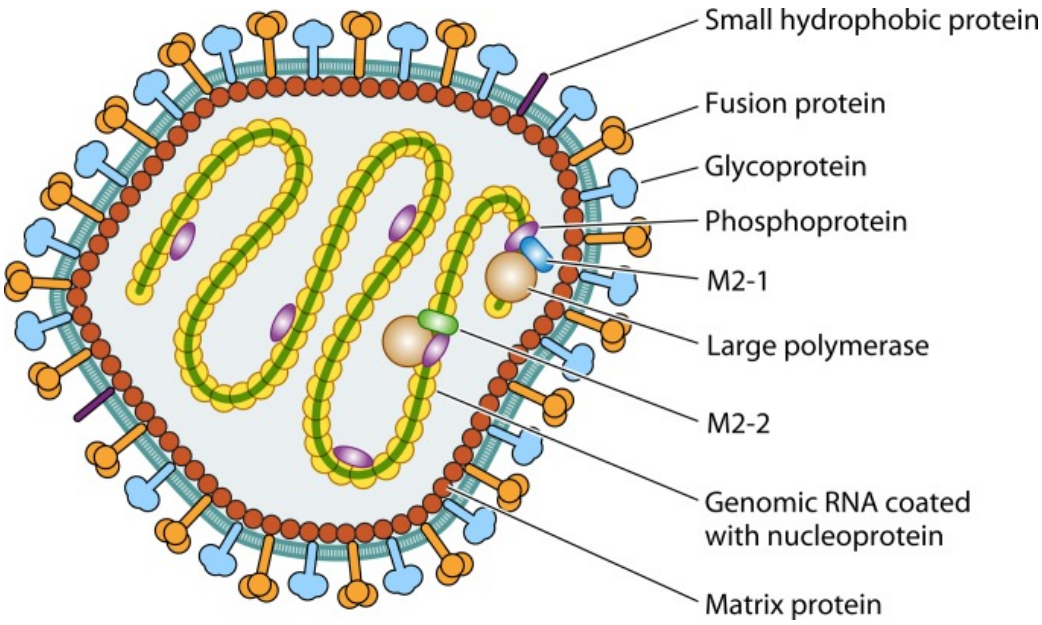

Figure 1-1. HMPV virion structure. From Wen & Williams 2015, *Clin. Vaccine Immunol.* (34).

All viruses that belong to the pneumovirus and paramyxovirus families (the P*neumovirinae* subfamily to which HMPV previously belonged was elevated to its own family in 2016 (23)) use at least one mechanism to antagonize the host innate immune response, which promotes infection. However, HMPV has no gene with sequence homology to other pneumo or paramyxovirus interferon antagonists (e.g. RSV NS1/NS2 (35)) (**Figure 1-2**), and thus it is important to define the proteins that HMPV uses to

evade the host response. A number of unique HMPV genes have a role in innate immune evasion. These will be discussed below.

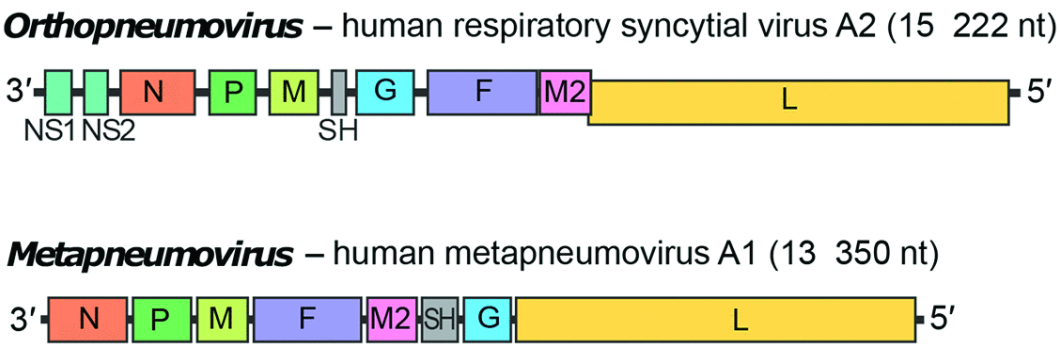

Figure 1-2. Comparison of RSV and HMPV genomes. From Rima et al. 2017, *J. Gen. Virol*. (36).

Influenza virus

When studying the immune response and immune regulation during respiratory virus infection, it is important to determine which elements of the immune response are virus-specific, and which are a feature of the lung environment in general. In this thesis I use mouse-adapted strains of influenza A virus (IAV) as a secondary model of respiratory virus infection, to determine whether my findings regarding Tregs and PD-L1 are virus- or lung-specific.

IAV is a common cause of respiratory virus infection in all age groups. Similar to HMPV, people who are very young, elderly, or immunocompromised tend to bear the highest burden of severe infection that requires hospitalization during influenza season (37). However, during pandemics of novel IAV subtypes, healthy young adults are often hardest hit due to a lack of heterosubtypic immunity, where exposure to one subtype of influenza can confer a small degree of resistance to infection by other subtypes (38).

IAV is a member of the Orthomyxoviridae family, which are characterized by segmented, negative-sense, single-stranded RNA genomes (39). IAV subtypes are defined by the antigenicity of the hemagglutinin (HA) and neuraminidase (NA) surface glycoproteins on the viral envelope (40). Due to its segmented genome, IAV can undergo reassortment to generate viruses with new HA and NA combinations. IAV also undergoes antigenic drift, which contributes to the reduced efficacy and duration of protection afforded by the yearly influenza vaccine.

T cell immunity to IAV is important, both in clearing the virus as well as in affording some cross-protection between IAV subtypes. It is generally thought that a universal vaccine to IAV will require one that generates a robust T cell immunity (41, 42). Because of the essential role of T cell immunity in IAV infection, immune regulation by Tregs or inhibitory receptors may alter both the response to acute infection as well as the memory response to future challenge, as we will see below.

Innate immune response to HMPV

The innate immune system serves as a first line of defense against microbial infection, and programs the initiation of the adaptive immune response a few days later. Viral infections can be severe in individuals who lack innate immune signaling (43, 44), indicating the essential role of this system. In the laboratory setting, cells or mice deficient in steps of innate immune signaling permit increased HMPV replication, as I report in chapter IV of this thesis.

Pattern recognition receptors (PRRs) recognize pathogen-associated molecular patterns (PAMPs), essential viral or bacterial components. Binding of a PRR to its

PAMP triggers signaling cascades that lead to induction of proinflammatory cytokines and other proteins. For example, double-stranded RNA, which is produced during infection by RNA viruses, is recognized in the cytoplasm by the RIG-I-like receptors RIG-I and MDA5 (45, 46).

HMPV double-stranded RNA is sensed by RIG-I (47, 48) and MDA5 (49) in the cytoplasm. Additionally, some Toll-like receptors (TLRs) have roles in sensing viruses. For example, in endosomal compartments, TLR3 senses double-stranded viral RNA, while TLRs 7 and 8 detect single-stranded RNA; however, thus far no studies have shown that HMPV infection specifically activates TLR3 or 8. TLR7 detects HMPV specifically in plasmacytoid dendritic cells (47).

RIG-I and MDA5 activate MAVS, which activates IRF3 and NF-κb, leading to transcription of IFNs and other proinflammatory molecules. TLR-7 signals through MyD88 and IRF7, also inducing transcription of proinflammatory genes (reviewed in (50)). Others have found that HMPV is recognized by a MyD88-dependent pathway in human DCs (51); this pathway could be triggered by TLR-7 or another TLR.

A principal product of signaling via PRRs is type I and III interferons. Type I interferons consist primarily of α and β interferons, though other interferons, including ε and ω, have been described (52). IFNα comes in multiple isoforms, which differ in tissue expression and affinity for their receptor, IFNAR (52). Type III interferon, or IFNλ, also exists in multiple subtypes that have different expression patterns and affinity for the IFNλ receptor, IFNLR (53). Type I and type III interferons act in an autocrine and paracrine manner to establish an antiviral state in infected and neighboring cells.

The role of type I IFN in HMPV infection was recently uncovered using a mouse model of infection. Mice deficient in the IFNAR receptor had higher virus titer but less inflammation compared to wild-type counterparts, indicating that IFN contributes to virus control but has the off-target effect of increasing weight loss and airway dysfunction in HMPV infection (54). HMPV infection also induces expression of IFNλ, which restricts virus replication and reduces inflammation (55).

The type I IFN receptor is composed of two subunits, IFNR1 and IFNR2. IFNR1 is associated with tyrosine kinase 2 (TYK2), while IFNR2 associates with the JAK1 tyrosine kinase. Binding of IFNα/β to IFNAR leads to activation of JAK1 and TYK2, which phosphorylate STAT1 and STAT2. pSTAT1 and pSTAT2 form a heterodimer, and associate with IRF9 to form the IFN-stimulated gene factor 3 (ISGF3) complex. ISGF3 translocates into the nucleus to act as a transcription factor for interferon-stimulated response elements (ISREs), which transcribe a variety of antiviral genes (52). Hundreds of interferon-stimulated genes (ISGs) have been identified, including antiviral mediators such as Mx1, tetherin, and IFITM proteins, interferon regulators such as SOCS, and even STAT-1, STAT-2, and IRF9 in a positive feedback loop (56, 57).

STAT1 also forms a homodimer upon Type II interferon signaling through the IFNγ receptor and is involved in signaling of a variety of cytokines (58). On the other hand, STAT2 is uniquely used in Type I and III interferon signaling and thus represents a point of convergence in the innate antiviral response. As a result, it is a natural target of some viruses to promote infection, which will be discussed below. One goal of the work in chapter IV of this thesis was to determine whether STAT2 is targeted by HMPV.

Innate immune inhibition by HMPV

In Chapter IV, I show HMPV antagonizes the innate immune molecules STAT1 and STAT2 in a species-specific manner. Other strategies of innate immune evasion by HMPV have also been uncovered. Many viruses encode proteins that interfere with innate immunity. Viral proteins can interfere with essentially any step in the innate immune response from virus recognition to interferon signaling. Some of these include virus sequestration of the genome away from intracellular sensors, binding of STAT proteins, or degradation of ISGs (reviewed in (59)).

Viruses related to HMPV in the pneumovirus and paramyxovirus families use a variety of strategies to inhibit steps in the innate immune pathway (reviewed in (60)). For instance, the V protein of multiple paramyxoviruses binds the RNA sensor MDA5 to inhibit detection (61) and inhibits signaling via RIG-I (62, 63). The HPIV3 M protein induces mitochondrial degradation, preventing signaling through MAVS (64).

Interestingly, HMPV does not encode homologous proteins to those that have well-established anti-innate immune roles in paramyxo- and pneumoviruses. HMPV is genetically similar to RSV, yet it lacks the NS1 and NS2 proteins that are used by RSV for interferon inhibition/inhibition of STAT1/STAT2 (35) or the V proteins of paramyxoviruses. However, HMPV is able to antagonize the innate immune system (65, 66) via other proteins.

Considerable work has gone into trying to identify which HMPV proteins mediate immune inhibition. With its small genome lacking homology to known anti-IFN proteins in other viruses, it is understandable that multiple HMPV proteins may antagonize

different steps of innate immunity. The HMPV proteins P, G, SH, and M2-2 have been reported to play a role in immune inhibition (**Figure 1-3**) (47, 51, 55, 66-71).

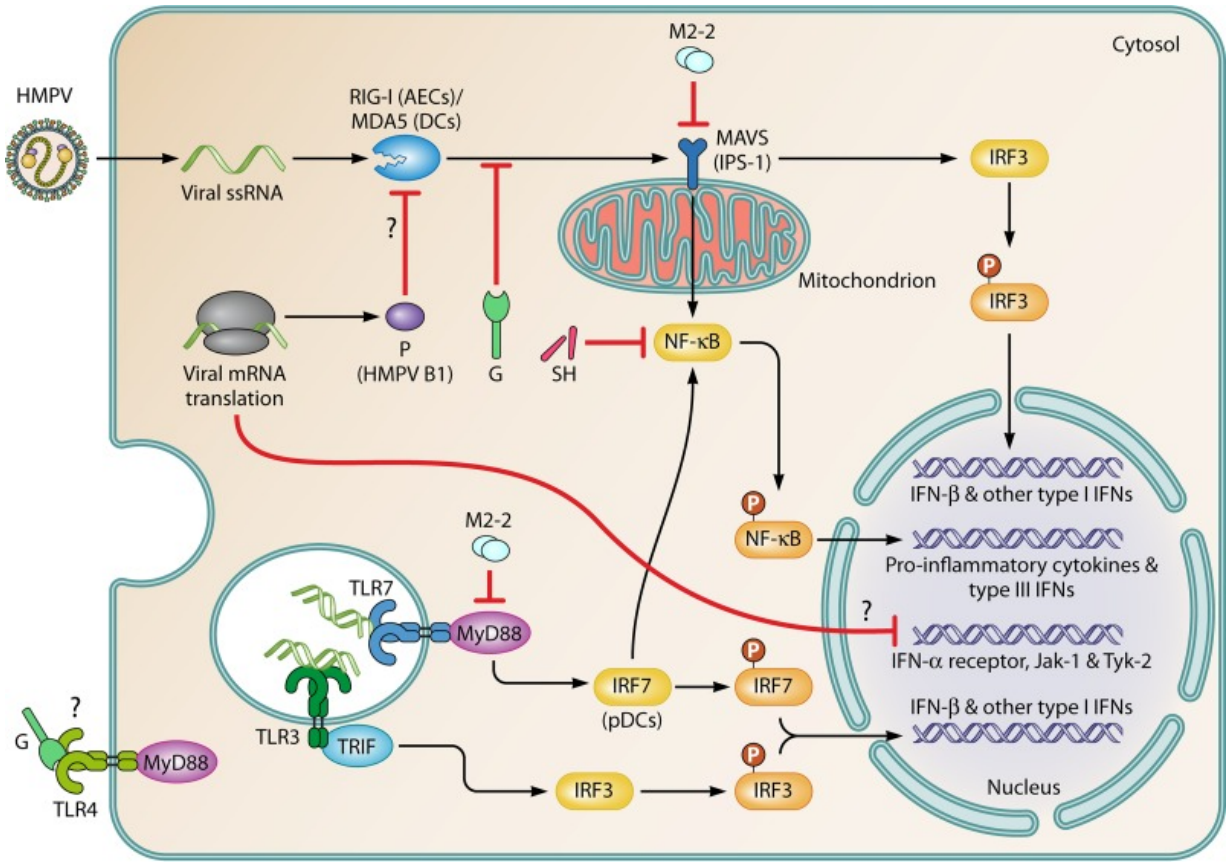

Figure 1-3. Mechanisms of HMPV evasion from innate immune recognition. From Céspedes et al. 2016, *Clin. Microbiol. Rev.*

SH, through an unknown mechanism, downregulates expression and phosphorylation of STAT1 (69). HMPVΔSH fails to inhibit this phosphorylation in human cells—however, this work did not study whether there is a similar inhibition in murine cells. SH also inhibits NF-κB phosphorylation as well as the transcription of cytokines controlled by this transcription factor (66). Interestingly, a HMPVΔSH strain is significantly restricted in the lungs of experimentally challenged hamsters and mice (72,

73). This finding in mice is notable, as in this thesis I show that HMPV inhibition of innate immunity is host species dependent.

The HMPV phosphoprotein (P) has a putative role in RIG-I inhibition, but in an HMPV-subtype specific manner. Investigators found that a HMPV B1 strain inhibits RIG-I, which is dependent on P, but an A1 strain fails to achieve this inhibition (47).

HMPV M2-2 interacts with and inhibits MAVS in human airway epithelial cells. Virus deficient in M2-2 fails to inhibit IFNβ production by infected cells. The middle and C-terminal thirds of M2-2 are required for this phenotype (71). Infection of DCs by an HMPV strain lacking M2-2 leads to increased production of proinflammatory cytokines compared with WT HMPV. In these cells, M2-2 associates with MyD88, and cotransfection of M2-2 and MyD88 leads to reduced IFNβ transcription (51). A HMPVΔM2-2 virus may be a vaccine candidate, as there was significantly less virus replication despite neutralizing antibody production against the strain in a hamster model (30).

HMPV G protein has the most evidence to implicate it in anti-host immunity. Infection of cells with HMPVΔG leads to increased IRF and NF-κB phosphorylation and nuclear translocation as well as increased IFNα/β and proinflammatory cytokines (66). The cytoplasmic C-terminus of G specifically interacts with the RIG-I N-terminal CARD domain in order to inhibit RIG-I mediated signaling (66, 67). HMPV also regulates production of IFNλ through the G protein. Just as HMPVΔG allows for increased IFNα/β production, it allows for increased IFNλ. In mice, HMPVΔG allows for 13-fold higher induction of IFNλ in the pulmonary tissue (55).

Others have found that HMPV G interferes with signaling through TLR4 in DCs (70). In an *in vitro* reporter cell line model, recombinant MPV F protein stimulates TLR4 (74), similar to how TLR4 recognizes the fusion protein of RSV (75).

In vivo, infection by HMPVΔG leads to increased IFNα production but decreased neutrophil recruitment, though it is unclear whether G is directly involved in recruitment of neutrophils or if the immune response to HMPVΔG is altered by the changed inflammatory environment in response to this virus mutant (68). HMPVΔG has also been proposed as a vaccine candidate due to its restricted replication in hamsters (72).

HMPV downregulates JAK1/TYK2 levels via proteasome degradation and reduces IFNAR cell-surface expression, though the viral protein involved is unknown (76). HMPV can also inhibit inflammatory signaling through IL-6 by inhibition of phosphorylation and nuclear translocation of STAT3, via blockade of phosphorylation of JAK2 (77). It is possible that the SH protein, which decreases STAT1 phosphorylation (69), could act by inhibiting activation of JAK/TYK kinases.

Additionally, SH and G also have putative roles in curtailing the adaptive immune response by inhibiting virus uptake by DCs and inhibiting DC activation of CD4+ T cells (78).

Together, it is clear that HMPV antagonizes innate immunity through a variety of mechanisms, and more work is required to fully understand the impact of each viral protein on different stages of innate immunity. The goal of chapter IV of this thesis was to further elucidate the innate immune antagonism by HMPV.

Interference of STAT signaling by viruses

Many viruses, including most, if not all, pneumo- and paramyxoviruses, inhibit STAT1, STAT2, or both to promote viral infection (reviewed in (60, 79)). The relatively ubiquitous nature of STAT1 being required for multiple signaling pathways likely constrains this protein evolutionarily. STAT1 is 98% conserved between humans, the natural host for HMPV infection, and mice, the widely used animal model of infection. In contrast, STAT2 is much less conserved between species: there is only ~70% amino acid similarity between humans and mice (**Figure 1-4**)(80, 81).

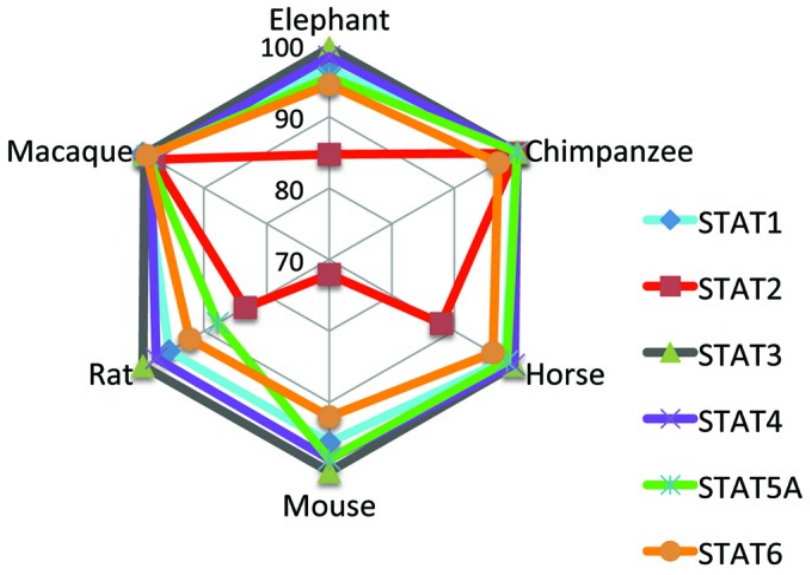

Figure 1-4. STAT2 is less conserved than other STAT proteins. From Chowdhury 2013, *JAK STAT.*

Inhibition of STAT proteins occurs by many mechanisms, from STAT degradation to inhibition of nuclear translocation. These and other strategies have been used by pneumo-and paramyxoviruses.

HMPV degrades STAT1 and inhibits phosphorylation via SH protein, though my work in this thesis contrasts with that of others who found that HMPV did not degrade STAT2 (65, 69). The RSV nonstructural proteins NS1 and NS2 degrade STAT2 by proteasomal degradation via E3 ligase (82-86). RSV NS1/NS2 also upregulate SOCS proteins (87), which form a negative feedback on signaling through STATs by ubiquitination and inhibition of JAK phosphorylation (reviewed in (88)). In addition to targeting STAT2, RSV NS1/2 proteins also interfere with other steps in the type 1 IFN response (reviewed in (79)).

Paramyxoviruses most commonly inhibit STAT1 and STAT2 via alternative isoforms of the viral P phosphoprotein (reviewed in (60)). Table 1-I illustrates the ubiquitous nature yet unique mechanisms of STAT inhibition by a variety of paramyxoviruses.

STAT2 as a host determinant of virus tropism

Because STAT2 is divergent between species, viral mechanisms to specifically inhibit STAT2 are often species-specific. It seems probable that virus antagonism of STAT2 has driven sequence divergence: viruses that preferentially infect one organism develop strategies to combat signaling via STAT2, which push this protein to mutate in the arms race between host and virus. Over time, viruses became so specialized for one version of STAT2 that they lost the capacity to antagonize this protein in other hosts. For a number of viruses, STAT2 contributes to host-species restriction, although other mechanisms of innate immune evasion are also used. As a consequence, STAT2 can be a barrier for adaptation of a virus to a new species.

Table 1-I. STAT inhibition by paramyxoviruses

Virus	Protein	STAT Target	Mechanism	Reference
hPIV1	C	STAT1/2	Inhibit phosphorylation, form perinuclear aggregates	(89)
hPIV2	V	STAT1/2	Protein destabilization and degradation	(90, 91)
hPIV5	V	STAT1/2	Degradation of STAT1 in STAT2 dependent manner	(90, 92, 93)
Sendai	C	STAT1/2	Binding of STAT1 by C inhibits phosphorylation; STAT1 required for STAT2 inhibition	(94-96)
		STAT1	Ubiquitination and degradation	(97-100)
Hendra	V	STAT1/2	Inhibition of nuclear translocation	(101)
Nipah	V	STAT1/2	Tripartite complex formation of V+STAT1/2 alters subcellular distribution and prevents nuclear translocation	(102-104)
	P, V, W	STAT1	Inhibition of phosphorylation and sequestering in cytoplasm or nucleus	(105, 106)
Measles	V	STAT1/2	Inhibition of phosphorylation and nuclear translocation	(107-111)
	N	STAT1/2	Inhibition of nuclear translocation	(110, 112)
Mumps	V	STAT1/2	Inhibition of phosphorylation and nuclear translocation	(113, 114)
		STAT1	Ubiquitination and degradation	(115, 116)

HPIV5 (formerly known as simian virus 5) replicates efficiently in human cell lines but not in mouse cells (117). The V protein of hPIV5 allows virus replication in human cells (118). Differences between the human and murine forms of STAT2 are responsible for the V protein's reduced capacity to dampen innate immunity and allow for replication in mouse cells (119). In a mouse model engineered to express the human version of

STAT2, transgenic hSTAT2 mice have significantly higher virus titer compared to littermate controls (93).

RSV also inhibits STAT2 in a species-specific manner. After stable transfection of the STAT2-deficient U6A human fibroblast cell line with either hSTAT2 or mSTAT2, RSV infection inhibits phosphorylation of hSTAT2 but not mSTAT2 in a dose-dependent manner (82).

STAT2 is also a host restriction factor for flavivirus infections. The NS5 protein of dengue virus antagonizes STAT2 (120, 121), but NS5 fails to antagonize murine STAT2 (122). Similarly, Zika virus is restricted in host species tropism by STAT2, which is inhibited by NS5 in human cells (123). As with hPIV5, a mouse expressing human STAT2 is competent for Zika virus replication (124). It seems likely that the same host species restriction exists for other viruses that antagonize STAT2 signaling, although these studies have yet to be reported.

In Chapter IV, I report that HMPV is restricted from antagonizing STAT1/2 in murine cells compared to human or monkey cells, and that the murine form of STAT2 is a source of this restriction. No data on host species restriction or HMPV antagonism of STAT2 had previously been reported.

A consequence of the divergence of STAT2 proteins is that mouse models for human viruses may not properly reflect the innate immune response of natural infection, as virus proteins cannot antagonize mouse STAT2 efficiently. If a virus cannot dampen the IFN response, the degree of inflammation by flow cytometry or histology may be greatly exaggerated compared to that in human disease. On the other hand, as we will

see below, overabundant inflammation is a potential sequela for respiratory viruses, even in the natural human host.

Adaptive immunity to respiratory viruses and cell-mediated immunopathology

A balance between the adaptive immune response to respiratory viruses and immune regulation of this response is necessary to ensure virus clearance while limiting immunopathology.

When a virus bypasses physical barriers to infect an epithelial cell in the lung, dendritic cells phagocytose the virus, process viral proteins in the inflammasome, upregulate surface co-stimulatory molecules, and traffic to regional lymph nodes where antigen is presented to $CD4^+$ and $CD8^+$ T cells. Educated effector T cells expand and travel to the lung parenchyma, where they encounter and kill infected epithelial cells. Cytotoxic $CD8^+$ T cells (CTLs) are the principal cells involved in clearing viral infections, including respiratory viruses, and are important for HMPV clearance (125-128). To kill virus-infected cells, CTLs release proinflammatory cytokines such as IFNγ, and create pores in cell membranes via perforin to allow granzymes to induce programmed cell death. However, once a CTL has followed a chemokine gradient toward infected lung tissue, multiple off-target complications are possible. First, the lung is the site of essential gas exchange, but massive immune cell infiltration into the airways increases the interstitial space between the airway and the capillaries, interfering with this function. Second, cytokines produced by CTLs can damage uninfected cells as well as the virus-infected cells. Left unchecked, CTLs can cause devastating injury to the lung, an organ that heals poorly after injury. Acute lung injury and acute respiratory distress

syndrome can result from pneumonia and other severe lung infections (129), leading to permanent deficits in lung function due to emphysematous changes or irreversible fibrosis.

Despite this potential for bystander injury, robust T cell effector function is required for clearing pathogens from the lung, emphasized by the fact that some of the most severe cases of lower viral respiratory infections are in immunocompromised persons with poor T cell function (130). However, the potential for damage induced by effector T cells must be kept in check. The immune system uses a variety of mechanisms to ensure that effector T cells are not allowed to go unchecked. Some of these include regulation of CTLs by $CD4^+$ regulatory T cells (Tregs) and inhibitory receptors expressed by $CD8^+$ T cells.

$CD8^+$ T cell impairment in respiratory virus infection

$CD8^+$ T cell function is reduced after infection by multiple respiratory viruses. After RSV infection, the frequency of IFNγ-producing virus-specific $CD8^+$ T cells is significantly reduced in the lung compared to those in the spleen (131, 132). Additionally, pulmonary lymphocytes stimulated *ex vivo* fail to degranulate (133) and to exert efficient cytolytic activity compared to splenocytes after RSV infection (131). Pulmonary $CD8^+$ T cell impairment occurs regardless of mouse strain used (131, 134). Reduced $CD8^+$ T cell function in primary infection also occurs during infection by hPIV5 (135), pneumonia virus of mice (PVM) (136), influenza (133, 137, 138), HMPV (138), and intranasal vaccinia virus (137). Of note, $CD8^+$ T cell impairment occurs only in the pulmonary compartment. Secondary challenge with RSV (131, 137), HMPV (138, 139),

vaccinia virus (137), hPIV5 (135), PVM (136), and influenza (137, 138) also leads to impaired $CD8^+$ T cell responses. Mechanisms of pulmonary $CD8^+$ T cell impairment have been elucidated in recent years and include regulatory T cells and inhibitory receptor signaling pathways, which I discuss in chapters II and III of this thesis (**Figure 1-5**).

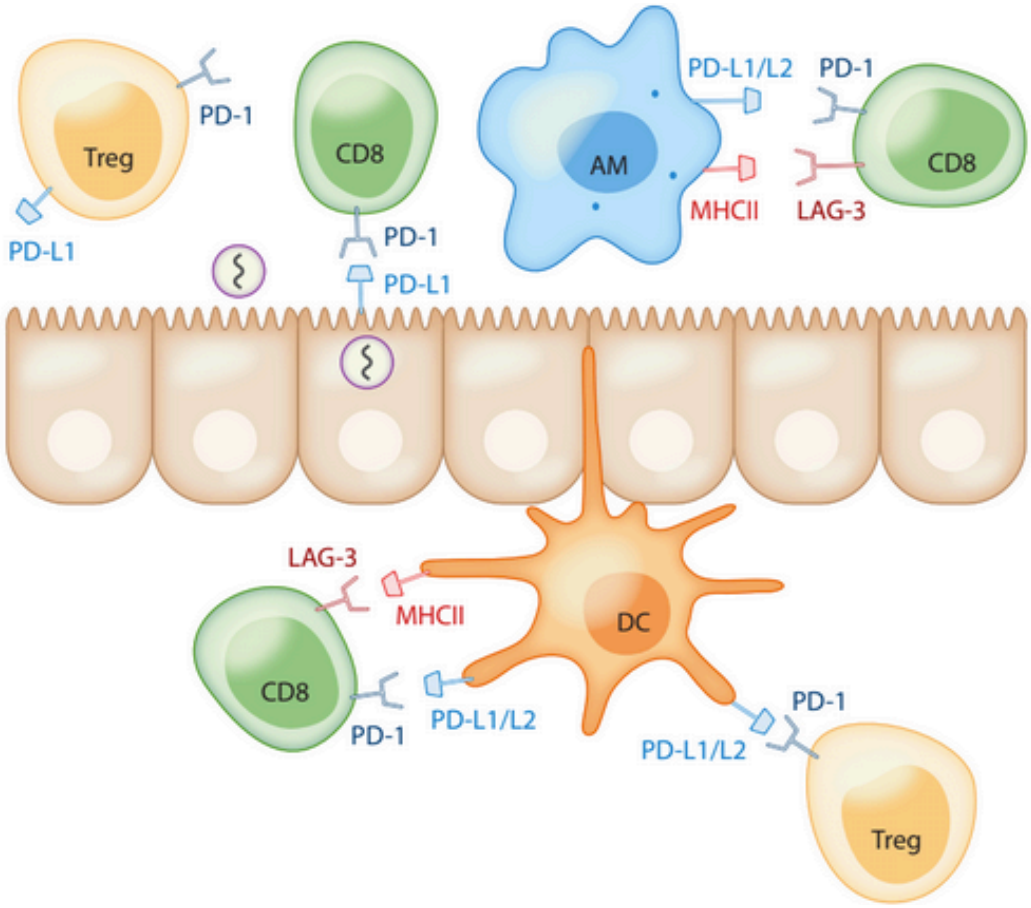

Figure 1-5. T cell impairment in respiratory virus infection. Suppression and regulation of $CD8^+$ T cell function is mediated by Tregs and inhibitory receptors. Virus infection promotes expression of PD-L1 and other inhibitory ligands on infected epithelial cells and APCs (such as dendritic cells (DC) and alveolar macrophages (AM)), while signaling through the TCR upregulates inhibitory receptor expression on T cells. Tregs suppress $CD8^+$ T cells and modulate APC function. From Rogers & Williams 2018, *Annu. Rev. Virol.*

$CD4^+$ Regulatory T cells

In chapter II, I investigate the role of $CD4^+$ regulatory T cells (Tregs) in respiratory virus infection. Tregs are master regulators of the immune system. While there are multiple cell types that are capable of suppressor function, the name Treg refers to a subset of $CD4^+$ cells that are suppressive and require the transcription factor FoxP3 for differentiation and maturation (140). Tregs are essential for immune homeostasis. Individuals with nonsense mutations of the gene that encodes FoxP3 develop IPEX syndrome (immune dysregulation, polyendocrinopathy, enteropathy, X-linked syndrome), which is associated with severe autoimmunity and is universally fatal without treatment. Mice with genetic deletion or disruption of FoxP3 develop a similar autoimmune disorder called scurfy, which leads to death within 3 weeks of birth (141).

Although Tregs require FoxP3 for development, expression of FoxP3 is not limited to these cells. Effector $CD4^+$ and $CD8^+$ T cells in humans can transiently upregulate FoxP3 upon activation (142). While murine Tregs are most often identified by the expression of CD4 and FoxP3 using flow cytometry, human $FoxP3^+$ cells require further analysis to confirm suppressor function. The difficulty of definitively identifying human Tregs (as well as the difficulty in collecting cells from patients) has meant that studies of human Tregs in respiratory virus infection are relatively uncommon. Most studies of Tregs during respiratory virus infections have used mouse models.

There are two types of Tregs: thymically derived Tregs (tTreg) and peripherally induced Tregs (called pTreg when induced *in vivo*, iTreg when induced *in vitro*) (143). Both sets arise from the common lymphoid progenitor and mature in the thymus. tTregs emerge directly from the thymus as a $FoxP3^+$ cell and are thought to function in

prevention of autoimmunity (144-146). pTregs, in contrast, emerge from the thymus as a naive $CD4^+$ cell and do not adopt the Treg phenotype until stimulated with the correct cytokines, such as TGFβ and IL-2, in the peripheral tissues (147). Generally speaking, pTregs are thought to be more active in the context of foreign antigen or infection, such as by HMPV or other respiratory viruses (144-146).

Reports indicate that FoxP3 expression in pTregs and iTregs may be unstable (148). This is due to evidence that tTreg DNA is demethylated at a FoxP3 locus, the Treg-specific demethylated region (TSDR) (149, 150). In contrast, iTregs that have been generated *in vitro* do not demethylate the TSDR (149-151). Chemical DNA methylation inhibitors promote stability of FoxP3 expression on iTregs (149). In contrast, when TGFb is removed from the iTreg culture, or when iTregs are adoptively transferred into wild-type mice, most, but not all, iTregs lose FoxP3 expression (148, 150, 151) and suppressor function (151). On the other hand, while some pTregs can lose FoxP3 expression, their TSDR tends to be demethylated. Furthermore, even when pTregs lose FoxP3 expression, upon restimulation these cells can regain FoxP3 expression and suppressor function, indicating that the regulatory nature of the pTreg population is more stable than that of iTregs (152, 153).

Both types of Tregs perform regulatory functions by a variety of mechanisms (**Figure 1-6**). Tregs express inhibitory cytokines such as TGFβ, IL-10, and IL-35, which inhibit effector cell function and proliferation. Through abundant surface expression of CD25, which is a component of the high-affinity IL-2 receptor, Tregs can act as an IL-2 “sink”, removing it from the environment. Since IL-2 promotes function of $CD8^+$ T cells, competition for IL-2 by Tregs can cause $CD8^+$ T cells to lose their functional capacity

(154). Another major Treg function is the ability to adjust dendritic cell function via interaction of receptors such as CTLA-4, PD-1, or LAG-3 with their cognate ligands. Tregs also produce adenosine via CD39/CD73, which interrupts effector T cell function. Lastly, Tregs can exhibit cytolytic function to kill effector cells via perforin and granzyme A or B (155, 156). Tregs likely use a variety of these methods in their control of immunopathology during lung infections, and I explore some of these in chapter II of this thesis.

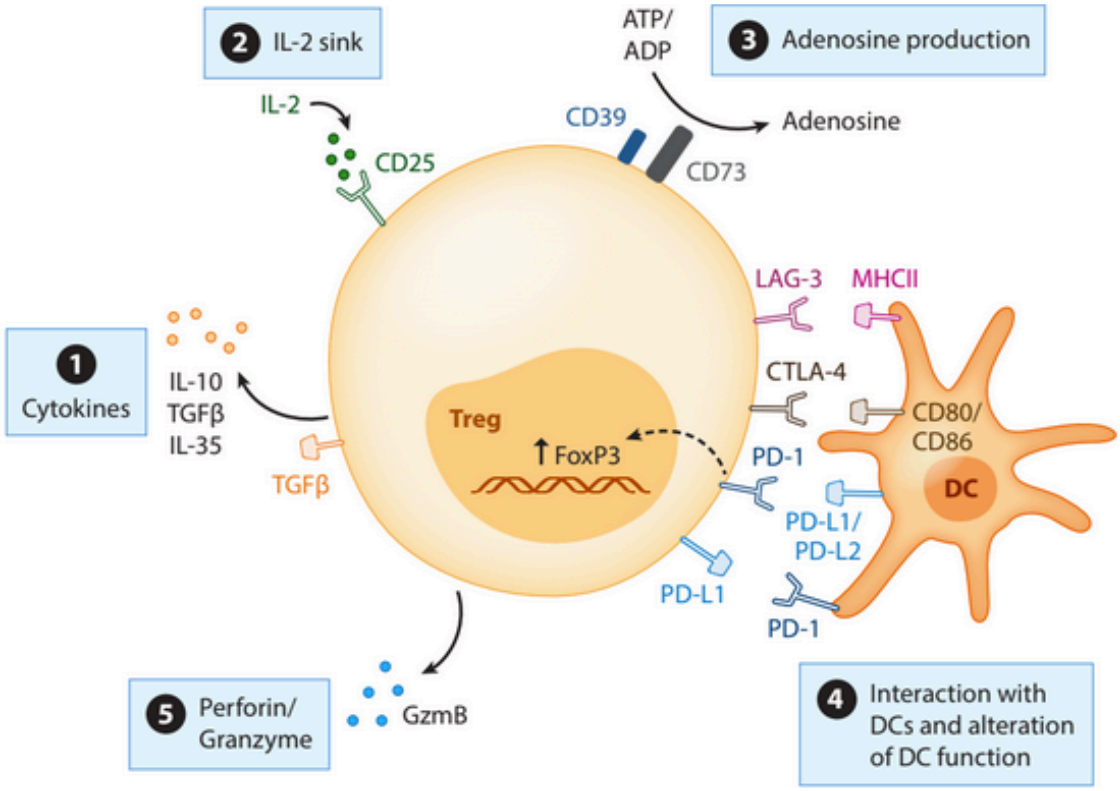

Figure 1-6. Tregs function by a variety of mechanisms. 1) Tregs produce inhibitory cytokines, including IL-10, IL-35, and secreted- and surface-bound (157, 158) TGFβ. **2**) Tregs sequester IL-2 from the inflammatory environment via the high-affinity IL-2 receptor, CD25. **3**) Tregs use CD39 and CD73 to convert ATP/ADP into adenosine, which suppresses effector T cells. **4**) Tregs modulate APC function via interactions between inhibitory receptors and ligands, including PD-1/PD-L1 and CTLA-4/CD80&CD86. PD-1 Signaling on Tregs promotes expression of FoxP3 (159). **5**) Tregs produce perforins and granzyme to directly kill effector T cells. From Rogers & Williams 2018, *Annu. Rev. Virol.*

Treg Mouse Models

To study the requirements for Tregs in virus infection models, multiple methods have been used to deplete these cells in mice. When they were first described, Tregs were defined by the abundant expression of CD25 (160); therefore, antibodies (Ab) against CD25 were used for depletion. In mice, the PC61 Ab can reduce Treg percentages by ~50%, and those Tregs that remain are less functional due to blockade of CD25 (161, 162). However, anti-CD25 Ab treatment can be nonspecific, since effector T cells express the same receptor upon activation (163). Additionally, in the lung many Tregs express FoxP3 but do not express CD25 (164, 165), though in our own studies we found that a minority of pulmonary $CD4^+$ cells express FoxP3 without CD25 (unpublished data). These differences may be due to differing genetic backgrounds or microbiota between mouse colonies at different institutions.

Once FoxP3 was identified as a master regulator of Tregs (166), two mouse models were developed for specific depletion of $FoxP3^+$ cells. Since complete genetic absence of FoxP3 causes fatal autoimmunity, complete knockouts are impractical. Instead, two groups independently developed mice that express the human diphtheria toxin (DT) receptor under the control of the FoxP3 promoter (167, 168). These mice, called $FoxP3^{DTR}$ (167) or DEREG (168), have become the gold standard for studies involving complete depletion of Tregs in mature mice, but only became widely available in the past several years. Therefore, the Treg respiratory virus literature contains reports using both anti-CD25 Ab and DT-mediated depletion, with important differences in observations and conclusions depending on the method used.

In my thesis work I primarily use FoxP3^{DTR} mice, though I also validate findings using anti-CD25 Ab. One important limitation of both DT-mediated Treg depletion models is that DT may have off-target effects, even though mice do not express DTR. For example, cells that nonspecifically take up antigen from the environment, such as DCs and macrophages, could also take up DT, leading to killing of these cells. Furthermore, since FoxP3 expression can be unstable on Tregs (148, 152, 153) or can be expressed on activated effector cells (169), it is possible that DT treatment can deplete non-Tregs or can fail to capture some Tregs. In one study using DEREG mice, authors found that after DT treatment, a population of Tregs emerged that did not express DTR, whereas in a setting of systemic inflammation, DT treatment of WT mice could be fatal (170). In this thesis work I attempted to control for some of these limitations. I measured FoxP3 expression on CD8$^+$ T cells and could not detect FoxP3 on these cells. I also injected WT mice with DT to control for nonspecific DT activity, and found no difference in CD8$^+$ T cell function between DT-treated WT mice and PBS-treated FoxP3^{DTR} mice after HMPV infection. However, it is possible that other assays would reveal detrimental effects of DT treatment in WT mice or that DT may deplete cells other than Tregs or may fail to deplete some Tregs in FoxP3^{DTR} mice.

Tregs in respiratory virus infection

Until my thesis work, no reports existed on the role of Tregs in HMPV infection. However, there were studies of Tregs in RSV and influenza infections. As will be seen below, discrepancies exist depending on the study and the virus, which makes it critical to understand whether Tregs are beneficial or detrimental in HMPV infection.

Additionally, it is important to determine which findings are virus-specific, and which can be generalized to other respiratory virus infections.

RSV

Little is known about how Treg populations change after natural RSV infection in humans. Infants who are severely infected with RSV and require hospitalization have decreased circulating Tregs compared to uninfected controls (171). However, whether this decrease is due to recruitment of Tregs to the infected lungs, or due to depression in Treg numbers, cannot be determined without invasive techniques.

Mouse models provide a tractable method of studying RSV infection and the Treg response to RSV. After inoculation of mice with RSV, Treg populations (defined in these studies as either $CD4^+$ $CD25^+$ cells or $CD4^+$ $FoxP3^+$ cells) expand in the lung, mediastinal lymph nodes, and BAL fluid, while the splenic population of Tregs remains largely unchanged (165, 172, 173). This expansion in the lung is in part due to proliferation of Tregs already in the tissue rather than solely from recruitment from the blood. Furthermore, these cells express common T cell activation markers (165). Tregs are a major source of IL-10, a well-established anti-inflammatory cytokine (174). IL-10 receptor blockade or knockout worsens RSV disease severity, although without a difference in viral titers, suggesting that Treg-secreted IL-10 suppresses $CD8^+$ T cell effector function during RSV infection (175, 176). Pulmonary Tregs also express granzyme B (GzmB) after RSV infection (177). Mice with GzmB-deficient Tregs exhibit increased weight loss, inflammatory lung infiltrate, and increased effector T cells after

RSV infection, suggesting that another mechanism of Treg function during RSV infection is perforin/granzyme-mediated cytolytic killing of effector $CD8^+$ T cells (177).

Tregs, like other $CD4^+$ T cells, have T cell receptors (TCRs) that recognize a specific peptide presented in the context of an MHC-II molecule. A significant proportion of $FoxP3^+$ $CD4^+$ T cells in RSV-infected mice recognize an epitope in the viral M protein (178). Immunization of mice with this same peptide leads to reduced clinical illness and immunopathology without a defect in virus clearance, suggesting that induction of epitope-specific Tregs suppresses immunopathology (179).

Depletion of Tregs during RSV infection using the anti-CD25 Ab method leads to peak virus titers that are similar in depleted and control animals; however, virus clearance is paradoxically delayed in treated animals even though $CD8^+$ T cells are highly functional in the absence of Tregs (165, 173). In other mouse infection models, such as with herpes simplex virus (HSV), anti-CD25 Ab treatment accelerates virus clearance (180), indicating that the effects of Treg depletion on virus infection may be organ-specific. Treg-depleted mice have fewer RSV-specific $CD8^+$ T cells in the lung at day 6, despite a larger number of total $CD8^+$ T cells in the tissue, which may account for this discordant result. Moreover, Treg depletion is correlated with an increase in the number of virus-specific cells in the mediastinal lymph nodes, which suggests that mice depleted of Tregs fail to recruit RSV-specific $CD8^+$ T cells from the lymph nodes to the site of infection in a timely manner, causing a delay in virus clearance (165, 173). Furthermore, the peak of the virus-specific $CD8^+$ T cell response in Treg-depleted mice is delayed by at least 3 days (173). Thus, while Tregs suppress $CD8^+$ T cell effector function, Tregs also may be required to initiate the $CD8^+$ T cell response.

RSV infection is cleared by day 8 regardless of whether Tregs are present or not (173); thus, one possible role for Tregs in lung infection is ramping down the effector $CD8^+$ T cell response once the virus is no longer present to prevent immunopathology. In support of this idea, Treg depletion during RSV infection is associated with increased weight loss and a prolonged reduction in airway function as well as increased inflammation (165, 172, 173).

After anti-CD25 Ab treatment, the ratio of the immunodominant to secondary dominant $CD8^+$ T cell epitopes is skewed in favor of the immunodominant epitope. This finding suggests that Tregs serve to balance immunodominance, which may also assist in efficient virus clearance (173). Decreasing immunodominance may be a beneficial adaptation in the evolutionary battle between host and pathogen. If a virus can escape by mutating one epitope (such as the case with HIV), then such a change might put selective pressure on the immune system to be able to mount responses against multiple epitopes in the same pathogen.

In contrast to the delay in viral clearance seen with anti-CD25 Ab treatment, when mice are depleted of Tregs before RSV infection using DT injection of DEREG mice, peak virus titer is reduced and virus clearance is accelerated (177). However, when using the $FoxP3^{DTR}$ mouse, Treg depletion has no effect on viral titers (181). The discordant results using different methods to answer the same question are somewhat unsatisfying. However, one likely explanation for the variation in virus clearance is that anti-CD25 Ab treatment does not eliminate Tregs completely and also may deplete $CD25^+$ effector cells. Intriguingly, perhaps there could be different roles for $CD25^+$ and $CD25^-$ Tregs in RSV and other lung infections. Importantly, immunopathology is

increased when Tregs are reduced, regardless of the Treg depletion method, emphasizing the critical regulatory role of these cells.

A gain-of-function approach to enhance Treg number and activity via IL-2/anti-IL-2 antibody immune complexes leads to lessened weight loss and immune cell infiltrate without an effect on viral clearance (177), again demonstrating a role for Tregs in controlling inflammation and suggesting a potential treatment to reduce disease severity.

RSV, Tregs, and Asthma

Much of the literature analyzing the role of Tregs in RSV infection focuses on the fact that RSV infection in infancy can predispose to the development of asthma later in life (182). HMPV can also predispose to asthma (18), though the link between RSV and asthma is much more concrete. Asthma is characterized by mucus production, airway hypersensitivity, and airway remodeling mediated by T_H2 cells, type 2 innate lymphoid cells (ILC2s), eosinophils, and other sources of type 2 inflammation (183). Repeated infection of young mice with RSV leads to increased sensitivity to allergens and a skewing towards type 2 immunity, characterized by expression of IL-5 and IL-13, increased mucus production, and airway hyperresponsiveness (184). Treg depletion during RSV infection is associated with increased T_H2-associated molecules in BAL fluid (181), as well as an influx of eosinophils (177, 181). Additionally, late in infection of Treg-depleted mice, the majority of $CD4^+$ T cells in the BAL fluid express the type 2 transcription factor GATA-3, a hallmark of T_H2 cells, while very few express the type 1

transcription factor T-bet that drives T_H1 differentiation (181). These studies indicate that Tregs serve to suppress T_H2 cells and type 2 cytokines in RSV infection.

RSV reinfection skews the $CD4^+$ T cell response towards T_H2 and T_H17 cells and away from Tregs (185). Recurrent RSV infection is associated with Tregs that express IL-13 and GATA-3 and have reduced capacity to suppress proliferation of naive effector cells (184). Even after secondary RSV infection, virus-specific Tregs do not expand as robustly as in primary infection (186). These results indicate that under repeated RSV challenge, Tregs lose their regulatory nature and instead acquire features of effector cells. Incubation of Tregs with the type 2 cytokines IL-4 and IL-13 promote GATA-3 expression by Tregs, suggesting that RSV infection leads to a self-perpetuating cycle of type 2 cytokines inducing type-2-like Tregs, which themselves can produce type 2 cytokines (184). Additionally, Tregs are known to constrain T_H2 cells over T_H1 cells (187-191); therefore, ineffective Treg function could result in a further pathogenic T_H2 loop. If Tregs are permanently altered to a type-2 phenotype in patients infected with RSV, and perhaps with other respiratory viruses that predispose towards asthma, this skewing could explain, at least in part, the predisposition towards allergic asthma. In chapter II of this thesis I explore the role of Tregs in controlling type 2 immunity in both HMPV and influenza infection, and propose that in respiratory virus infections in general, strong Treg activity is important for dampening down type 2 immunity and potentially reducing the risk of type 2 mediated consequences, including asthma.

Influenza A virus (IAV) and Tregs

While influenza and RSV are both respiratory virus infections, the immune response to each of these differs, and as seen below, the role of Tregs in each virus may be fundamentally different, or may simply reflect differences in mouse models and study protocols.

Similar to RSV, the Treg population expands in the lung in response to IAV infection in mice, with a peak in total Treg number at day 7-8 in the lung. In contrast, the Treg percentage in the spleen and mediastinal lymph nodes decreases during IAV infection, while the absolute number increases (192, 193). The Treg peak precedes the peak of the effector $CD8^+$ T cell response on day 11 (192). IAV-induced Tregs express activation markers, are capable of suppressing effector T cell proliferation, and proliferate after incubation with IAV antigen in an MHC class II-dependent manner, indicating that at least a portion of the Tregs recognize IAV-specific epitopes (192). IAV-specific Tregs express the type 1 transcription factor T-bet and produce IL-10 in response to influenza virus infection, which decreases IFNγ production from virus-specific $CD8^+$ effector T cells (193).

Anti-CD25 Ab treatment increases the number of IFNγ-producing IAV-specific $CD8^+$ T cells in the spleen and peritoneum (194) and the number of $CD4^+$ and $CD8^+$ T cells in the lung (193). Treg depletion using $FoxP3^{DTR}$ mice enhances the number of IAV-specific $CD8^+$ T cells in mediastinal lymph nodes, while decreasing the proportion of these cells (195), similar to that observed with RSV (165, 173). Furthermore, Treg depletion markedly skews the distribution of epitope-specific $CD8^+$ T cells towards immunodominant epitopes (194). While immunodominance is important in successful

antiviral $CD8^+$ T cell responses, these high-affinity $CD8^+$ T cells might also have more off-target effects and contribute to more immunopathology. Therefore, the presence of Tregs during natural infection may direct the immune response towards less dominant epitopes to preserve tissue (194). Although anti-CD25 treatment altered the $CD8^+$ and $CD4^+$ T cell immune response to IAV in one study, it did not affect the $CD8^+$ or $CD4^+$ T cell compartments, alter disease severity, or change peak virus titer in other work (196). These conflicting findings may result from different dosage and frequency of anti-CD25 Ab treatment for Treg depletion, as there is no recognized standard dosage for this antibody.

Several lines of evidence show that Tregs are important for lung recovery by other mechanisms after IAV clearance. Depletion of Tregs using DEREG mice during resolution of infection leads to delayed weight loss recovery without a change in virus clearance. Additionally, in WT mice infected with IAV, the number of Tregs in the lung correlates with the recovery of body weight (197). Furthermore, mice with a selective Treg deficiency in amphiregulin, an epidermal growth factor receptor ligand, have increased weight loss and lung damage upon IAV infection, despite no difference in viral loads (198). This is distinct from a suppressive function of Tregs on effector cells, as the frequency of epitope-specific $CD8^+$ or $CD4^+$ T cells and the cytokine production by effector cells is unchanged in mice with Tregs that are sufficient or deficient in amphiregulin (198). Thus, the arms of effector immune suppression and tissue healing appear to be independent in Tregs after IAV infection.

Pharmacologic enhancement of Treg function can reduce IAV-related immunopathology. Treg-mediated resolution of IAV infection in mice is improved by

administration of a DNA methyltransferase inhibitor, which increases suppressive activity and proliferation of Tregs (199). Depletion of Tregs using FoxP3^{DTR} mice prior to drug treatment fails to accelerate lung repair, indicating that the DNA methyltransferase inhibitor specifically alters Tregs to promote resolution of lung injury (199). Treatment of IAV-infected animals with an ICOS agonist delays viral clearance but reduces immunopathology, which is associated with expansion of Tregs and increased IL-10 production (200).

Treg-mediated suppression may contribute to susceptibility to re-infection. After recovery from primary IAV or bacterial pneumonia or during secondary pneumonia, the proportion and number of pulmonary Tregs is higher than in uninfected mice or during primary infection (201). Treg depletion during recovery from IAV pneumonia does not change clearance of the primary pneumonia, but upon secondary bacterial pneumonia, challenged mice mount a greater CD4$^+$ T cell response and clear bacteria more effectively (201).

CD8$^+$ T cell exhaustion and inhibitory receptors

CD8$^+$ T cell impairment in acute respiratory virus infection is similar to the antigen unresponsiveness (CD8$^+$ T cell exhaustion) that occurs during chronic viral infections such as lymphocytic choriomeningitis virus (LCMV), hepatitis C virus (HCV), and human immunodeficiency virus (HIV), and cancer (reviewed in (202-204)). In these infections, constant antigenic stimulation of CD8$^+$ T cells leads to a loss of effector functions in a progressive and hierarchical manner, with IL-2 production lost first, followed by TNFα, and finally IFNγ late in infection (205). Inhibitory receptors, such as PD-1, Tim-3, LAG-3,

and others are key mediators of T cell exhaustion in chronic infections and cancer (202-204). Therapies directed against these inhibitory molecules ("checkpoint inhibitors") have shown tremendous promise in cancer immunotherapy (reviewed in (206)). As discussed below, these receptors also contribute to $CD8^+$ T cell impairment in acute respiratory virus infection.

Characteristics of inhibitory receptors

Programmed cell death-1 (PD-1) has been the most widely investigated inhibitory receptor in respiratory infections. Binding of PD-1 by either of its ligands, PD-L1 (207) or PD-L2 (208), leads to inhibition of signaling through the T cell receptor (202-204). Specifically, signaling through PD-1 leads to recruitment of the tyrosine phosphatases SHP-1 and SHP-2 (209), which dephosphorylate Zap-70, CD3ζ (210), and CD28 (211). Ultimately this signaling has the downstream effect of inhibiting PI3K/Akt and Ras pathways (212) and leads to broad effects in the cell, including downmodulation of T-bet and Eomes, two signatures of effector $CD8^+$ T cells (213), inhibition of cell cycle progression (212), and metabolic changes (214). Signaling through the TCR upregulates expression of PD-1, while interferons and other cytokines stimulate expression of PD-L1 and PD-L2 (215). The net effect of these signaling pathways is to inhibit key effector $CD8^+$ T cells functions including cytokine secretion and degranulation.

Blockade of PD-1/PD-L1 signaling by Abs in chronic LCMV infection rescues exhausted $CD8^+$ T cells, allowing them to exert cytotoxic function, produce cytokines, and decrease viral burden in mice (216). Abs directed at PD-1 or PD-L1 are FDA-

approved for cancers such as melanoma, non-small lung cancer, and colon cancer, and are being investigated for treatment of many others (217). Studies of circulating $CD8^+$ T cells in patients with HIV, hepatitis C, and hepatitis B have also shown PD-1-mediated exhaustion of T cells (218-222), and clinical trials of PD-1 blockade in hepatitis C and HIV have been conducted. Other inhibitory receptors, including CTLA-4, LAG-3, Tim-3, TIGIT, and 2B4, also mediate exhaustion in chronic infection and cancer (223, 224), and some mediate T cell impairment in respiratory virus infection.

Initial studies of T cell exhaustion in chronic infection led to the paradigm that persistent antigen stimulation due to chronic infection led to PD-1-mediated T cell exhaustion, while T cells in acute infections expressed PD-1 as an activation marker. Mice infected with the acute LCMV Armstrong strain transiently express PD-1 on epitope-specific T cells; however, this expression declines by day 8 post-infection and PD-L1 blockade during acute LCMV infection has no effect on virus-specific $CD8^+$ T cell function (216). Moreover, mice acutely infected with Friend retrovirus upregulate PD-1 on virus-specific cells, yet these cells are functional (225). However, some acute infections are improved by inhibition of PD-1/PD-L1 signaling. For example, rabies infection in PD-$L1^{-/-}$ mice is less severe, with lower viral loads and increased numbers of $CD8^+$ T cells migrating to the CNS (226). Blockade of PD-L1 in mice infected with neurotropic coronavirus leads to significantly more functional virus-specific $CD8^+$ T cells in the CNS (227). However, while infected mice deficient in PD-L1 have lower viral loads, they also have more morbidity, reflecting the importance of PD-1-mediated immune regulation in this sensitive tissue (227). There is a similar need to preserve tissue integrity and function between the CNS and lung, considering that disruptions in

either of these organs bode poorly for survival.

PD-1-mediated T cell impairment in acute respiratory virus infection

The role of PD-1 in mediating pulmonary $CD8^+$ T cell impairment was recently discovered using HMPV and IAV infections as models for respiratory virus infection (138, 228). Mice infected with respiratory viruses develop progressive dysfunction of cytokine secretion and degranulation in lung but not splenic $CD8^+$ T cells. Both lung and spleen virus-specific $CD8^+$ T cells from infected mice upregulate PD-1; PD-1 expression is transient on splenic cells but prolonged on lung $CD8^+$ T cells and correlates with their decrease in functionality (138). Ab blockade of PD-L1 or genetic ablation of PD-1 leads to significantly more functional epitope-specific $CD8^+$ T cells. $CD8^+$ T cell function is also improved in the absence of PD-1/PD-L1 signaling in secondary challenge with HMPV and influenza (138, 139, 228). While PD-L1 blockade is associated with decreased viral load in primary (138) and secondary (139, 228) infection, airway dysfunction is elevated in the absence of PD-1/PD-L1 signaling (138), illustrating the immunoprotective role of $CD8^+$ T cell regulation.

Lung $CD8^+$ T cell impairment differs in some ways from $CD8^+$ T cell exhaustion during chronic infection and appears to occur more rapidly. Impaired pulmonary HMPV-specific $CD8^+$ T cells on day 7 have a gene expression profile that resembles the signature of exhausted $CD8^+$ T cells on day 30 during chronic LCMV infection (229). Moreover, $CD8^+$ T cell impairment proceeds even if HMPV infection is abolished by neutralizing Ab during the first 24 hours post-infection (unpublished data).

PD-1-mediated $CD8^+$ T cell impairment may vary with disease severity. Comparison of moderate and severe influenza infection shows significantly reduced virus-specific $CD8^+$ T cell function in severely ill mice (230). Additionally, PD-1, PD-L1, and PD-L2 expression is higher on influenza-specific $CD8^+$ T cells in severe infection compared to moderate infection. Ab blockade of PD-L1 restores virus-specific $CD8^+$ T cell function in severely ill mice, but does not have an effect on mice with moderate infection. PD-L1 blockade correlates with a reduction in viral titers for the severely ill mice, but without a change in weight loss or survival (230). Blockade of PD-L1 in mice infected with RSV leads to enhanced function of bulk $CD8^+$ T cells. The treatment also increases weight loss and lung inflammation but does not affect viral titers (231).

A number of studies have explored the role of PD-1/PD-L1 signaling in respiratory viral infection of humans. RSV infection leads to upregulation of PD-L1 on human lung epithelial cells (232, 233). In *in vitro* co-culture of RSV-infected primary bronchial epithelial cells with $CD8^+$ T cells, PD-L1 blockade increases cytokine production and cytolytic activity by $CD8^+$ T cells, and ultimately reduces viral loads in the infected cells (233). Human rhinovirus-infected DCs upregulate PD-L1, leading to impairment of co-cultured $CD8^+$ T cells; Ab blockade of PD-L1 partially reverses the $CD8^+$ T cell impairment and allows proliferation (234). Rhinovirus infection of primary bronchial and nasal epithelial cells leads to induction of both PD-L1 and PD-L2 expression, and nasal epithelial cells from rhinovirus-infected patients show upregulation of PD-L1 and PD-L2 mRNA (235). Human PBMCs stimulated *in vitro* with pandemic H1N1 influenza demonstrate induction of PD-L1 on DCs and both PD-L1 and PD-1 on T cells; blockade of PD-L1 in these cultures decreases $CD8^+$ T cell apoptosis

and increases cytokine production (236). Patients infected with pandemic influenza virus also have increased PD-L1 expression on DCs and T cells compared to healthy controls (236). Our group has found that both PD-1 and PD-L1 are upregulated in the lungs of autopsy specimens from patients with fatal RSV, influenza, or PIV-3 infection, with PD-L1 expression on both epithelial and hematopoietic cells (138).

One unanswered question that I explore in chapter III of this thesis is which cells are required for expression of PD-L1 to engage PD-1 and mediate $CD8^+$ T cell impairment. Many different types of cells are capable of expressing PD-L1 (215), and in respiratory virus infection, expression of PD-L1 on epithelial cells and dendritic cells has been observed (231-235, 237). PD-L1 expression on inflammatory DCs is increased after RSV infection compared to expression on other cell types (231). Anti-PD-L1 treatment of e*x vivo* co-cultures of $CD8^+$ T cells with either epithelial cells or DCs from RSV-infected mice leads to significant restoration of T cell function only in the DC co-cultures, whereas anti-PD-L1 treatment of epithelial/$CD8^+$ T cell co-cultures show no difference (231). Collectively, these results suggest that DCs provide the PD-L1 signal to bind PD-1 in T cell impairment; however, conditional cell-specific knockouts of PD-L1 are necessary to prove that DCs provide this signal *in vivo*.

The contribution of PD-1-mediated $CD8^+$ T cell impairment in vaccine responses is unclear. One murine influenza vaccine model showed that limited $CD8^+$ T cell function was associated with high levels of PD-1 expression induced by alum (238). In contrast, PD-1 modulation enhances $CD8^+$ T cell memory responses in mouse models of HPV, HIV, and cancer vaccination (239-241). VLP-based vaccination of mice against HMPV initially leads to $CD8^+$ T cells that are more functional and express lower levels of PD-1

and other inhibitory receptors. However, HMPV challenge of these mice still leads to $CD8^+$ T cell impairment and inhibitory receptor expression similar to mice that had been previously infected with HMPV and then challenged (128), indicating that devising methods to sustain virus-specific T cell function might be necessary in vaccine development for respiratory viruses.

Other inhibitory receptors may contribute to $CD8^+$ T cell impairment. In both primary and secondary HMPV infection, virus-specific lung $CD8^+$ T cells upregulate expression of Tim-3, LAG-3, and 2B4 in addition to PD-1 (139, 229, 237). Though PD-1 mediates early $CD8^+$ T cell impairment, $CD8^+$ T cell impairment still occurs at later time points in the absence of PD-1 (237). *In vitro* blockade of Tim-3, LAG-3, and 2B4, either alone or in combination with PD-L1 blockade, restores IFNγ production by virus-specific $CD8^+$ T cells. However, *in vivo* blockade of Tim-3 does not change $CD8^+$ T cell function or viral titers. Blockade of LAG-3 in either the presence or absence of PD-1 enhances $CD8^+$T cell function, but does not reduce viral titer (237). Thus, the role of other inhibitory receptors in regulating antiviral immunity vs. immunopathology in respiratory viral infection is complex and requires further exploration.

Project Goals and Hypotheses

In this thesis, I address a number of knowledge gaps regarding the field's current understanding of HMPV infection and respiratory virus infections in general. The first aim of my thesis was to elucidate the role of Tregs in HMPV infection, as this was completely unknown before my work. Considering that there was no consensus of the role of Tregs in other respiratory virus infections, I thought it was essential to address

whether these cells were beneficial or detrimental to HMPV infection. I hypothesized that Tregs were detrimental to HMPV infection. As will be seen in chapter II, this is true later in infection; however, I discovered that these cells are necessary for immune priming to HMPV and influenza.

My second aim was to address the contribution of PD-L1 on different cell types in respiratory virus infection, as there was no clear consensus of whether these cells were required on infected epithelial cells, DCs, another cell type, or some combination in respiratory virus infection. I initially hypothesized that antigen presenting cells would provide the essential PD-L1 signal. Though I was unable to either prove or disprove this hypothesis, in chapter III I report that deficiency of PD-L1 on hematopoietic cells appears to drive increased inhibitory receptor expression on $CD8^+$ T cells, pointing to a potential feedback mechanism of PD-L1 controlling inhibitory receptor levels.

My final aim was to understand mechanisms of species restriction of HMPV infection. While there were previously data regarding inhibition of STAT1 by HMPV, there were no reports that HMPV antagonizes STAT2. Due to my initial preliminary data that showed that HMPV titers were significantly higher in $STAT2^{-/-}$ mice compared to WT, I hypothesized that HMPV inhibits STAT2. I further hypothesized that this inhibition was species-specific. In chapter IV I confirm both hypotheses: HMPV inhibits primate, but not murine, STAT2. I also report for the first time mouse-to-mouse passage of HMPV, which indicates that murine adaptation of the virus may be achieved via this method.

CHAPTER II

$CD4^+$ regulatory T cells exert differential functions during early and late stages of the immune response to respiratory viruses[*]

Introduction

Acute respiratory infection by HMPV, influenza, and other viruses leads to $CD8^+$ T cell functional impairment (131, 133, 137, 138). Optimal immune responses to viral infections require a careful balance of effector responses to clear infection and regulatory mechanisms to prevent immunopathology (242-245).

$CD4^+$ regulatory T cells (Tregs) are a principal mediator of immune regulation and have been implicated in a variety of diseases, including autoimmunity, cancer, and infectious disease (246, 247). Studies of respiratory virus infections have yielded conflicting data about the role of Tregs in these different models. In this study, we sought to understand the role of Tregs in HMPV infection. We further sought to differentiate the roles of Tregs at different time points of respiratory virus infection. Other groups have found that Tregs are important for priming the adaptive immune response (165, 248, 249), but have not investigated whether these cells are beneficial or detrimental later in infection.

---

[*] This chapter contains excerpts from the manuscript published in *The Journal of Immunology*. Rogers MC, Lamens KD, Shafagati N, Johnson M, Oury TD, Joyce S, Williams JV. 2018. $CD4^+$ Regulatory T cells exert differential functions during early and late stages of the immune response to respiratory viruses. *J. Immunol*. vol. 201, pp. 1253-1266.

We found that Tregs are increased and become activated in the murine lung in response to HMPV and that Treg depletion leads to significantly more functional anti-viral $CD8^+$ T cell responses and reduced HMPV peak virus titer. Treg depletion immediately before inoculation with either HMPV or influenza reduces the frequency of virus-specific $CD8^+$ T cells in the lung and delayed virus clearance. In contrast, depletion after inoculation enhances $CD8^+$ T cell function with no defect in $CD8^+$ T cell frequency and also accelerates clearance of influenza. In the absence of Tregs during the priming stage of infection, dendritic cells and $CD8^+$ T cells fail to migrate efficiently. The absence of Tregs before inoculation leads to type 2 immune skewing characterized by increased type 2 innate lymphoid cells (ILC2s) and IL-4^+ $CD4^+$ cells, which was not seen when Treg depletion was delayed to 2 days post-inoculation. Furthermore, Treg depletion skews the T_H1:T_H2 cell ratio as well as the ILC1:ILC2 ratio in favor of type 2, indicating that Tregs are strong suppressors of both innate and adaptive type 2 immunity.

Results

Tregs are increased and activated in response to HMPV

To determine the Treg response to HMPV infection, we inoculated WT mice with HMPV and measured the frequency of Tregs in the lung, bronchoalveolar lavage (BAL) fluid, and spleen at day 6 post-inoculation. Compared to mock-infected mice, Tregs were significantly increased in the lungs and BAL fluid (**Figure 2-1A**). We next measured the absolute number of $FoxP3^+$ $CD4^+$ T cells in the lung and spleen throughout the course of infection. Treg numbers peaked in the lung at day 4 of

infection, while splenic Tregs did not change significantly in number during infection (**Figure 2-1B**). To assess the activation state of these cells, we measured expression of the inhibitory receptor PD-1 on the cell surface of pulmonary Tregs. PD-1 is involved in activation, maintenance, and function of Tregs (250). PD-1 was significantly upregulated on Tregs over the course of infection, suggesting that they were becoming activated (**Figure 2-1C**). In contrast, PD-1 expression on splenic Tregs did not change during infection (data not shown). To further characterize the Treg phenotype, Tregs were stained for surface expression of LAG-3, TGFβ, GITR, and neuropilin-1, and intracellular expression of Helios, at day 6 of infection. The median fluorescence intensity of activation markers was higher on Tregs in infected mice compared to mock-infected mice, and Tregs from HMPV-infected animals expressed lower levels of Helios and neuropilin-1, two suggested markers of thymic Tregs (251-253) (**Figure 2-1D-E**). These results indicate that Tregs respond to HMPV infection by becoming activated and increasing in number and frequency.

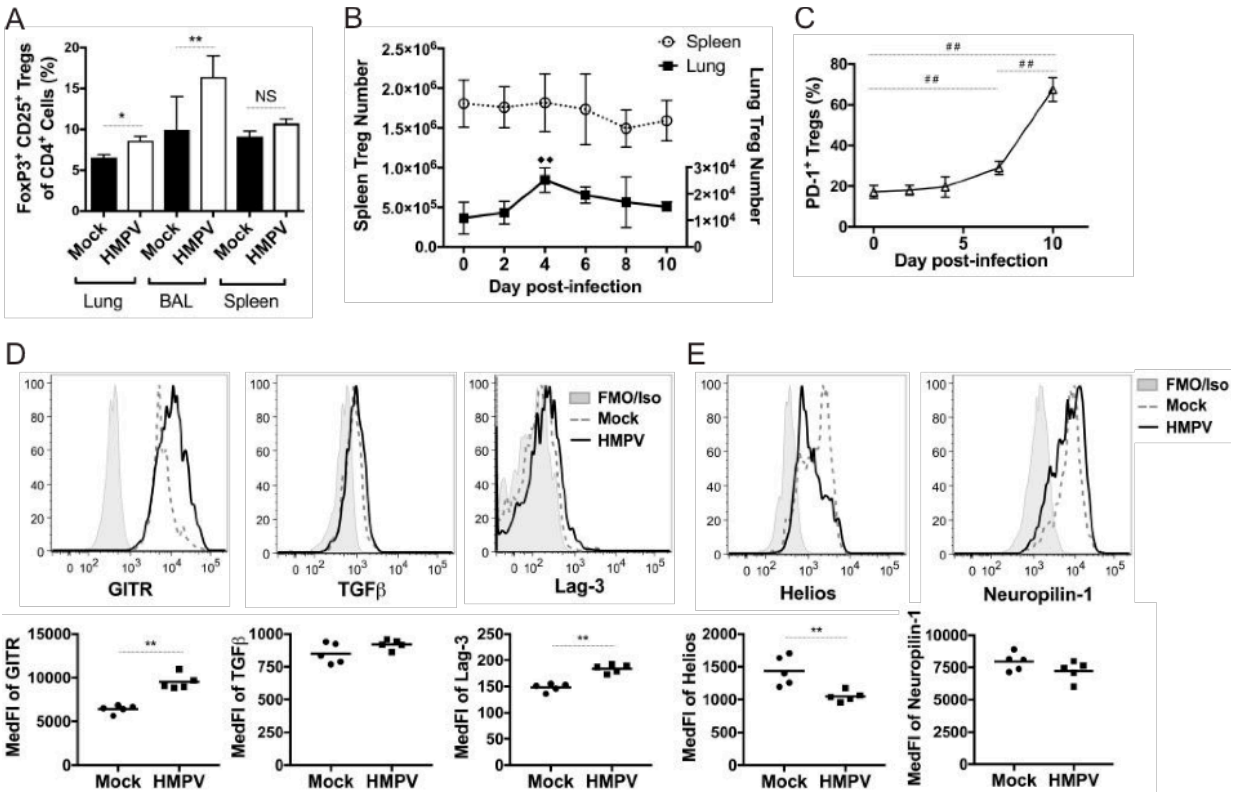

Figure 2-1. Tregs become increased and activated in the lungs of HMPV-infected mice
C57BL/6J mice were intranasally inoculated with HMPV and the percentage (**A**) of $CD4^+$ $CD25^+$ $FoxP3^+$ Tregs was quantified in various organs at day 6 of infection compared to naïve mice. (**B**) The absolute number of pulmonary and splenic $FoxP3^+$ cells was quantified for the duration of HMPV infection. (**C**) The expression of PD-1 on Tregs was measured throughout infection. The expression of Treg activation markers (**D**) and thymic Treg markers (**E**) was measured in mock and infected mice at day 6 and median fluorescence intensity (MedFI) was calculated. Shaded gray represents isotype control (GITR, TGFβ, Helios, Neuropilin-1), or FMO (fluorescence minus one) control (Lag-3) when isotype staining was brighter than sample staining, dashed line represents mock infection, and solid line represents HMPV-inoculated. *p<0.05, **p<0.01, Student's t test; ##p<0.01, One-way ANOVA with Tukey's post-hoc test. ◆◆ indicates significant compared to day 0, p<0.01, one-way ANOVA with Tukey's post-hoc test. N=3-6 mice/group, combined 2 repeat experiments (A-C) or representative of 2-3 experiments (D-E).

Treg depletion leads to enhanced anti-HMPV responses during infection

We next tested whether Tregs inhibit the HMPV-specific $CD8^+$ T cell response during infection. For these experiments, we used $FoxP3^{DTR}$ mice, which express the human diphtheria toxin (DT) receptor downstream of the FoxP3 promoter, so that Tregs

are specifically eliminated by injection of DT (167). In our study, DT injection reduced Treg numbers by >95% in the lung (data not shown). FoxP3^{DTR} mice were depleted of Tregs before and throughout HMPV infection, and the virus-specific CD8$^+$ T cell response was measured by flow cytometry. At days 7 and10 of infection, the percentage of pulmonary CD8$^+$ T cells that recognized the immunodominant HMPV F528 epitope (138), as well as a secondary dominant epitope, N11 (138), was significantly reduced in Treg-depleted mice (**Figure 2-2A,E** and data not shown). However, this reduced frequency was primarily due to an increase in the total number of CD8$^+$ T cells in DT-treated mice, as the absolute number of epitope-specific cells did not significantly differ between DT-treated and control mice at day 7 (**Figure 2-2B**) or day 10 (**Figure 2-2F**). Similarly, at day 7 the percentage of HMPV-specific IFNγ-producing CD8$^+$ T cells was lower in Treg-depleted mice (**Figure 2-2A**), with an IFNγ mean fluorescence intensity (MFI) similar to controls (**Figure 2-2D**). At day 10, however, Treg-depleted mice had significantly increased numbers of IFNγ$^+$ cells (**Figure 2-2F**) with greater IFNγ production per cell (**Figure 2-2H**). To quantify the frequency of functional cells, the percentage of IFNγ$^+$ cells was divided by the percentage of tetramer$^+$ cells in each mouse. Treg-depleted mice had significantly more functional CD8$^+$ T cells at both days 7 and 10 of infection (**Figure 2-2C,G**). This increase in functionality per cell was also seen for a secondary dominant epitope, N11 (data not shown). To ensure that DT treatment had no off-target effects (170), WT mice were injected with DT on the same days, and the CD8$^+$ T cell response was quantified. No difference was seen in CD8$^+$ T cell functionality in DT-treated WT mice compared to PBS-treated FoxP3^{DTR} mice (data not shown). These data indicate that the absence of Tregs allows CD8$^+$ T cells to

become more functional in response to infection, even though the relative frequency of epitope-specific CD8$^+$ T cells is reduced relative to bulk CD8$^+$ T cells infiltrating the lung.

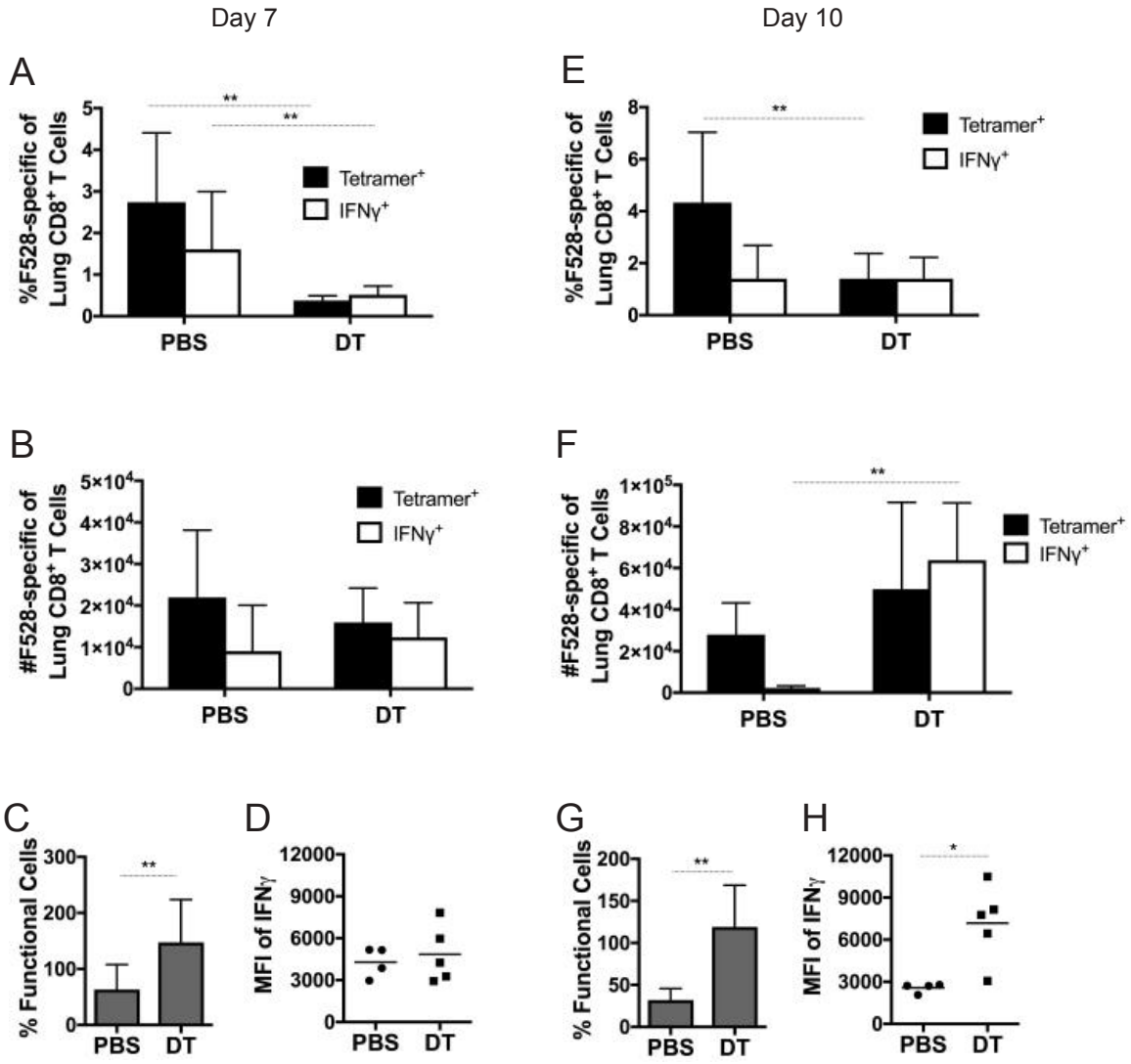

Figure 2-2. Treg depletion leads to an enhanced HMPV-specific CD8$^+$ T cell response. FoxP3^{DTR} mice were depleted of Tregs by injection of DT or injected with PBS before and during infection with HMPV. The percentage (**A,E**), absolute number (**B,F**), and functionality (**C,G**) of the pulmonary CD8$^+$ T cell response was analyzed by flow cytometry at day 7 and day 10. Mean fluorescence intensity (MFI) of the IFNγ signal was quantified at days 7 (**D**) and 10 (**H**). Functionality was calculated by dividing %IFNγ$^+$/tet$^+$. *p<0.05, **p<0.01, Student's t test. N=4-5 mice per group, combined 2 repeated experiments (A-C, E-G) or representative of 2 repeated experiments (D, H).

Tregs inhibit immune control of HMPV replication while decreasing inflammation

Since Treg depletion led to enhanced $CD8^+$ T cell function, we next tested the biological effect on HMPV infection. We depleted Tregs in $FoxP3^{DTR}$ mice as above, inoculated them with HMPV, and at various times post-inoculation homogenized and quantified lung virus titer by plaque assay. At day 5 of infection, which is the peak of HMPV replication in B6 mice (138), HMPV titers were significantly lower in DT-treated mice compared to PBS-treated controls (**Figure 2-3A**). The kinetics of virus clearance on days 7 and 9 were not altered in the absence of Tregs. Lung sections were stained with H&E and scored histologically at days 7 and 10 (**Figure 2-3B-D**) to determine whether reduced viral titers came at the cost of increased immunopathology. While DT- and PBS-treated mice had similar lung histology at day 7, DT-treated mice exhibited greater perivascular lymphohistiocytic inflammation than PBS controls at day 10 post-inoculation. Additionally, Treg-depleted mice had a greater number of lung fields that scored 3 or higher (greater than 50% inflammation) compared to PBS controls. However, Treg-depleted, infected mice scored similarly to Treg-depleted, mock-infected mice, which suggests that increased inflammation was due primarily to the absence of Tregs rather than to damage mediated by the virus itself. Taken together, these data suggest that Tregs inhibit immune control of peak HMPV virus replication but restrain immune-mediated pathology.

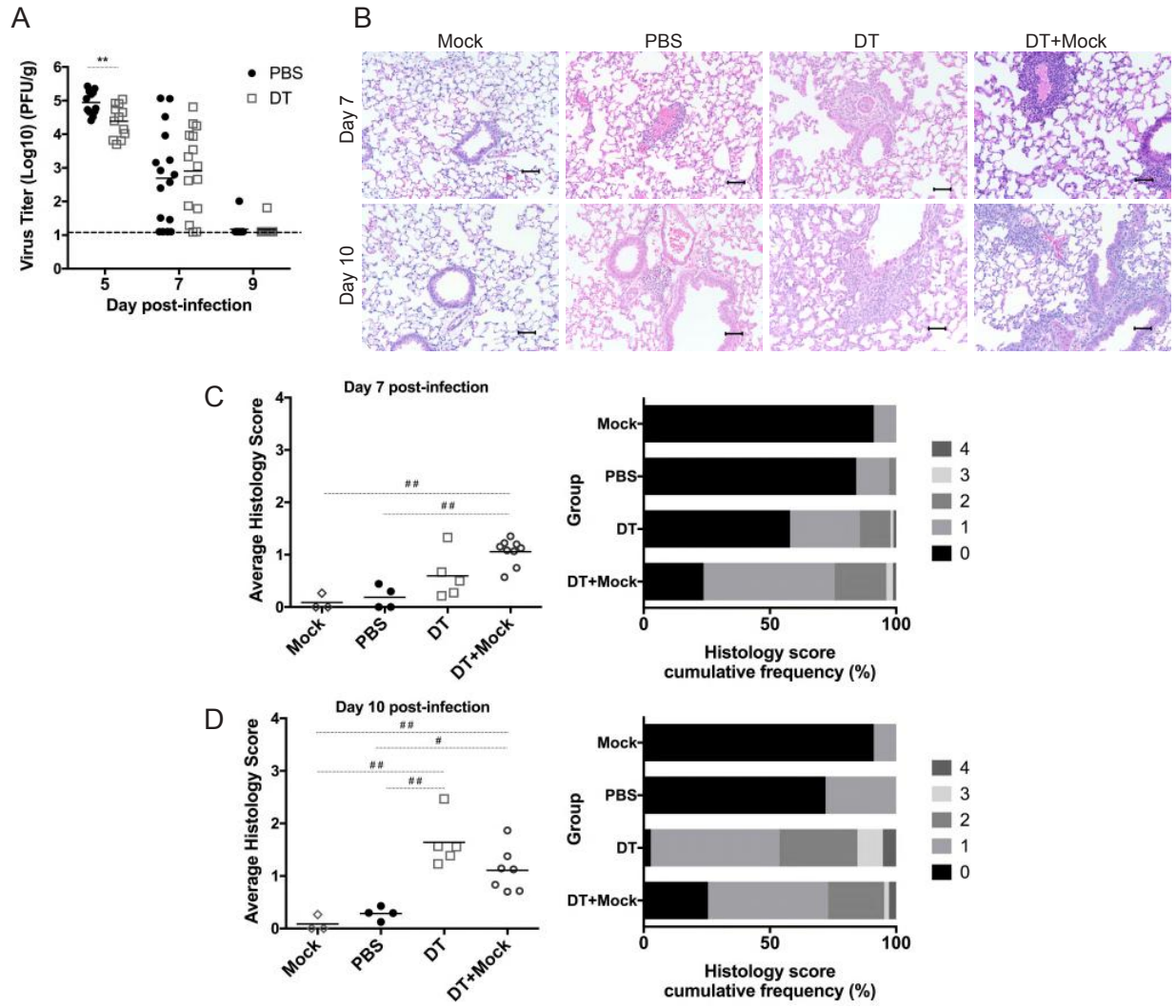

Figure 2-3. Treg depletion reduces virus titers but increases histopathology. FoxP3 ^{DTR} mice were injected with PBS (Mock) or DT (DT+Mock) and mock-infected, or were injected with PBS (PBS) or DT (DT) and inoculated with HMPV. (**A**) Lungs were harvested at indicated times post-inoculation to quantify virus titer by plaque assay. Lung specimens were taken at days 7 and 10 and stained with H&E (**B**), and scored by a pathologist (**C,D**). Histological scoring was calculated by percent inflammation per field of view, with scores of 0, 1, 2, 3, and 4 representing 0%, 1-25%, 26-50%, 51-75%, and 76-100%, respectively. **p<0.01, Student's t test, $^{\#}$p<0.05, $^{\#\#}$p<0.01, One-way ANOVA with Tukey's post-hoc comparison. N=3-6 mice/group, combined 4 repeated experiments (A) or representative of 3 repeated experiments (B-D).

Depletion and blockade of Tregs using αCD25 treatment improves anti-HMPV CD8$^+$ T cell response

As a complementary approach, and because previous studies of RSV demonstrated different outcomes depending on the method of Treg depletion (165, 177, 181, 249, 254), we depleted and blocked Tregs *in vivo* using PC61, an antibody against CD25 that has been commonly used for Treg depletion in WT mice. Since a variety of dosages and schedules have been reported in the literature for respiratory virus infection (165, 249, 254), we performed a pilot study to define the optimal dose for our model. We determined that i.p. injection of 500 μg at days -3 and 0 had the greatest effect on Treg frequency in the lung while sparing CD8$^+$ T cells (data not shown). Mice that received αCD25 had increased HMPV-specific and functional CD8$^+$ T cells, as measured by production of IFNγ and CD107a, an indicator of cytotoxic granule release (255), despite only a modest reduction in Treg percentages (**Figure 2-4A-D**). Furthermore, αCD25-treated mice exhibited increased IFNγ production by CD8$^+$ T cells (**Figure 2-4E**). αCD25-treated mice had slightly lower virus titers than isotype-treated controls, which approached statistical significance (**Figure 2-4F**). This intermediate phenotype compared to Treg depletion in FoxP3^{DTR} mice was likely due to the fact that αCD25 is not sufficient to completely eliminate all Tregs (**Figure 2-4A**). These findings indicate that αCD25 treatment directed at Tregs during HMPV infection has a similar, though less robust, effect on CD8$^+$ T cell cytokine production and degranulation and virus clearance compared to complete elimination using FoxP3^{DTR} mice.

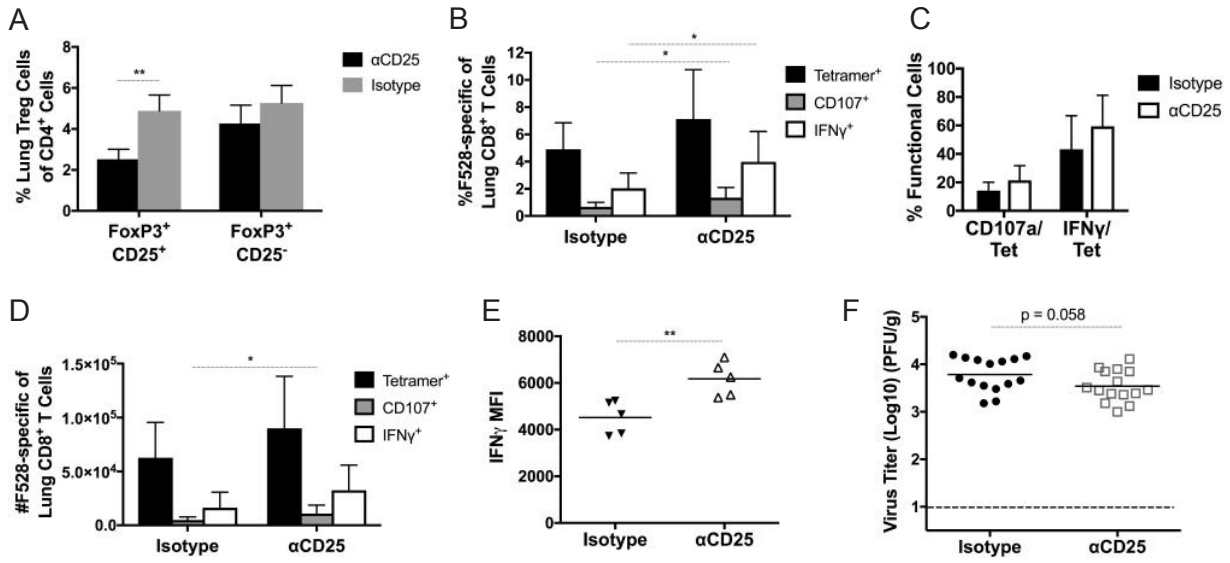

Figure 2-4. Depletion and blockade of Tregs with αCD25 restores CD8$^+$ T cell function. WT mice were injected with 500 ug anti-CD25 antibody or isotype at days -3 and 0 of HMPV infection. Treg percentages (**A**), percent CD8$^+$ T cell response (**B**), function (**C**), and absolute number (**D**) were quantified at day 7 of infection. (**E**) Mean fluorescence intensity (MFI) of IFNγ signal was measured at day 7. (**F**) HMPV virus titer was calculated at day 5 of infection. *p<0.05, **p<0.01, Student's t test. N=2-6/group, combined 2-3 experiments (B-D,F) or representative of 2 experiments (A,E).

Treg depletion early or late in HMPV infection reveals differential functions of Tregs

Since Treg depletion throughout infection led to a decreased proportion of HMPV-specific CD8$^+$ T cells (Figure 2-2A,D), we hypothesized that Tregs might be necessary to prime the adaptive immune response to HMPV. To test this, we depleted Tregs before and throughout infection (DT), only before inoculation with HMPV (early), or from 2 days post-inoculation onward (late) (**Figure 2-5A**). At day 7 of infection, Tregs in the "early" group were restored to nearly the same level (8.42% +/- 0.41) as the PBS group (9.93% +/- 0.60). Mice that were depleted of Treg later had a greater frequency and absolute number of HMPV-specific and IFNγ-producing CD8$^+$ T cells at day 7 of infection (**Figure 2-5B,C**). In contrast, mice that underwent Treg depletion only before

inoculation had decreased $CD8^+$ T cell percentages and similarly functional cells as those that received DT throughout (**Figure 2-5D**). All mice had similar day 5 titer (**Figure 2-5E**); however, mice that received late depletion had significantly reduced virus titers at day 7 compared to those mice that had Tregs depleted early (**Figure 2-5F**). Both DT and early groups had delayed virus clearance compared to PBS-treated mice. Histologic analysis showed that both early and late Treg depletion led to increased lung immunopathology (**Figure 2-5G**), with the early group having more instances of inflammation scores of 2 or higher (**Figure 2-5H**). Lung sections were also stained with Periodic acid-Schiff (PAS) to detect mucus. Early Treg-depleted groups had marked PAS positivity in large and small airways. DT and late groups had less PAS positivity than the early group, while the PBS-treated mice had rare PAS positivity in bronchioles (**Figure 2-5I**). These data indicate that Treg depletion after inoculation is sufficient to enhance function while also maintaining the number and frequency of HMPV-specific $CD8^+$ T cells. Additionally, these findings suggest that Tregs play a role at the onset of infection for the recruitment of $CD8^+$ T cells but then impair $CD8^+$ T cell function later on to prevent immune pathology.

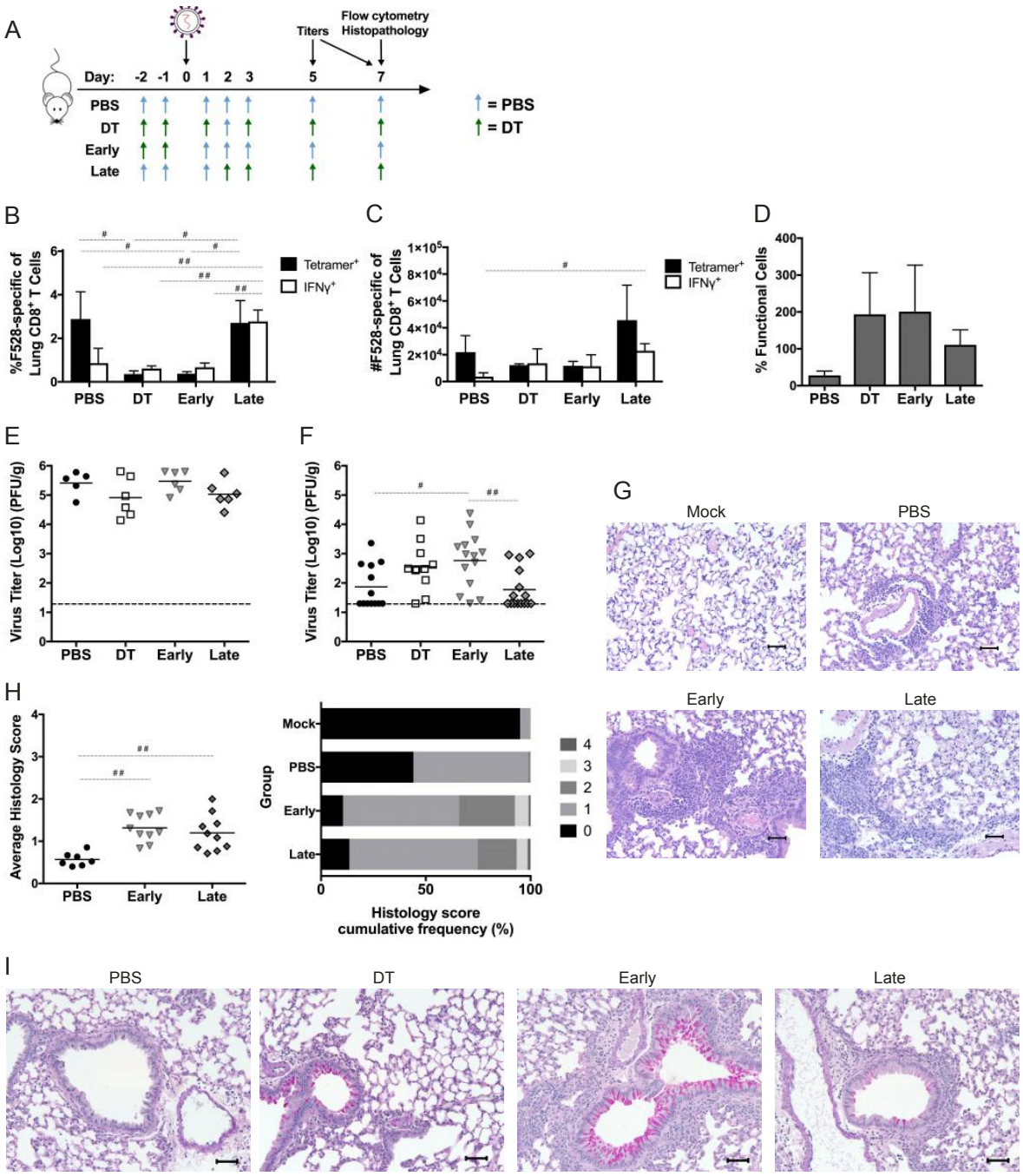

Figure 2-5. CD8$^+$ T cells fail to mount a robust response and clear virus efficiently when Tregs are depleted before inoculation. (**A**) FoxP3^{DTR} mice were depleted of Tregs by injection of DT on days -2 and -1 (Early); on days 2, 3, and 5 (Late); or before and throughout the course of infection (DT); or injected with PBS before and throughout (PBS). Mice were inoculated with HMPV. The pulmonary CD8$^+$ T cell response was analyzed by flow cytometry at day 7 for frequency (**B**), absolute number (**C**), and percent functionality (**D**). Virus titers were measured via plaque assay at days 5 (**E**) and 7 (**F**). Histological sections were stained with H&E (**G**) and scored (**H**) as in Figure 2-3, or stained with Periodic-acid Schiff (PAS) (**I**). $^{\#}p<0.05$, $^{\#\#}p<0.01$, One-way ANOVA with Tukey's post-hoc comparison. N=4-6 mice/group, pooled from 2-3 experiments (E-H) or representative of 3-4 experiments (B-D, I).

Absence of Tregs during priming phase of infection impairs migration of DCs and CD8$^+$ T cells to lymph nodes and lung

We next sought to understand the mechanism of how a lack of Tregs at the priming stage of the immune response leads to a deficient proportion of HMPV-specific CD8$^+$ T cells in the lung (Figures 2-2A, 2-5B). In the absence of Tregs, dendritic cells (DCs) exhibit reduced migration to lymph nodes in response to HSV infection (248). To determine whether depletion of Tregs leads to impaired DC migration from the lung to the draining mediastinal lymph nodes (MLN), we instilled CFSE-labeled, HMPV peptide-loaded bone marrow derived DCs (BMDCs) intratracheally into mice that had either been depleted of Tregs or given PBS control. We found that at 22 hours post-instillation, significantly fewer CFSE$^+$ BMDCs were found in the MLN of Treg-depleted mice compared to PBS controls (**Figure 2-6A,B**). There was a similar reduction of BMDCs in Treg-depleted mice at 40 hours post-instillation, though this was not statistically significant (**Figure 2-6B**). To better understand the mechanism of this reduction, we measured levels of the chemokine CCL21, a ligand for CCR7 on DCs and other cells, and found that CCL21 was reduced in MLNs of infected Treg-depleted mice compared to infected PBS controls (**Figure 2-6C**). We next asked whether a reduction of DCs led to decreased expansion of HMPV-specific CD8$^+$ T cells in the MLN. We measured the percentage of CD8$^+$ T cells specific for the HMPV epitopes F528 and N11 as well as the expression of CD69, an early marker of activation, on these cells at day 4 of infection in the MLN. We found that despite a phenotype that suggested impaired DC migration in Treg-depleted mice, there was a significantly greater frequency of HMPV-specific CD8$^+$ T cells, as well as more activated CD8$^+$ cells, in the MLN compared to PBS controls

(**Figure 2-6D**). However, when we measured HMPV-specific $CD8^+$ T cell recruitment to the lung at day 4 (the earliest time point that we could detect HMPV-specific $CD8^+$ T cells in the lung (data not shown)), Treg-depleted mice had significantly fewer epitope-specific $CD8^+$ T cells by frequency and number compared to PBS controls, suggesting a failure of migration in the absence of Tregs (**Figure 2-6E,F**). The frequency of HMPV-$specific^+$ $CD8^+$ T cells in MLN at day 3 of infection was less than 0.05% for either group (data not shown), which suggests that the difference in MLN and lung $CD8^+$ T cell frequency was not due to earlier migration of HMPV-specific $CD8^+$ T cells from the MLN to the lung in control mice.

To better understand the mechanism of how Treg depletion leads to impaired $CD8^+$ T cell migration to the lung, we measured a variety of chemokines that contribute to T cell migration in lung homogenate at day 5 of infection in PBS, Early, and DT treatment groups by qrtPCR (**Table 2-I)**. We found that CXCL11, CCL4, CX3CL1, and IL-15 were reduced up to 2-fold in the lungs of DT and Early groups compared to PBS controls (**Figure 2-6G,H**). These data indicate that in the absence of Tregs, cell migration in response to HMPV infection is impaired.

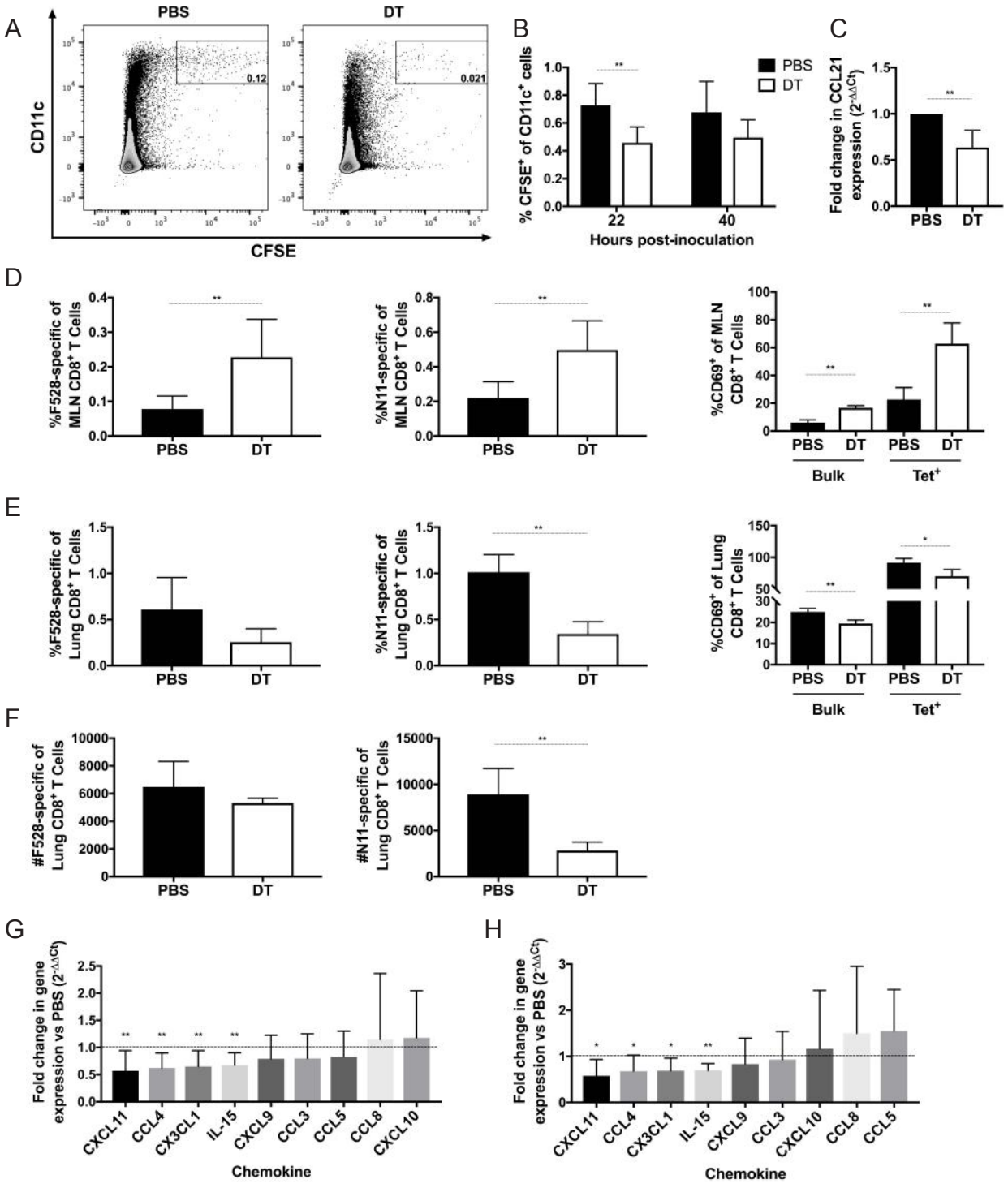
A
PBS
DT
CD11c
CFSE
0.12
0.021
B
% CFSE+ of CD11c+ cells
PBS
DT
22
40
Hours post-inoculation
C
Fold change in CCL21 expression (2-ΔΔCt)
PBS
DT
D
%F528-specific of MLN CD8+ T Cells
%N11-specific of MLN CD8+ T Cells
%CD69+ of MLN CD8+ T Cells
Bulk
Tet+
E
%F528-specific of Lung CD8+ T Cells
%N11-specific of Lung CD8+ T Cells
%CD69+ of Lung CD8+ T Cells
F
#F528-specific of Lung CD8+ T Cells
#N11-specific of Lung CD8+ T Cells
G
Fold change in gene expression vs PBS (2-ΔΔCt)
CXCL11
CCL4
CX3CL1
IL-15
CXCL9
CCL3
CCL5
CCL8
CXCL10
Chemokine
H
Fold change in gene expression vs PBS (2-ΔΔCt)
CXCL11
CCL4
CX3CL1
IL-15
CXCL9
CCL3
CXCL10
CCL8
CCL5
Chemokine

Figure 2-6 (previous page). Treg deficiency leads to impaired DC and CD8$^+$ T cell migration early in infection. FoxP3^{DTR} mice were depleted of Tregs via i.p. injection of diphtheria toxin at days -2 and -1 (DT) or given PBS control (PBS). BMDCs were generated and matured overnight in the presence of 100 ng/ml LPS and 10 μM HMPV F528 peptide. Mature BMDCs were labeled with CFSE and intratracheally instilled into mice at day 0. (**A,B**) 22 and 40 hours post-instillation, mediastinal lymph nodes were collected from mice, and the percentage of CFSE$^+$ CD11c$^+$ cells was quantified via flow cytometry. (**C**) Mice were depleted of Tregs as above, and inoculated with HMPV. At day 2 post-inoculation, mediastinal lymph nodes were harvested, and expression of CCL21 was measured by qRT-PCR. At day 4 of infection, mediastinal lymph nodes (**D**) and lungs (**E,F**) were harvested, and the frequency, number, and activation status of CD8$^+$ T cells recognizing the HMPV epitopes F528 and N11 were measured by flow cytometry. Chemokines were measured by qRT-PCR at day 5 of infection in the lung, and the fold change of DT (**G**) or Early (**H**) groups was compared to PBS controls. *p<0.05, **p<0.01, Student's t test. N=2-5 mice/group, combined from 2-3 independent experiments (A-C,G,H) or representative of 2 experiments (D-F).

Table 2-I. Chemokines with a role in T cell migration

Chemokine	Role in T cell migration	Reference
CXCL11	Recruit CD4$^+$ and CD8$^+$ effector T cells (Teff) to sites of inflammation	(256-258)
CCL4 (MIP-1b)	Made by activated CD8$^+$ T cells	(259)
CX3CL1	Attract and induce endothelial adhesion of activated T cells	(260, 261)
IL-15	Induce migration of CD8 Teff to lung	(262)
CXCL9	Recruit CD4$^+$ and CD8$^+$ Teff to sites of inflammation	(257)
CCL5 (RANTES)	Recruit CD4$^+$/CD8$^+$ T cells	(263)
CCL3 (MIP-1a)	Attract CD8$^+$ T cells to airways	(264)
CXCL10	Recruit CD4$^+$ and CD8$^+$ Teff to sites of inflammation	(257)
CCL8 (MCP-2)	Attract human T cells (limited data in mice)	(265)

Early Treg depletion leads to type 2 immune skewing, while late depletion maintains type 1 response

To further investigate the mechanism of how early Treg depletion alters the lung environment and delays virus clearance, we analyzed protein levels of cytokines and chemokines in lung homogenates in the groups defined in Figure 2-5A at days 5 and 7 post-HMPV inoculation. At day 5 of infection, IL-10 was lower in DT, early, and late treated groups compared to control mice. IL-5 levels were significantly higher in both DT and early treated mice, while type 1 cytokines IL-2 and IFNγ were higher in PBS controls and late depleted mice (**Figure 2-7A**). We found that type 2 cytokines, including IL-4, IL-5, IL-13, and eotaxin, were increased at day 7 in mice that received early Treg depletion (**Figure 2-7B**). Furthermore, early Treg depletion led to even higher IL-5 and IL-13 levels than DT treatment throughout infection, indicating that the timing of Treg depletion was critical for this phenotype. To determine which cells are responsible for the type 2 cytokine skewing, we stimulated lung cells from infected mice in the 4 treatment groups *ex vivo* with PMA/ionomycin. We used flow cytometry to immunophenotype $CD4^+$ T cells and measure type 2 innate lymphoid cell (ILC2) numbers and cytokine production. We found that after early Treg depletion, there was a greater frequency of IL-4-producing $CD4^+$ T cells than after DT, late depletion, or PBS control (**Figure 2-7C**). Additionally, early Treg depletion led to greater numbers of ILC2s compared to late depletion (**Figure 2-7D**; for gating strategy see **Figure 2-8**) as well as greater production of IL-5 and IL-13 from these cells (**Figure 2-7E,F**). Since previous studies have used a variety of markers to identify ILC2s (which may differ between tissue type and mouse strain) (266-270), we further stained the ILC2 population for ST2,

CD25, and KLRG-1 (**Figure 2-9A**). We found that although the overall absolute number of cells varied depending on the marker of interest, all revealed nearly identical patterns of increased ILC2s in Treg-depleted mice (**Supplemental Figure 2-9B**). When IFNγ (produced by ILC1s) and IL-13 (from ILC2s) were measured on bulk ILCs, the DT and early groups had a smaller proportion of IFNγ$^+$ ILC1s compared to IL-13$^+$ ILC2s (2.5:1), while this ratio was maintained near 5:1 in PBS-treated and late groups (**Figure 2-7G**). These data indicate that early Treg depletion is associated with skewing of both innate and adaptive cells towards a type 2 phenotype and that Tregs control the ratio of both innate and adaptive type 1 and type 2 immune cells.

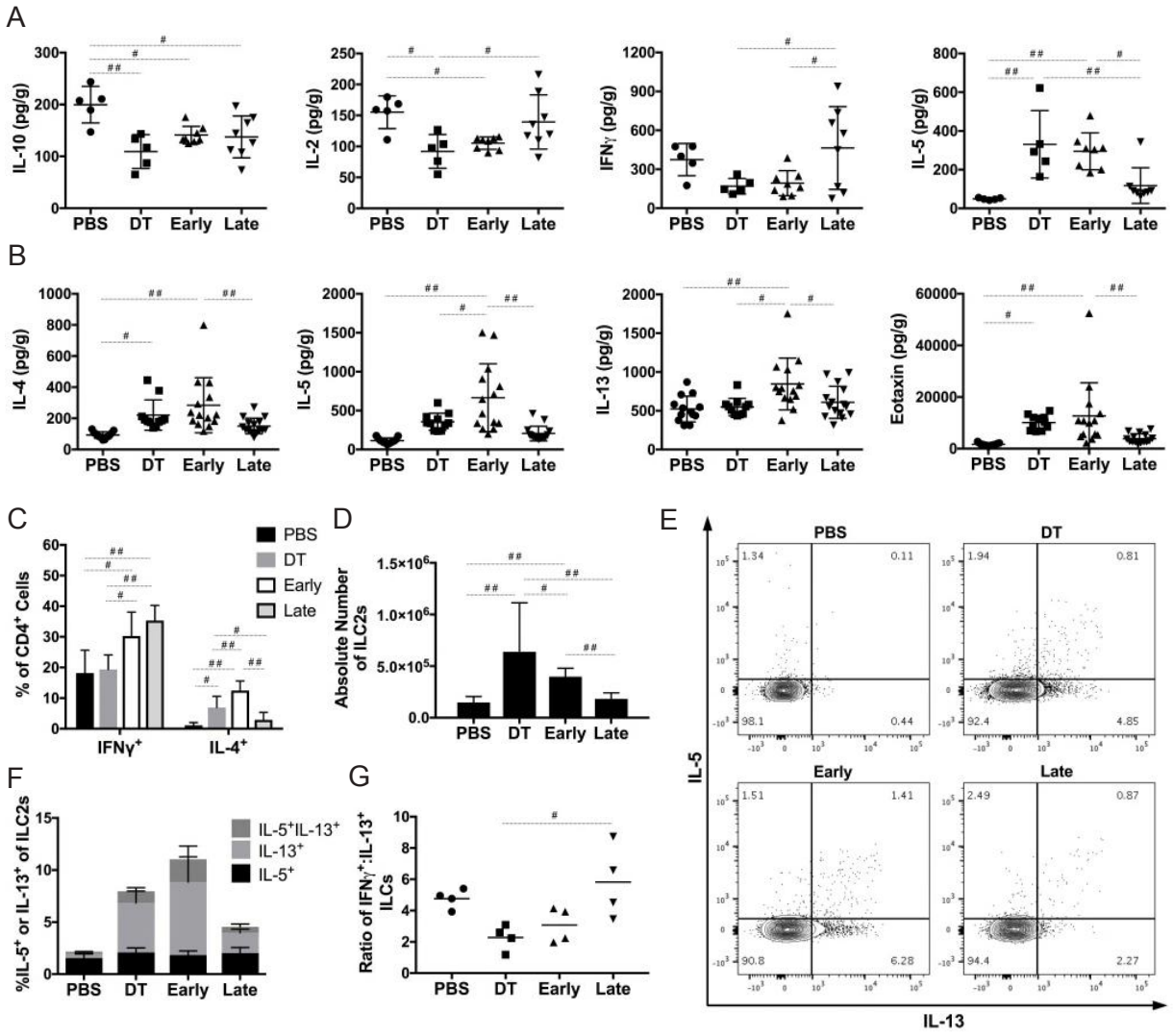

Figure 2-7. Early Treg depletion leads to imbalance of T_H2 cytokines, T_H2 cells, and ILC2s. Cytokines and chemokines were measured by Luminex multiplex analysis of lung homogenate of groups from Figure 2-5A at day 5 (**A**) and 7 (**B**). FoxP3^{DTR} mice were depleted of Tregs and inoculated as in Figure 2-5, and CD4$^+$ cells (**C**) and ILC2s (**D-F**) were quantified and phenotyped by flow cytometry at day 7 post-inoculation. (**G**) The ratio of IFNγ^+ to IL-13$^+$ ILCs was calculated. CD4$^+$ cells and ILC2s were stimulated prior to staining in C and E-G. For panel G, pan-ILCs were defined as CD45$^+$, CD127$^+$, Lin$^-$, CD90$^+$; for panels D-F, ILC2s were defined as pan-ILC markers plus ICOS$^+$ (see Figure 2-9). $^{\#}p<0.05$, $^{\#\#}p<0.01$, One-way ANOVA with Tukey's post-hoc comparison. N=4-6 mice/group, pooled from 2-3 independent experiments (A-D) or representative of 2 independent experiments (E-G).

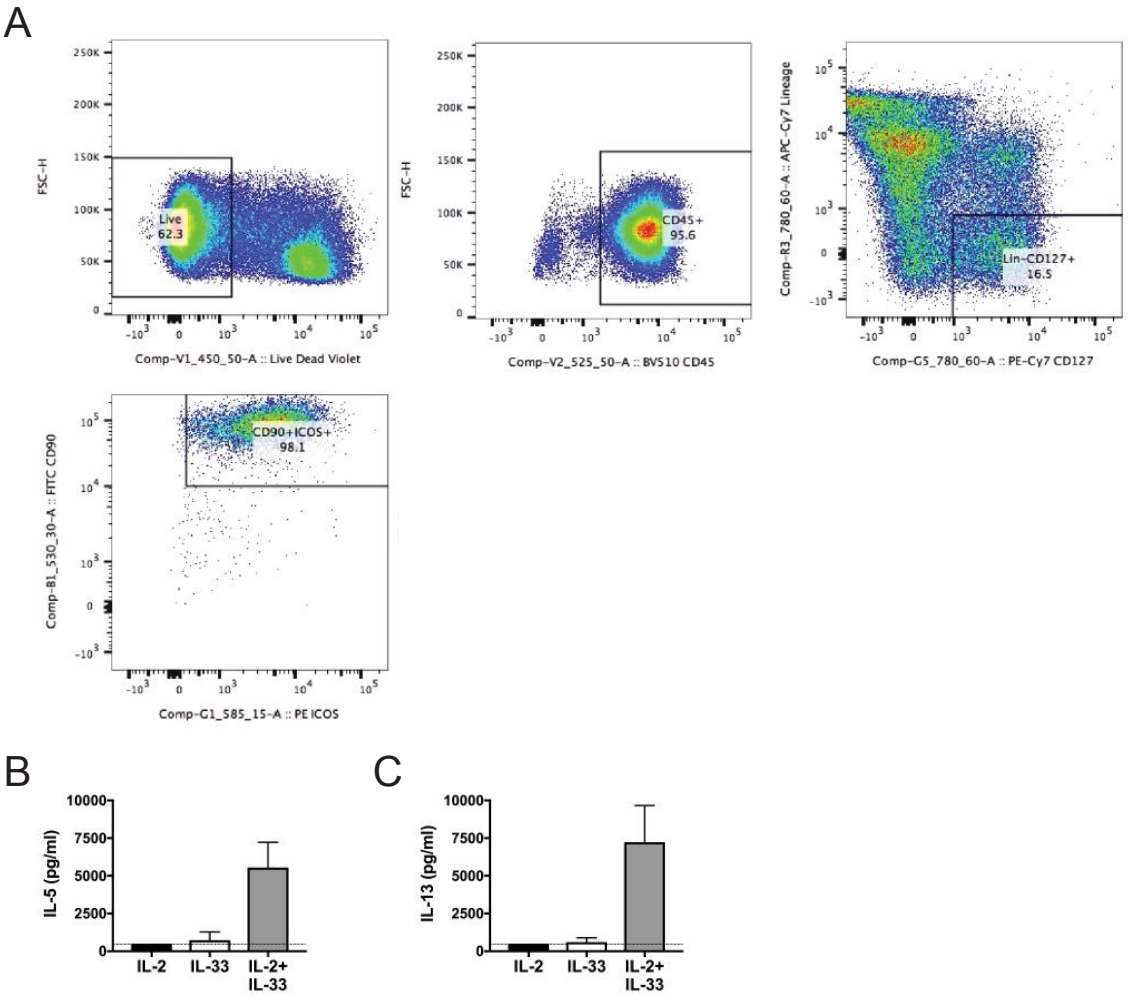

Figure 2-8. Gating strategy for ILC2s. (**A**) ILC2s were identified as CD45^{+}, Lineage^{-}, CD127^{+}, CD90^{+}, ICOS^{+}. ILC2s were sorted according to the above gates and production of IL-5 (**B**) and Il-13 (**C**) was measured by ELISA after stimulation with IL-2 and/or IL-33.

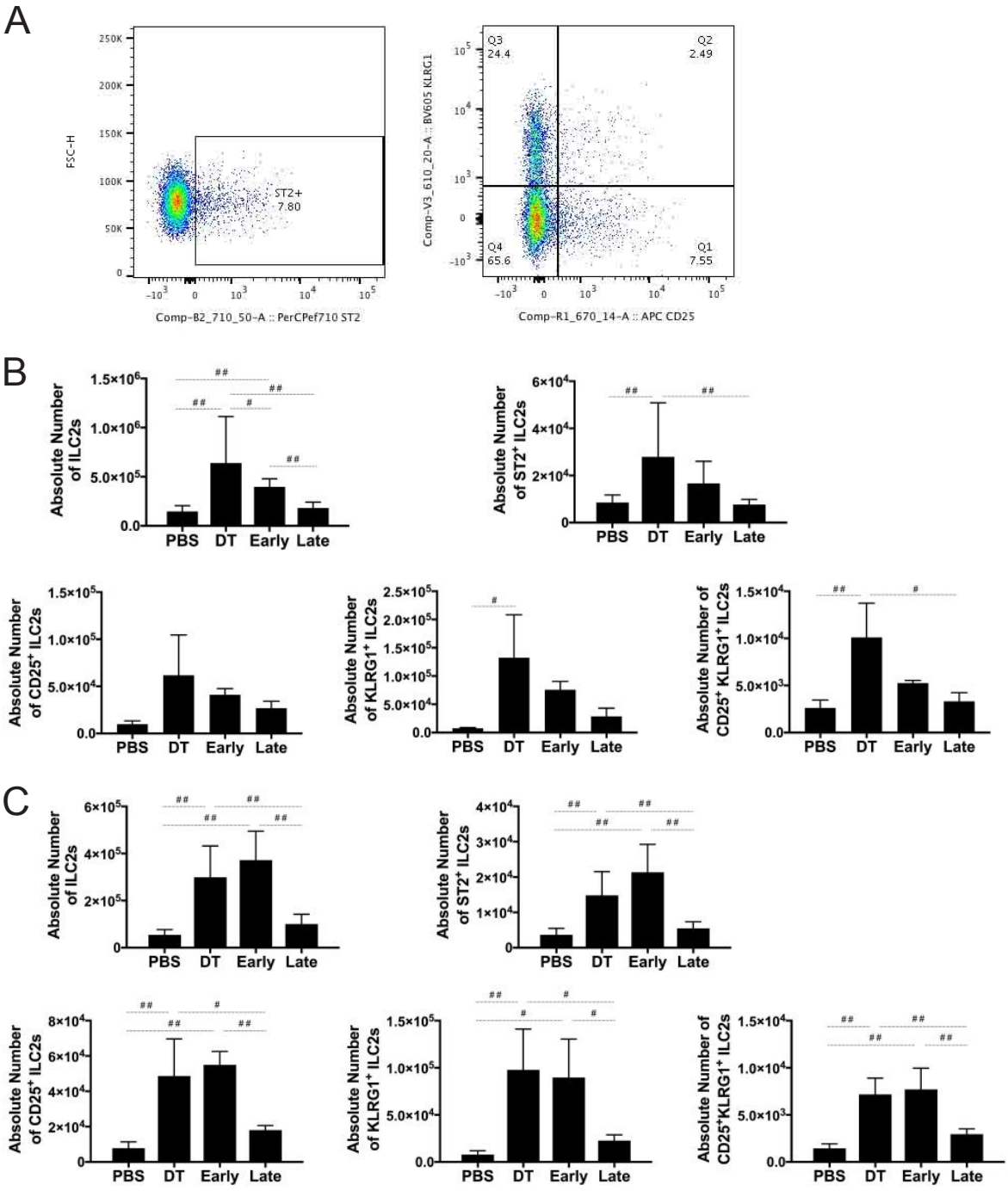

Figure 2-9. ILC2 markers. Gating strategy (**A**) and quantification of ST2$^+$ CD25$^+$, KLRG-1$^+$, or CD25$^+$KLRG-1$^+$ ILC2s from FoxP3^{DTR} mice treated with DT or PBS at the indicated time points and infected with HMPV (**B**) or influenza (**C**). $^{\#}p<0.05$, $^{\#\#}p<0.01$, One-way ANOVA with Tukey's post-hoc comparison. N=4-6 mice/group, pooled from 2-3 independent experiments (B,C).

Tregs have differential roles in early and late influenza virus infection

To determine whether the roles of Tregs early and late in infection was specific to HMPV or could be generalized to other respiratory viruses, we depleted Tregs either early or late during infection with influenza x31, a mouse adapted H3N2 strain. Since x31 is a mouse-adapted strain, mice had increased morbidity than with HMPV infection (19% vs. 5% body weight loss at day 7 post-inoculation, data not shown). As we observed with HMPV, at day 7 post-inoculation, mice depleted of Tregs either early or throughout infection had significant reductions in epitope-specific $CD8^+$ T cells as well as significantly fewer IFNγ-producing cells compared to PBS-treated mice (**Figure 2-10A,B**). Although late Treg depletion led to significantly more IFNγ production by $CD8^+$ T cells compared to DT- or early-treated groups, the frequency of epitope-specific cells in the late group was not equivalent to the PBS control group, in contrast to that observed in HMPV infection (Figure 2-5B). This difference may be attributable to the increased severity of the mouse-adapted influenza virus infection. Mice depleted of Tregs at any time point had a trend towards more functional $CD8^+$ T cells than PBS-treated mice (**Figure 2-10C**). At day 7 of infection, virus titers in the late group were reduced by 100-fold compared to early and DT groups, and 10-fold compared to PBS controls (**Figure 2-10D**). When we analyzed helper T cell skewing, there were significantly more IL-4^+ CD4 cells as well as more IL-4 produced per cell in the early and DT groups (**Figure 2-10E,F**). Absolute numbers of ILC2s were significantly increased in early-depleted mice (**Figure 2-10G and Figure 2-9C**). The early group had a higher proportion of IL-5/IL-13^+ ILC2s as well as more IL-5 per cell (**Figure 2-10H,I**). These

data suggest that the temporal differences in the role of Tregs are conserved between infections by multiple respiratory viruses.

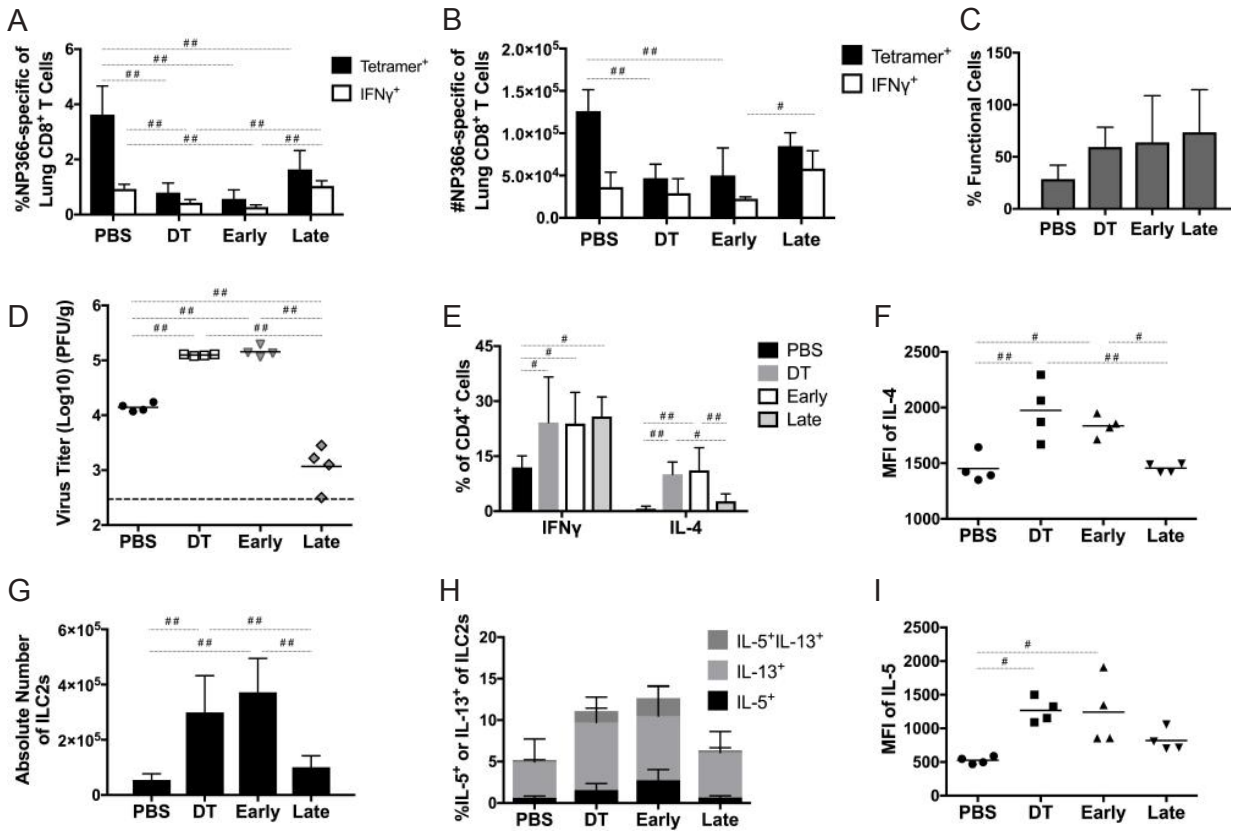

Figure 2-10. Tregs exert differential functions in the early and late immune response to influenza infection. FoxP3^{DTR} mice were depleted of Tregs early, late, or throughout infection as in Figure 2-5, then inoculated with 50-100 PFU influenza x31. (**A-C**) At day 7 of infection mice were sacrificed and the influenza-specific CD8$^+$ T cell response was quantified. (**D**) Virus titers were measured at day 7 of infection. Cytokine production from CD4$^+$ cells was measured at day 7 (**E,F**), and numbers (**G**) and cytokine production from ILC2s (**H,I**) was also measured. $^{\#}p<0.05$, $^{\#\#}p<0.01$, One-way ANOVA with Tukey's post-hoc comparison. N=4 mice/group, combined from 2-3 experiments (E,G) or representative of 2-3 independent experiments (A-D,F,H-I).

Neither early nor late depletion of Tregs affects the CD8$^+$ T cell memory recall response to HMPV

Since early Treg depletion led to a reduction in HMPV-specific CD8$^+$ recruitment to the lung and delayed virus clearance during primary infection (Figure 2-5), we hypothesized that depletion of Tregs immediately before primary infection would also impair the recall response to subsequent HMPV challenge. To test this, we depleted Tregs before, throughout, or immediately after HMPV inoculation as in Figure 5 until day 5 post-infection. We let the primary infection clear and then challenged the mice with the same strain of HMPV 30-35 days after initial infection. In a pilot experiment, we found that multiple mice that received DT (from DT, early, and late groups) died around day 14 post-infection, likely from lethal autoimmunity caused by a lack of thymic Tregs (data not shown). To account for this, we adoptively transferred 1.5-2x10^6 naive CD4$^+$ cells from a congenic donor at day 6 post-infection. Interestingly, after adoptive transfer the mice in the DT group nevertheless succumbed to autoimmunity around day 14 post-infection, likely because the naive cells were not sufficient to counteract the 9-day absence of Tregs, which suggests that there is a "point of no return" when autoimmunity cannot be reversed by Treg adoptive transfer. In contrast, all but one mouse in the other groups survived to at least day 35, when the experiment concluded. After secondary challenge, mice were euthanized at day 5 or 7 post-challenge for analysis of HMPV-specific CD8$^+$ cells by flow cytometry. Overall CD8$^+$ percentages were significantly higher in both early and late groups, possibly indicating ongoing autoimmunity in these mice (**Figure 2-11A**). We found that all groups had similar percentages and numbers of CD8$^+$ T cells specific to F528 and N11, primary and secondary dominant epitopes in B6 mice (**Figure**

2-11B,C and data not shown). Additionally, similar proportions of $CD8^+$ T cells from each group produced IFNγ in response to peptide (**Figure 2-11D**). These results indicate that timing of Treg depletion skews the effector CTL response during primary infection but does not affect the formation of the effector $CD8^+$ memory response.

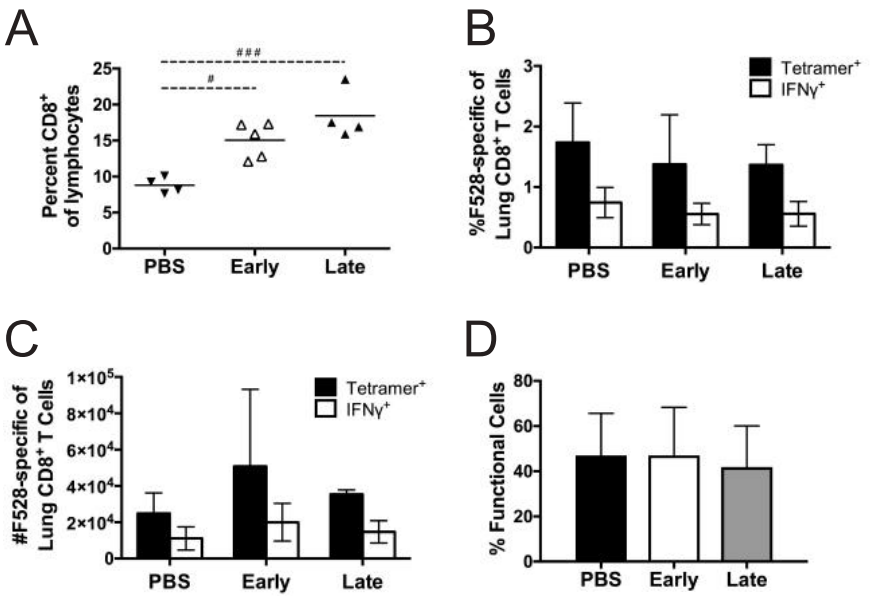

Figure 2-11. Early or late Treg depletion during primary infection does not affect memory recall response to secondary challenge. Tregs were depleted early or late in HMPV infection, as in Figure 2-5. At day 6, 1.5-2x10^6 naïve $CD4^+$ cells were adoptively transferred into Treg depleted mice. At day 30-35, mice were challenged with the same strain of HMPV and sacrificed at day 5 post-infection. Percent $CD8^+$ lung lymphocytes (**A**), percent virus-specific $CD8^+$ T cells (**B**), absolute number of virus-specific $CD8^+$ T cells (**C**), or percent functionality (**D**) were determined at day 5 by flow cytometry. $^{\#}p<0.05$, $^{\#\#\#}p<0.001$, One-way ANOVA with Tukey's post-hoc comparison. N=3-5 mice/group, representative of 2 experiments.

Tregs do not function additively or synergistically with PD-1 to impair $CD8^+$ T cell responses to HMPV and other respiratory viruses

Here we found that depletion of Tregs restores $CD8^+$ T cell function and reduces HMPV titers. We previously found that blockade of the ligand for the inhibitory receptor

PD-1 also restores function and reduces virus titer (138). Therefore, to determine whether these two mechanisms for $CD8^+$ T cell impairment work coordinately, we used a combination of Treg depletion and PD-L1 blockade. $FoxP3^{DTR}$ mice were depleted of Tregs and given anti-PD-L1 Ab for the duration of HMPV infection. The $CD8^+$ T cell response at day 7 of infection (**Figure 2-12A-D**) was not significantly different in mice that received the combined treatment compared to mice that received DT alone. Additionally, virus titer was equivalent for mice receiving combined treatment or either DT or antibody blockade alone (**Figure 2-12E**). These data suggest that a threshold may exist over which a $CD8^+$ T cell cannot become more functional or that anti-PD-L1 may be working through its effect on PD-1 expressed by Tregs, so in the absence of these cells the PD-L1 treatment has reduced efficacy.

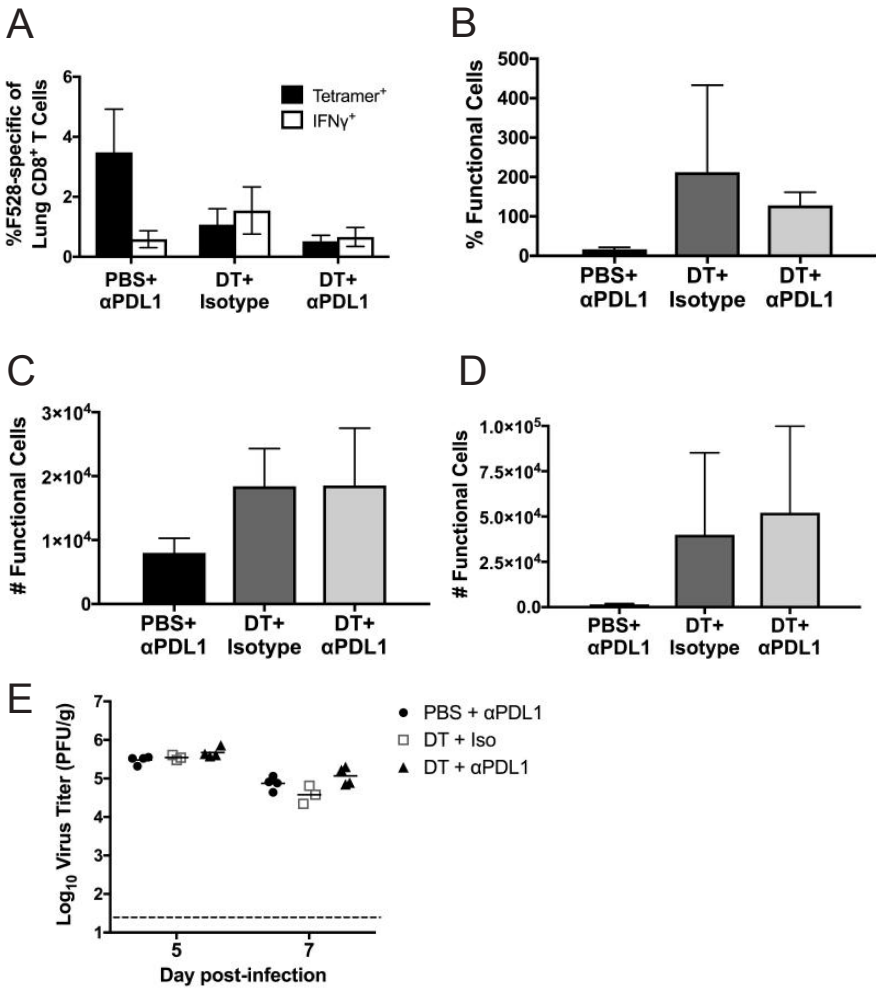

Figure 2-12. Treg depletion combined with PD-L1 blockade does not enhance CD8$^+$ T cell function more than Treg depletion alone. FoxP3^{DTR} mice were depleted of Tregs by injection of diphtheria toxin throughout infection and were given either blocking antibody against PD-L1 or an isotype control on the same days. Mice were infected with HMPV. The percentage (**A,B**) and absolute number (**C,D**) of the pulmonary CD8$^+$ T cell response was analyzed by flow cytometry at day 7. (**E**) Lungs were harvested at days 5 and 7 post-infection to quantify virus particles by plaque assay. N=3-4 mice/group.

Discussion

The results from these studies demonstrate the importance of timing for determining whether Tregs are detrimental or beneficial during respiratory virus infection. We found that a complete absence of Tregs during the entire course of HMPV infection led to enhanced CD8$^+$ T cell function and reduced peak virus titer; however,

the magnitude of the HMPV-specific $CD8^+$ T cell response was not increased. This observation led us to question whether the timing of Treg depletion could influence the $CD8^+$ T cell response. We found that Tregs were required early in infection for enhancing the $CD8^+$ T cell response through DC and $CD8^+$ T cell migration and that early depletion led to impaired virus clearance for both HMPV and influenza. In contrast, when Treg depletion was delayed until 2 days post-inoculation, the frequency of virus-specific $CD8^+$ cells was maintained, while the functionality of these cells was enhanced. Furthermore, late Treg depletion enhanced the clearance of influenza. However, despite their role in immune priming, we did not see that Treg depletion affected the $CD8^+$ T cell memory response. Additionally, Tregs and PD-1 blockade did not act synergistically to restore $CD8^+$ T cell function. These results suggest that Tregs play an important role in priming the immune response to respiratory virus infections, but they are dispensable and in some ways even detrimental after the immune response has already been initiated.

The findings from our studies contrast with results from other respiratory viruses. The closest human pathogen to HMPV is RSV. Previous studies that explored the role of Tregs in the immune response to RSV found that while Treg depletion led to a greater percentage of functional epitope-specific $CD8^+$ cells, virus clearance was delayed (165, 249, 254) or unchanged (181). In contrast, for HMPV, we saw that Treg depletion led to lower peak virus titer but unchanged virus clearance. These discordant findings could simply be due to the fact that even though these are both pneumoviruses, they are distinct viruses. In addition, RSV is often studied using BALB/c mice, while the experiments in this study were conducted using C57BL/6 mice. Most previous studies of

Tregs in RSV relied on αCD25 antibodies to deplete and block Tregs (165, 249, 254). However, in this study αCD25 treatment led to increased cytokine production and cytotoxic degranulation, with a trend towards reduced peak virus. It is possible that these differences using αCD25 antibodies can be explained by different dosing schedules. αCD25 may have targeted effector cells in those earlier studies, since effector $CD8^+$ and $CD4^+$ T cells can upregulate CD25 upon activation. If this was the case, then the reduced CD4/CD8 response could have delayed virus clearance in those previous reports. DT-mediated depletion of $FoxP3^+$ cells has become standard for Treg depletion studies. One RSV study using DEREG (168) mice, which also allow for DT-mediated Treg depletion, demonstrated lower viral titers with DT treatment, similar to our findings for HMPV infection (177).

This study primarily relied on $FoxP3^{DTR}$ mice to deplete Tregs. It is important to acknowledge the inherent limitation of DT-mediated depletion. While this method is regarded as the best technique currently available, off-target effects of DT are possible. DCs could non-specifically take up DT or could be affected by DT in the process of phagocytosing apoptotic Tregs. In the experiments in figure 6, we did not attempt to distinguish whether the observed reduced DC migration could be due to these nonspecific effects. Others have found that DT treatment of WT mice revealed nonspecific effects of DT (170); however, when we treated WT mice with DT, we did not see changes in $CD8^+$ T cell function or histopathology (data not shown).

Additionally, use of $FoxP3^{DTR}$ mice relies on the assumption that all Tregs express FoxP3. Since there was increased histopathology and weight loss in DT-treated $FoxP3^{DTR}$ mice regardless of whether they were infected with HMPV or not (Figure 3), it

is likely that a majority of Tregs were depleted by this method, though it is possible that some Tregs were not depleted if they had a transient reduction of FoxP3 expression.

It is also possible that some $FoxP3^+$ cells were not Tregs but were depleted with DT treatment. Some have found that effector T cells can transiently upregulate FoxP3, though we did not detect FoxP3 expression on $CD8^+$ T cells in this study (data not shown). Though we defined Tregs as $CD4^+$ FoxP3-expressing cells (and measured percentage and numbers of both $FoxP3^+$ and $FoxP3^+CD25^+$ cells) and measured expression of activation markers of these cells, we did not confirm their regulatory capacity with an *ex vivo* suppression assay.

Tregs of thymic origin (tTregs) are often primarily involved in preventing autoimmunity, while Tregs derived from a naïve $CD4^+$ cell (pTregs) are typically specific to exogenous antigen and therefore dampen the immune response to pathogens and other foreign insults (144-146). Some controversy exists over markers to discriminate thymically or peripherally derived Tregs; therefore, we used both Helios and neuropilin-1 to phenotype the Tregs responding to HMPV infection. Both of these markers have been suggested to have higher expression on tTregs, even if some tTregs or pTregs either do or do not express either of these molecules (271). In our experiments, we found that Tregs in the lungs of mice inoculated with HMPV had fewer $Helios^+$ cells compared to those from mock-infected mice, which suggests that more of the Tregs responding to HMPV might be peripherally derived. However, our results cannot definitively conclude whether the increased number of Tregs seen at days 4 and 6 in the lung are specifically due to maturation of naïve $CD4^+$ cells into pTregs.

When we measured the effect of early and late Treg depletion, we found that the absence of Tregs before inoculation reduced epitope-specific $CD8^+$ T cells in the lung tissue (Figures 2-5, 2-10). This reduction is consistent with earlier studies (165, 248, 249) that suggested that Tregs are important for priming $CD8^+$ T cells at the beginning of infection.

Our finding of delayed BMDC trafficking and reduced CCL21 levels in Treg-depleted mice is consistent with data from herpes simplex virus that showed that Tregs are necessary early in HSV infection for DC trafficking to lymph nodes (248). We show that this is also true for respiratory virus infection, and by pre-loading the BMDCs with antigen, we further find that DC trafficking is impaired regardless of antigen uptake efficiency.

Additionally, we found that $CD8^+$ T cell trafficking to the lung was impaired in mice that had been depleted of Tregs before infection. Even though Treg depletion led to reduced DC trafficking to the mediastinal lymph node, there was still a greater frequency of HMPV-specific $CD8^+$ T cells in the lymph node in Treg-depleted mice. This could have been due to an overall increased proliferative capacity of these cells in the absence of Tregs. However, these HMPV-specific cells were reduced both by frequency and number in the lung of Treg-depleted mice compared to PBS controls. Because the absolute number of these cells was lower in the lungs of Treg-depleted mice at day 4, it is unlikely that the difference in frequencies between the groups at this time point was simply due to overabundant proliferation of bulk $CD8^+$ T cells triggered by an absence of Tregs immediately before infection.

It is possible that the reduced HMPV-specific $CD8^+$ T cell numbers and frequencies could be due to decreased proliferation of these cells once they had migrated from the MLN to the lung, rather than due to strict deficiencies in migration. However, when we measured lung expression of a variety of chemokines that promote T cell migration, we found that Treg-depleted mice had significantly reduced levels of CXCL11, CCL4, CX3CL1, and IL-15, which supports a mechanism of a failure of virus-specific $CD8^+$ cells to traffic efficiently to the lung.

Of the chemokines measured, CXCL11 (also known as I-TAC (Interferon-inducible T-cell alpha chemoattractant)) had the greatest fold reduction in expression in Treg-depleted mice compared to PBS controls (Figure 2-6G,H). CXCL11 is related to CXCL9 and CXCL10, but has the highest affinity of the three for the CXCR3 receptor on activated T cells (258). CXCL11 is strongly induced by IFNγ (256), which was reduced in the lungs at day 5 of infection in the absence of Tregs (Figure 2-7A). Therefore, a potential mechanism for the observed reduction in virus-specific $CD8^+$ T cells at day 7 in the lung is that the absence of Tregs leads to reduced IFNγ in the lung early in infection, which causes reduced CXCL11 levels, and finally, deficient effector $CD8^+$ T cell migration to the infected lung.

Interestingly, when Tregs were depleted 2 days after influenza inoculation, there was a significant reduction in viral titer at day 7 post-inoculation compared to all other groups (Figure 2-10D). This accelerated virus clearance was unique to influenza, as at day 7 of HMPV infection, titers were equally low in the late and PBS groups (Figure 2-5F). This discrepancy may be attributable to differences in the kinetics of HMPV and

influenza clearance or differential roles of Tregs between the two infections and merits further investigation.

Early Treg depletion in both infections was associated with immunological skewing towards a type 2 biased response. It is unclear whether this type 2 skewing contributed to the reduction in virus-specific effector T cells during early Treg depletion or whether type 2 skewing also occurs in the population of virus-specific effector cells in the absence of Tregs. A future study could assess this by quantifying the ratio of IFNγ^+/IL-4$^+$ CD4$^+$ cells after stimulation with a pool of HMPV peptides representing CD4$^+$ epitopes; however, MHC-II epitopes have not yet been identified for HMPV.

Tregs constrain T_H2 cells more strongly than they do T_H1 or T_H17 cells in respiratory virus infection (181, 272, 273). There not only was skewing towards T_H2 CD4$^+$ cells following early Treg depletion, but there were also increased numbers and function of type 2 ILCs and an increased ratio of ILC2s to ILC1s in Treg-depleted mice (Figures 2-7, 2-10). This finding is consistent with other groups that demonstrated that Tregs suppress ILC2s (274, 275), but here we further demonstrate that Tregs also control the innate type 1 to type 2 ratio.

Overall, our findings and those from other groups indicate that Tregs exert tight control over both innate and adaptive type 2 responses in the lung, which is important when considering the pathogenic role of T_H2 and ILC2s in immune-mediated diseases such as asthma (276). Treg control of type 2 immunity is especially significant given the known association between infection by respiratory viruses such as HMPV or RSV and subsequent asthma (277). It would be worth investigating whether Treg numbers or function during respiratory infection in early life could have predictive value on the

predisposition to future allergic asthma and perhaps could be manipulated during infection in order to reduce this risk.

We have demonstrated that Tregs constrain the antiviral $CD8^+$ T cell response in HMPV infection, allowing higher virus titers while reducing immunopathology. Tregs are essential during the priming phase of respiratory virus infection, and depletion of these cells immediately before infection impedes immune cell migration and virus clearance. Interestingly, early Treg depletion skews both the innate and adaptive immune response towards a type 2 bias in viral respiratory infection.

Our findings and those of other groups emphasize the fine-tuning required to balance the antiviral immune response against harmful immunopathology. Moving the dial too far in either direction could lead to establishment of chronic infection or potentially severe reductions in lung function. Immunopathology is already a potential consequence of the increasing use of immunomodulatory drugs in diseases such as cancer. As immunomodulatory therapies such as PD-1 blockade are used more widely, off-target effects such as immune-related lung injury associated with common respiratory viruses could become more frequent. An understanding of the mechanisms regulating the lung immune response to viruses is essential to managing these therapeutic complications.

Materials and Methods

Mice and viruses

C57BL/6 and $FoxP3^{DTR}$ (Alexander Rudensky (167)) mice were purchased from The Jackson Laboratory. Animals were bred and maintained in specific pathogen free

conditions in accordance with the Institutional Animal Care and Use Committees of Vanderbilt University and University of Pittsburgh. 6-14 week-old age- and sex-matched mice were used in all experiments. HMPV (clinical strain TN/94-49, subtype A2) and influenza virus (strain HK/x31, H3N2) were grown and titered in LLC-MK2 or MDCK cells as previously described(138, 278). For all animal experiments, mice were anesthetized with ketamine-xylazine and intranasally inoculated with $1x10^6$-$5x10^6$ PFU HMPV or 50-100 PFU influenza x31, in a 100-μL volume. Mock-infected mice were inoculated with the same volume of UV-inactivated virus or mock cell lysate after we had determined that UV inactivated virus and cell lysate performed equally (data not shown). Viral titers were measured by plaque assay as previously described (278, 279). For bronchoalveolar lavage, mice were euthanized and lavaged twice with 1 ml cold PBS.

Flow cytometry

Pulmonary $CD8^+$ T cells were tetramer-stained as described previously (138). MHC class I tetramers for HMPV (H2-D^b/$F_{528–536}$ and H2-K^b/$N_{11–19}$) were generated as previously described (280). MHC class I tetramer for influenza (H2-D^b/$NP_{366-374}$) was obtained through the NIH Tetramer Core Facility. Lung Tregs were identified as viable (live/dead violet, Life Technologies), $CD4^+$ (clone RM4-5, eBioscience), $FoxP3^+$ (clone FJK-16s, eBioscience), +/- $CD25^+$ (clone PC61 or 3C7, Biolegend). Tregs were stained for PD-1 (clone RMP1-30), LAG-3 (clone C9B7W), GITR (clone YGITR 765), TGFβ (clone TW7-16B4) Helios (clone 22F6), all BioLegend, and Neuropilin-1 (clone 3DS304M, eBioscience), or with appropriate isotype control Abs (all BioLegend). (Cell

surface rather than intracellular TGFβ was measured, as reports have suggested that Treg suppression is mediated by cell surface-bound TFGβ rather than soluble TGFβ.(157, 158)) Cells were fixed and permeabilized with Foxp3/Transcription Factor Fixation/Permeabilization solution (eBioscience) before FoxP3 and Helios staining. Type 2 innate lymphoid cells (ILC2s) were stained for viability (live/dead violet, Life Technologies), CD45 (clone 30-F11), CD127 (clone A7R34), lineage cocktail (TER-119 (clone TER-119), CD45R/B220 (clone RA3-6B2), Ly-6G/Ly-6C (Gr-1) (clone RB6-8C5), CD3e (clone 145-2C11), CD11b (clone M1/70), CD4 (clone RM4-5), and FcεR1a (clone MAR-1)), CD90.2 (clone 30-H12), and ICOS (clone 15F9), all from BioLegend. ILC2 identity was validated by exposing sorted cells *ex vivo* to IL-2 and IL-33 and measuring production of IL-5 and IL-13 (Figure 2-8). ILC2s were also stained for ST2 (clone RMST2-2, eBioscience), CD25 (clone PC61, Biolegend), and KLRG-1 (clone 2F1/KLRG1, Biolegend). See figures 2-8 and 2-9 for ILC2 gating schematic. Flow cytometric data were collected using an LSRII or Fortessa cytometer (BD Biosciences) and analyzed with FlowJo software (FlowJo, LLC). MedFI refers to median fluorescence intensity, MFI refers to geometric mean fluorescence intensity.

Intracellular cytokine staining

Peptide restimulation and ICS for $CD8^+$ T cells were performed as previously described (138). For $CD4^+$ T cell and innate lymphoid cell ICS, lung cells were stimulated with PMA (50ng/ml) and ionomycin (1ug/ml) (Sigma) in the presence of 0.067% GolgiStop (BD) for 5 hours. After stimulation, cells were stained for viability (live/dead violet, Life Technologies) CD4 (clone RM4-5, eBioscience), IFNγ (clone

XMG1.2, BD), and IL-4 (clone 11B11, Biolegend), or ILC markers (for Fig 6F, pan-ILC markers CD45, CD127, Lineage, CD90; for all ILC2 ICS figures, pan-ILC markers plus ICOS)(see above for clones) and IL-5 (clone TRFK5, BD), IL-13 (clone eBio13A, eBioscience) and IFNγ (clone XMG1.2, BD).

In vivo Treg depletion

FoxP3^{DTR} mice were injected i.p. with 50 ng/kg diphtheria toxin (Sigma) in 200 µL PBS or with PBS alone for two days before inoculation and every other day thereafter, as previously described (167), or for the indicated days as described in figure legends.

In vivo antibody blockade

For CD25 depletion, C57BL/6 mice were injected i.p. with 500 µg in 200 µL PBS anti-CD25 mAb (clone PC61.5.3) or isotype control (clone HRPN) (both Bio X Cell) at days -3 and 0 of infection.

ILC2 Stimulation

ILC2s were stained with Live/Dead, CD45, Lineage markers, CD127, CD90, and ICOS (see above) and sorted using a BD FACSAria II. 2,500 sorted cells were plated in a total volume of 200 ul RPMI with 10% FBS in a round-bottom 96-well plate. ILC2s were stimulated with 10 ng/ml IL-2 and/or 10 ng/ml IL-33 (both PeproTech). After 5 days cell supernatant was collected and IL-5 and IL-13 were measured by ELISA according to manufacturer instructions (DY405 and DY413, R&D Systems).

Mediastinal lymph node harvest

At indicated time points post-inoculation, mediastinal lymph nodes were collected and placed into RPMI supplemented with 10% FBS (R10) on ice. All 3 nodes were analyzed when possible, but when only 2 were found, these were analyzed. Absolute numbers were not calculated due to the difference in numbers of lymph nodes collected between mice. A single-cell suspension was made by pushing the lymph nodes through a 70 μm nylon cell strainer (Falcon). Cells were washed with R10 and red blood cells were lysed (ACK lysing buffer, Gibco). Cells were then stained for flow cytometry. $CD8^+$ cells from mediastinal lymph nodes were stained for tetramers (see above) and CD69 (clone H1.2F3) (Biolegend).

Labeling and tracking of peptide-loaded BMDCs

Bone marrow derived dendritic cells (BMDCs) were generated as previously described (138). At day 7 of culture, BMDCs were matured overnight with 100 ng/ml LPS (Sigma-Aldrich) and 10 μM F528 HMPV peptide. The next day BMDCs were collected, counted, and resuspended in PBS. BMDCs were labeled as described (281) with some modifications. BMDCs were incubated in 8 μM CFSE (Molecular Probes) for 10 min at 37°C, then washed with RPMI supplemented with 10% FBS. BMDCs were allowed to rest for 1 hour at 37°C before $2x10^6$ BMDCs were intratracheally instilled into mice in a total volume of 50 μL. At various time points post-instillation, mediastinal lymph nodes were harvested and prepared for flow cytometry as above. Migratory BMDCs were identified as $CFSE^+$, $CD11c^+$ (clone N418, Biolegend).

Memory experiments

FoxP3^{DTR} mice were injected with diptheria toxin as described in figure legends, and intranasally infected with 1x10^6-5x10^6 PFU HMPV in a 100 µL volume. At day 6 post-infection, congenic donor CD45.1 mice were sacrificed and spleens were harvested to single cell population as previously described (Erickson JCI 2012). CD4+ cells were magnetically sorted by negative selection (Miltenyi). 1.5-2x10^6 naïve CD4$^+$ cells were injected intravenously. 30-35 days after primary infection mice were challenged again with 1x10^6-5x10^6 PFU HMPV intranasally and sacrificed 5-7 days post-challenge for analysis of the recall response.

Quantitative RT-PCR

Lung homogenate from the whole lung or total mediastinal lymph node homogenate was frozen at -80°C until use for qRT-PCR. RNA was extracted from the lung homogenate with the Ambion MagMAX-96 Viral Isolation Kit (ThermoFisher) on an Applied Biosystems MagMAX Express-96 Deep Well Magnetic Particle Processor (ThermoFisher) and stored at -80°C until further use. 5 µl of extracted RNA was used for qRT-PCR in 25 µl reaction mixtures on an ABI StepOnePlus Real-Time PCR System (ThermoFisher) using the AgPath-ID One-Step RT-PCR kit (ThermoFisher). TaqMan primers and probes were used according to the manufacturer's instructions (all ThermoFisher): IL-15 (Mm00434210_m1), CCL3/MIP-1a (Mm00441259_g1), CCL4/MIP-1b (Mm00443111_m1), CXCL9 (Mm00434946_m1), CXCL10 (Mm00445235_m1), CXCL11 (Mm00444662_m1), CCL8 (Mm01297183_m1), CCL5/RANTES (Mm01302427_m1), CX3CL1 (Mm00436454_m1), CCL21

(Mm03646971_gH). Cycling conditions were 50°C for 30 minutes, followed by an initial activation at 95°C for 10 minutes and 45 cycles of 15 seconds at 95°C, and 30 seconds at 60°C. All values were normalized to the housekeeping gene *Hprt*, and fold change in chemokine was measured in DT or Early groups compared to PBS groups using the ΔΔCt method.

Multiplex cytokine analysis

Lung homogenate from the whole lung (Day 5) or left lung (Day 7) was used for cytokine analysis by Bio-plex Mouse Cytokine 23-plex Assay (BioRad, Hercules, CA) according to manufacturer's instructions. The following cytokines and chemokines were measured: IL-1α, IL-1β, IL-2, IL-3, IL-4, IL-5, IL-6, IL-9, IL-10, IL-12p40, IL-12p70, IL-13, IL-17A, Eotaxin, G-CSF, GM-CSF, IFNγ, CXCL1, MCP-1, MIP-1α, MIP-1β, RANTES, TNFα. Observed concentrations were normalized to lung weight.

Histology

Either the left lobe or accessory lobe of the lung was inflated and fixed in formalin, then subsequently sectioned and stained with H&E or PAS. All fields of each H&E stained slide were scanned at 200x magnification and each field was scored as follows: 0: normal lung tissue; 1: >0 to 25% of tissue area with inflammation; 2: 25-50% of tissue area with inflammation; 3: 50-75% of tissue area with inflammation; 4: 75-100% of tissue area with inflammation (282). Scores were added for each slide and divided by total number of fields scored to calculate average score. Scale bars represent 50 um.

Statistical Analysis

Data analysis was performed using Prism v 6.0 (GraphPad Software). Comparisons between two groups were performed using an unpaired, two-tailed Student's t test, and significance is noted by asterisks (*). Comparisons between multiple groups were performed using a one-way ANOVA with Tukey's post-hoc test, and significance is noted by hash signs ($^{\#}$). Error bars on each graph represent SD unless otherwise noted. ** or $^{\#\#}$ denotes $p<0.01$, even when p values were calculated to be <0.001 or <0.0001

CHAPTER III

Genetic absence of PD-L1 does not restore $CD8^+$ T cell function during respiratory virus infection and delays virus clearance*

Introduction

A key mediator of T cell impairment is the action of inhibitory receptors, specifically PD-1 (138, 228, 233, 283), though others, including LAG-3, Tim-3, and 2B4 are also upregulated in respiratory virus infection and contribute to some degree of impairment (229, 237). PD-1 is induced on T cells following antigen exposure, whereas proinflammatory cytokines upregulate its ligands PD-L1 and PD-L2 (228, 232, 250, 284). PD-L1 is expressed or can be induced on most or all cells, while PD-L2 expression is restricted to antigen presenting cells (250, 285). In the lung and *in vitro*, respiratory virus infection leads to upregulation of PD-L1 on airway epithelial cells as well as dendritic cells (231-235, 237). PD-L1 is also highly expressed on alveolar macrophages at baseline (54).

One essential question in the field of T cell impairment is which PD-L1-expressing cells contribute the necessary "stop" signal to PD-1-expressing $CD8^+$ T cells? Work in LCMV infection and T cell exhaustion has suggested that, at least in chronic systemic infection, PD-L1 on hematopoietic cells reduces $CD8^+$ T cell function, while PD-L1 on somatic cells contributes to virus persistence (286). In cancer T cell

---

* This chapter contains unpublished data in preparation for submission. Rogers MC, Lamens KD, Tollefson ST, and Williams JV.

exhaustion, roles of PD-L1 on tumor cells and host immune cells have been hotly debated within the past year, and appear to vary in different cancers and different patients (287, 288).

However, the role of PD-L1 on different cell types in acute infections and in respiratory virus infections in particular has not been satisfactorily elucidated. *In vitro* and *in vivo* data have suggested that epithelial cells (228, 233) or DCs (231) are important for providing PD-L1 in respiratory virus infection; however, these relied on cell culture or antibodies that bind nonspecifically.

To address the role of PD-L1 on different cell types in $CD8^+$ T cell impairment, we used a genetic model of PD-L1 deficiency. Surprisingly, we found that PD-$L1^{-/-}$ mice challenged with HMPV or influenza showed a similar level of $CD8^+$ T cell impairment compared to WT counterparts, even though antibody blockade of PD-L1 has been shown to restore $CD8^+$ T cell function. Furthermore, virus clearance was delayed in PD-$L1^{-/-}$ mice compared to WT. The $CD8^+$ T cells from the impaired PD-L1-deficient mice expressed higher levels of inhibitory receptors both at baseline as well as after respiratory virus challenge. Antibody blockade of PD-L2 failed to restore function to the impaired cells, indicating that PD-L2 did not compensate for a lack of PD-L1. While reciprocal bone marrow chimeras between WT and PD-$L1^{-/-}$ mice did not restore $CD8^+$ T cell function after respiratory virus challenge, mice that received PD-$L1^{-/-}$ bone marrow had higher inhibitory receptor expression on $CD8^+$ cells. This discrepancy in inhibitory receptor expression suggests that cells of the hematopoietic compartment contribute to T cell impairment on $CD8^+$ T cells.

Results

PD-L1$^{-/-}$ mice have impaired T cell function and virus clearance

To test whether PD-L1$^{-/-}$ mice had improved T cell function after infection, we infected PD-L1$^{-/-}$ and WT mice with HMPV. Surprisingly, at both days 7 and 10 of infection, both PD-L1$^{-/-}$ and WT mice had similar a percentage of CD8^{+} T cells that were specific for the HMPV immunodominant epitope F528, and CD8^{+} T cells from PD-L1$^{-/-}$ or WT stimulated *ex vivo* had similar IFNγ production (**Figure 3-1A,B**). To determine the kinetics of HMPV clearance in these mice, lungs were harvested and virus was quantified by plaque assay after infection. HMPV replicated to higher peak titer in PD-L1$^{-/-}$ mice with delayed virus clearance compared to WT mice (**Figure 3-1C**). This result was contrary to previous findings of accelerated virus clearance with PD-L1 antibody blockade (138). To understand whether the increased impairment of PD-L1$^{-/-}$ mice was restricted to HMPV, mice were infected with murine adapted influenza PR8 both at high and low inoculum. Once again, virus-specific CD8^{+} T cells were similarly impaired between WT and PD-L1$^{-/-}$ mice (**Figure 3-2**). These data indicate that CD8^{+} T cells from PD-L1$^{-/-}$ mice are as impaired or even more impaired as those from WT mice, regardless of virus or viral load.

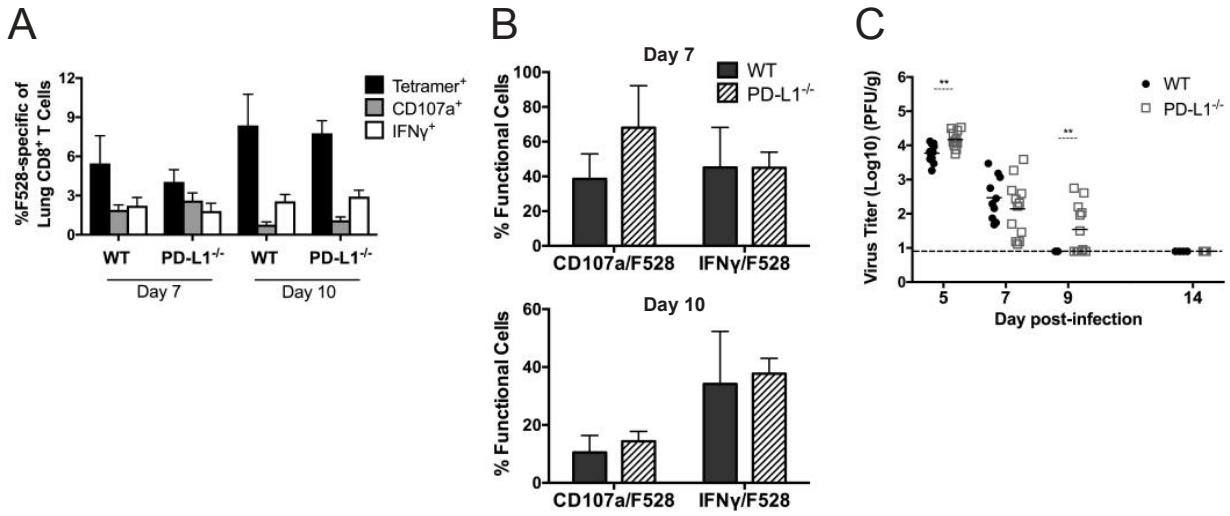

Figure 3-1. PD-L1$^{-/-}$ mice have an impaired CD8^{+} T cell response to HMPV infection. WT and PD-L1$^{-/-}$ mice were infected with 1x10^{6} PFU HMPV. Lung lymphocytes were harvested after infection and CD8^{+} T cells were analyzed by flow cytometry and intracellular cytokine staining. (**A**) Percentages of CD8^{+} T cells recognizing and producing cytokines in response to the immunodominant HMPV epitope F528 were quantified. (**B**) The percentage of functional F528-specific CD8^{+} T cells was calculated by dividing the percentage of tetramer^{+} into the percentage producing CD107a/IFNγ in response to peptide. (**C**) Virus titer was quantified from the lungs of WT and PD-L1$^{-/-}$ mice via plaque assay. N=5-7/group, combined from 2-3 independent experiments.

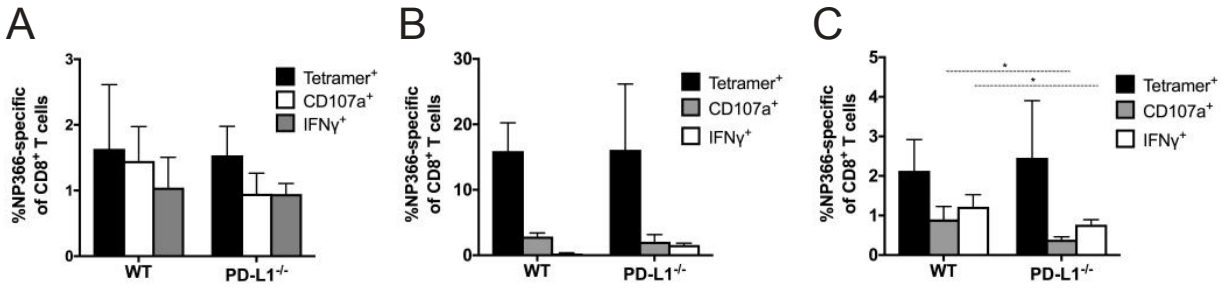

Figure 3-2. PD-L1$^{-/-}$ mice are impaired regardless of respiratory virus infection. WT and PD-L1$^{-/-}$ mice were infected with 50 (**A,B**) or 5 (**C**) PFU influenza PR8. Virus-specific CD8^{+} T cells were quantified and analyzed for function at day 7 (A,C) or day 10 (B) post-infection. *p<0.05, Student's t test. N=4-5/group, representative of 2 experiments.

PD-L1$^{-/-}$ mice upregulate multiple inhibitory receptors

Because PD-L1$^{-/-}$ mice had impaired T cell function and delayed virus clearance in the absence of PD-L1/PD-1 signaling, we hypothesized that other inhibitory receptors might compensate for a lack of signaling through PD-1. To test this, we measured expression of PD-1, LAG-3, Tim-3, and 2B4 in PD-L1$^{-/-}$ and WT mice. CD8^{+} T cells in naïve PD-L1$^{-/-}$ mice had inhibitory receptor expression that was at least twice that of CD8^{+} T cells in WT mice, and had higher expression per cell (**Figure 3-3A**). After HMPV infection, inhibitory receptor expression on bulk CD8^{+} T cells increased for both WT and PD-L1$^{-/-}$ mice, but remained significantly higher in knockout mice (**Figure 3-3B,C**). In contrast, inhibitory receptor expression on CD8^{+} T cells specific for the HMPV immunodominant epitope F528 was similar between WT and knockout mice (**Figure 3-3D,E**). These data suggest that increased inhibitory receptor expression could explain the predisposition for T cell impairment in PD-L1$^{-/-}$ mice.

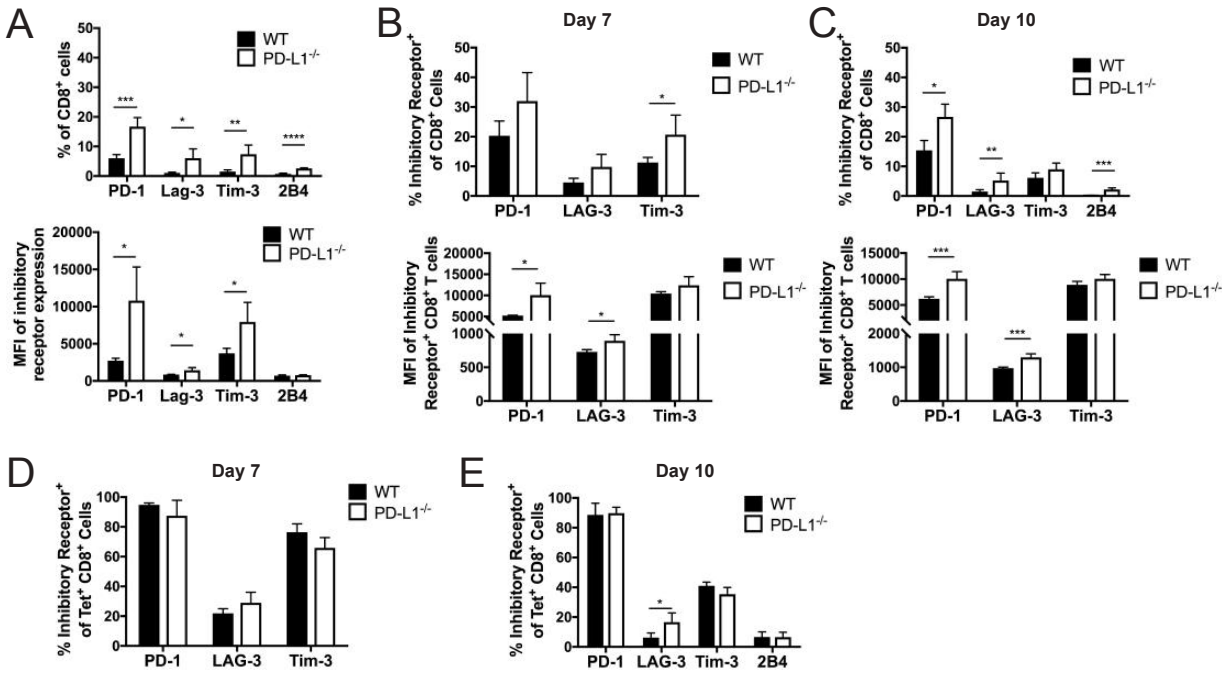

Figure 3-3. PD-L1$^{-/-}$ mice upregulate inhibitory receptors at baseline and during infection. (**A**) Expression of inhibitory receptors PD-1, Tim-3, LAG-3, and 2B4 on CD8^{+} T cells from naïve WT and PD-L1$^{-/-}$ mice and mean fluorescence intensity of inhibitory receptor expression. Inhibitory receptor expression and mean fluorescence intensity were measured on bulk CD8^{+} T cells at days 7 (**B**) and 10 (**C**) of HMPV infection in WT and PD-L1$^{-/-}$ mice. Inhibitory receptor expression was measured on F528-specific CD8^{+} T cells at day 7 (**D**) and 10 (**E**) of HMPV infection. *p<0.05, **p<0.01, ***p<0.001, ****p<0.0001, Student's t test. N=4-5/group, representative of 2 experiments.

Antibody blockade of PD-L2 does not restore T cell function in PD-L1$^{-/-}$ mice

Thus far, two ligands for PD-1 have been identified; PD-L1 is expressed on many cell types, while PD-L2 is restricted to antigen presenting cells (250, 285). PD-L2 has a higher affinity for PD-1, but PD-L2 signals tend to be significant only with high PD-L2 expression (289). In respiratory virus infection, signaling through PD-1 appears to occur predominantly through PD-L1, as antibody blockade of PD-L2 in WT mice has limited effect on CD8^{+} T cell function and combined PD-L1/PD-L2 blockade results in similar function as PD-L1 blockade alone (237). We hypothesized that in the genetic absence

of PD-L1, PD-L2 might compensate and explain the phenotype of impaired PD-L1$^{-/-}$ mice in Figure 3-1. To address this, we quantified expression of PD-L2 on pulmonary dendritic cells in WT and PD-L1$^{-/-}$ mice and found that, contrary to our hypothesis, PD-L2 was expressed on fewer CD11c^{+} MHCII^{+} DCs in PD-L1$^{-/-}$ mice during infection (**Figure 3-4A**). However, even lower levels of PD-L2 might provide effective inhibitory signaling in PD-L1$^{-/-}$ mice, especially considering the abundance of the PD-1 receptor on CD8^{+} T cells (Figure 3-3). To test whether PD-L2 compensated for the lack of PD-L1 in these mice, we performed antibody blockade of PD-L2 in WT and PD-L1 mice before and during the course of HMPV infection. We found that even in the absence of PD-L2 signaling, pulmonary CTLs in PD-L1$^{-/-}$ mice remained as impaired as those from WT mice (**Figure 3-4B-D**). These data indicate that compensation by PD-L2 is not responsible for the impaired CD8^{+} T cells in respiratory virus infection.

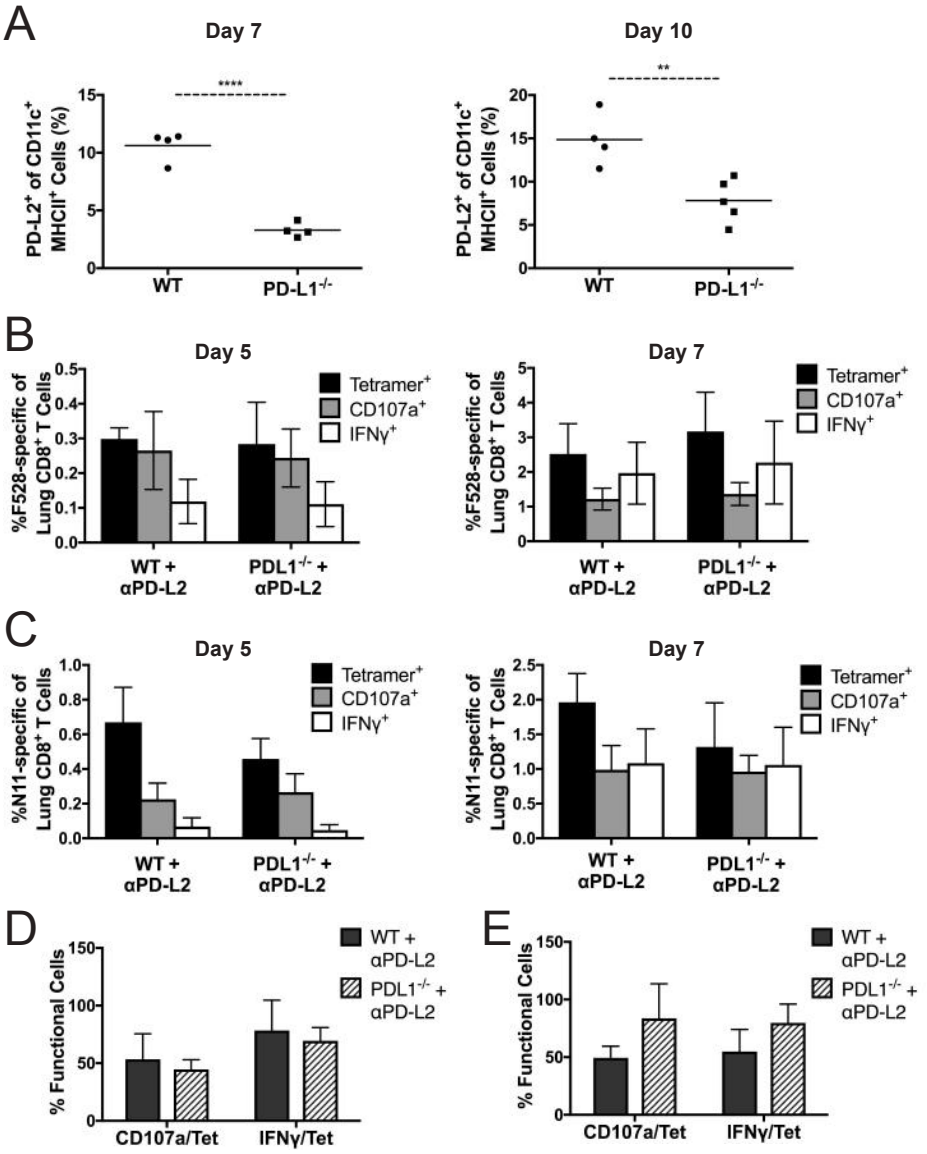

Figure 3-4. PD-L2 does not compensate for PD-L1 in PD-L1$^{-/-}$ mice. WT and PD-L1$^{-/-}$ mice were infected with HMPV. (**A**) At days 7 and 10 post-inoculation, PD-L2 was measured on CD11c^{+} MHCII^{+} dendritic cells by flow cytometry. (**B,C**) WT and PD-L1$^{-/-}$ mice were injected with anti-PD-L2 antibody at days -2, -1, and every other day thereafter during infection. Mice were infected with HMPV and CD8^{+} T cell functionality was analyzed on F528- and N11-specific cells by flow cytometry at days 5 and 7 of infection. Percent functionality of F528-specific (**D**) and N11-specific (**E**) CD8^{+} T cells was quantified at day 7 of infection. **p<0.05, ****p<0.0001, Student's t test. N=4-5 per group.

Bone marrow chimeras of WT/PD-L1$^{-/-}$ mice have equal T cell function, but hematopoietic PD-L1 appears to limit inhibitory receptor expression

Previous studies of LCMV infection showed that PD-L1 had a compartment-specific effect on CTL function and virus clearance (286). However, since LCMV is a systemic infection, we sought to determine whether PD-L1 has a differential role in the hematopoietic and somatic compartments of the lung during HMPV infection. We generated reciprocal bone marrow chimeras between WT and PD-L1$^{-/-}$ mice and infected these with HMPV. We found that CTLs from each group had equivalent functionality by percentage and absolute number (**Figure 3-5A,B**). Virus titers were not statistically significant between groups (**Figure 3-5C**). Interestingly, inhibitory receptor expression was highest on mice that had PD-L1$^{-/-}$ hematopoietic cells (either PD-L1/PD-L1 or WT/PD-L1), which may indicate an importance of the hematopoietic lineage for controlling inhibitory receptor expression (**Figure 3-5D**). Considering the somewhat contradictory prior reports that either DCs or epithelial cells are essential for contributing PD-L1 to T cell impairment (228, 231, 233), it is possible that both cell types are essential, at least in HMPV infection.

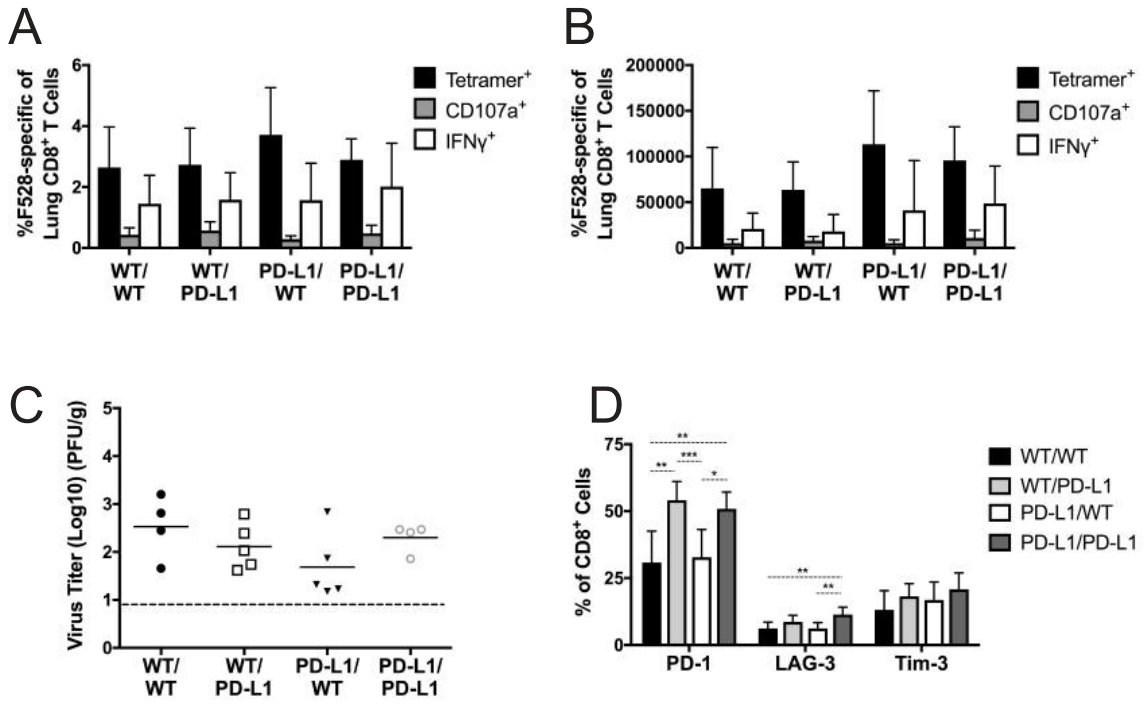

Figure 3-5. WT/PD-L1 reciprocal bone marrow chimeras do not have more functional CD8$^+$ T cells in response to HMPV infection. Bone marrow chimeras were generated by lethally irradiating WT and PD-L1$^{-/-}$ mice and transplanting 2x10^6 donor bone marrow cells 24 hours later. Bone marrow was allowed 8 weeks to reconstitute before infection. Mice were infected with HMPV, and the percentage (**A**) and absolute number (**B**) of F528-specific CD8$^+$ T cells were analyzed by flow cytometry. Virus titers were quantified via plaque assay at day 5 of infection (**C**) and inhibitory receptor expression was analyzed at day 7 of infection (**D**). X-axes and figure legends indicate somatic/hematopoietic genotype (e.g. WT/PDL1 = WT somatic cells and PD-L1$^{-/-}$ hematopoietic cells). *p<0.05, **p<0.01, ***p<0.001, One-way ANOVA with Tukey post-hoc test. N=4-5/group, representative of 2-4 experiments.

Discussion

In this study, we sought to elucidate the role of PD-L1 on different cell types by using a genetic PD-L1 knockout. Despite the fact that PD-L1 blockade or PD-1 knockout restores CD8$^+$ T cell function (138, 228, 283), we were surprised to find that genetic deficiency of PD-L1 still led to functional impairment of CD8$^+$ T cells, and further, resulted in delayed clearance of human metapneumovirus. Considering this level of impairment in PD-L1$^{-/-}$ mice, it is perhaps not surprising that bone marrow chimeras

between WT and PD-L1$^{-/-}$ mice did not show a change in CD8^{+} T cell function. However, the finding of increased inhibitory receptor expression in mice that had PD-L1 deficiency specifically in the hematopoietic lineage indicates that hematopoietic expression of PD-L1 is important for limiting the expression of PD-1 and other inhibitory receptors. Moreover, the higher inhibitory receptor expression on lung CD8+ T cells in PD-L1$^{-/-}$ mice both at baseline and during infection suggests that the lung environment favors T cell impairment.

It is notable that absence of PD-1 in respiratory virus infection leads to restored function (138) while absence of PD-L1, with or without PD-L2 signaling, does not restore T cell function. However, there is evidence that PD-1$^{-/-}$ and PD-L1$^{-/-}$ mice are fundamentally different. PD-1$^{-/-}$ mice eventually develop a lupus-like autoimmune response later in life (290). In contrast, PD-L1$^{-/-}$ mice have no apparent autoimmune phenotype (291), although one strain of PD-L1$^{-/-}$ mice may be more susceptible to experimental encephalitis (292). PD-1$^{-/-}$ mice are able to clear tumors that PD-L1$^{-/-}$ or PD-L1/L2$^{-/-}$ mice fail to clear (293). Systematic review of PD-1 and PD-L1 inhibitors in lung cancer found that PD-1 inhibitors had a slightly but significantly increased risk of pneumonitis and other autoimmune side effects compared to PD-L1 inhibitors (294, 295).

Several explanations are possible for the discordant phenotypes between PD-L1$^{-/-}$ and PD-1$^{-/-}$ mice. First, PD-L1, but not PD-L2, interacts in a bidirectional manner with the costimulatory molecule B7-1 (also known as CD80) (296). In canonical costimulatory APC-T cell signaling, B7-1 and B7-2 (CD86) on APCs bind to CD28 on T cells to enhance signaling through the T cell receptor (297). One mechanism of

downregulating this costimulation is that the coinhibitory receptor CTLA-4 competes with CD28 for binding to B7-1 and B7-2 (297). PD-L1 acts as an additional competitive inhibitory ligand for B7-1 but not B7-2 (296). An elegant model using an antibody that specifically blocked the interaction of PD-L1 with B7-1 but not PD-1 showed that PD-L1/B7-1 interactions are important for T cell tolerance, indicating that general PD-L1 antibody blockade may work through the interaction of PD-L1 with both B7-1 and PD-1 (298). If PD-L1/B7-1 interactions are important in immune system development, then the absence of these could account for the inhibitory receptor skewing and $CD8^+$ T cell impairment in PD-$L1^{-/-}$ mice.

Another explanation is the possibility of a third ligand for PD-1, which has been proposed by others (299). However, considering the extensive active research on PD-1, it seems unlikely that a third PD-1 ligand would not have been discovered in the almost 20 years since the discoveries of PD-L1 and PD-L2 (207, 208, 300, 301).

It is generally thought that PD-1 signaling requires ligation (302). However, some studies have suggested ligand-independent activity of PD-1 (303). Ligand-independent signaling has been identified for some receptors, including the B cell receptor (304) and EGFR (305). Ligand-independent signaling through these receptors activates different signaling pathways than ligand-dependent activation (304, 305), and if ligand-independent PD-1 signaling occurs, this has not been recognized in models where the measured output is the same signaling cascade that is activated by PD-1/PD-L interactions. A baseline level of “tonic” PD-1 signaling on tumor infiltrating lymphocytes (TILs) in the absence of ligation with PD-L1 or PD-L2 was reported (303). However, this study assumed that TILs did not express PD-L1; in contrast, baseline and inducible PD-

L1 expression on T cells has been reported (250) and even low ligand expression can provide the necessary signal through a receptor. To fully understand whether signaling through PD-1 is possible on CD8 T cells independently of ligantion, gene expression profiling of PD-L1$^{-/-}$ cells or PD-L1$^{fl/fl}$-CD8^{cre} cells after overexpression of PD-1 could be performed.

Finally, though some have suggested that the short cytoplasmic domain of PD-L1 indicates that reverse signaling is not possible (306), there is some evidence that PD-1/PD-L1 signaling may be bidirectional. (Though it should be mentioned that a significant body of work from the Pease lab that supported signaling through PD-L1 has since been retracted.) As mentioned above, PD-L1 and B7-1 appear to signal in a bidirectional manner (296), which would suggest that PD-L1 and PD-1 are capable of a similar interaction. In vitro, a PD-1-Ig fusion protein bound to PD-L1 on macrophages and activated an anti-inflammatory phenotype, characterized by increased IL-10 and decreased IL-6 production (307). Perhaps a bidirectional role of PD-L1 signaling is important for immune system development, which is altered in genetic depletion of PD-L1.

In this study, we used mice developed by the Chen lab, who described a putative costimulatory role for PD-L1 (291). In contrast, the PD-L1$^{-/-}$ mouse from the Sharpe lab did not reveal a costimulatory phenotype (292). We also characterized the PD-L1$^{-/-}$ mouse from the Sharpe lab and CD8^{+} T cells were impaired in response to respiratory virus infection in these mice as well (data not shown).

It is possible that the delayed virus clearance in PD-L1$^{-/-}$ mice was due to inefficient activity of a cell type other than CD8^{+} T cells. For example, CD4^{+} Th cells

could have a role in T cell impairment. $CD4^+$ epitopes tend to be in very low abundance in infected mice and have not yet been mapped for HMPV; nevertheless, it would be interesting to measure the function and contribution of virus-specific CD4+ T cells to T cell impairment in the presence or absence of PD-L1.

Future experiments to better understand the role of PD-L1 in respiratory virus infection will help elucidate the mechanism of PD-1-mediated T cell impairment. Considering that we saw increased expression of other inhibitory receptors in the absence of PD-L1, it would be interesting to block one or more inhibitory receptors, either *in vivo* or in an *ex vivo* ELISPOT assay, which has previously been utilized to understand the role of various inhibitory receptors in WT mice (237). More inhibitory receptors continue to be evaluated for a role in chronic infections (223); it would be worth understanding whether other receptors such as TIGIT or VISTA also play a role in T cell impairment.

T cell impairment mediated by inhibitory receptors continues to be an incompletely understood feature of respiratory virus infections. A more complete picture of how impairment proceeds and what steps in this process can be manipulated will provide important information of how the immune system specifically generates impaired T cells in lung infection but not other acute infections and may reveal potential strategies for manipulating this response in both therapeutics and vaccination.

Materials and Methods

Mice and Viruses

C57BL/6 mice were purchased from The Jackson Laboratories. PD-L1$^{-/-}$ (aka B7-H1$^{-/-}$) mice were obtained with permission from Liepeng Chen (291). Animals were bred and maintained in specific pathogen free conditions in accordance with the Institutional Animal Care and Use Committees of Vanderbilt University and University of Pittsburgh. 6-14 week-old age- and sex-matched mice were used in all experiments. HMPV (clinical strain TN/94-49, subtype A2) was grown and titered in LLC-MK2 cells (previously described (278). Influenza virus strain A/34/PR/8 (PR8; H1N1; ATCC) was grown in MDCK cells and titered in LLC-MK2 cells as described (138). For all animal experiments, mice were anesthetized with ketamine-xylazine and intranasally infected with $1x10^6$-$5x10^6$ PFU HMPV, or 10-50 PFU PR8, in a 100 uL volume.

Surface and tetramer staining

Lung and mediastinal lymph node lymphocytes were surface stained with tetramers as described previously (138, 308). MHC Class I tetramers for HMPV (H2-D^b/$F_{528–536}$ and H2-K^b/$N_{11–19}$) and for influenza (H2-D^b/$NP_{366–374}$) were generated as previously described (138, 280). Lung cells were stained for PD-1 (clone RMP1-30), TIM-3 (clone RMT3-23), LAG-3 (clone C9B7W), and 2B4 (clone m2B4 (B6) 458.1) or with appropriate isotype control Abs (all from BioLegend). Flow cytometric data were collected using an LSRII (BD Biosciences) and analyzed with FlowJo software (Tree Star).

Peptide restimulation and intracellular cytokine staining

Peptide restimulation and intracellular cytokine staining were performed as previously described (138).

Virus titration

Viral titers were measured by plaque assay as previously described (278).

In vivo antibody blockade

Mice were injected i.p. with 200 ug in 200 uL PBS with either anti–mouse PD-L2 (Bio X Cell, clone TY-25) or isotype control antibody for two days before infection and every other day thereafter.

Bone marrow chimeras

6-week-old WT and PD-L1$^{-/-}$ mice were irradiated with a total of 10 Gy (5 Gy 4 hours apart) to deplete bone marrow, either in a Cs_{137} irradiator or an x-ray irradiator. WT and PD-L1$^{-/-}$ bone marrow was obtained from femurs and tibiae of donor mice, lysed of erythrocytes, and resuspended to 2x10^6 cells/ml in PBS. Recipient mice were anesthetized with isofluorane and 2x10^6 bone marrow cells were injected retroorbitally 20-24 hours after irradiation. Mice were kept in sterile housing and given sulfamethoxazole/trimethoprim in their drinking water for 2 weeks post-transplant. Bone marrow was allowed to reconstitute for 8 weeks before experiments were performed.

Statistical analysis

Data analysis was performed using Prism v 6.0 (GraphPad Software). Comparisons between two groups were performed using an unpaired, two-tailed Student's T test. Comparisons between multiple groups were performed using a one-way ANOVA with a Bonferroni posttest. Error bars on each graph represent SD unless otherwise noted.

CHAPTER IV

STAT2 limits host species specificity of human metapneumovirus*

Introduction

It is essential to better understand the virus and host factors that are involved in promoting and restricting HMPV infection. The innate immune system is a first line of defense against microbial infection, and therefore many viruses encode at least one protein that interferes in some way with innate immunity in host cells (59). Pneumoviruses and parmamyxoviruses antagonize the host interferon signaling, specifically STAT1 and/or STAT2, in the course of natural infection (35, 60).

Despite being related to RSV and paramyxoviruses, none of the 9 virally encoded HMPV proteins have homology with pneumovirus or paramyxovirus inhibitors of STAT1 or STAT2 (26). In spite of this, HMPV inhibits phosphorylation of STAT1 in cell lines and primary human epithelial cells (65). Others found no inhibition of STAT2 by HMPV; however, these experiments used a relatively low multiplicity of infection (MOI) in cell culture (65).

In order to study HMPV infection *in vivo*, mouse models have been developed, most commonly using C57BL/6 mice. However, mice are only semi-permissive for HMPV: an inoculum of 10^5 or higher, depending on the HMPV strain, is required for productive *in vivo* infection ((278) and unpublished observations). Additionally, clinical

* This chapter contains unpublished data in preparation for submission. Rogers MC, Miranda-Katz M, Xu J, and Williams JV. 2018.

features of murine infection with HMPV do not adequately mimic human disease (309); how much of this is due to differences in mouse physiology, and how much is due to differences in the virus' ability to antagonize the human vs. mouse immune system, is unclear.

Studies of RSV, hPIV2, and hPIV5 have revealed that the murine version of STAT2 restricts these human viruses (82, 119). We hypothesized that HMPV is similarly restricted in a species-specific manner. We found that HMPV titers are significantly higher in $STAT2^{-/-}$ mice compared to WT, and that HMPV could be serially passaged *in vivo* in $STAT1^{-/-}$ and $STAT2^{-/-}$ mice. This led us to hypothesize that HMPV's capacity to antagonize STAT signaling may be limited to primates. Since STAT1 is so highly conserved, we further wondered whether HMPV antagonizes hSTAT2, and if species differences in STAT2 could drive host restriction of HMPV.

We found that HMPV was able to antagonize expression, phosphorylation, and nuclear localization of both STAT1 and STAT2 in primate cells, while murine cells maintained the capacity to upregulate and phosphorylate both molecules. STAT1 and STAT2 inhibition occurred independently, suggesting HMPV does not specifically antagonize the STAT1/STAT2 heterodimer. Transfection of U6A cells, which lack STAT2, with hSTAT2 or mSTAT2 revealed that suppression of both STAT1 and STAT2 were prevented by mSTAT2. In contrast, transfection of hSTAT2 into murine cells enabled inhibition of STAT1 and STAT2 by HMPV. These data show that HMPV fails to inhibit both STAT1 and STAT2 in the presence of murine STAT2 and suggest that HMPV antagonizes STAT2 to promote infection in humans.

Results

Serial passage of HMPV in STAT1$^{-/-}$ and STAT2$^{-/-}$ mice

Some respiratory viruses, including influenza, SARS-CoV, and MERS-CoV, have been serially passaged in mice to generate mouse adapted virus strains. These mouse-adapted viruses have provided important tools for studying viral and host determinants of disease and tropism (310-314).

We sought to generate mouse-adapted HMPV. However, viral titers in lung homogenate of infected C57BL/6 mice were not sufficiently high to productively infect a recipient mouse (data not shown). Attempts to passage in Rag-2$^{-/-}$ and IFNAR$^{-/-}$ mice were also unsuccessful (data not shown). However, HMPV titers are significantly higher in IFNAR$^{-/-}$ mice (54), indicating that type 1 interferon signaling restricts HMPV in mice *in vivo*. We therefore inoculated STAT1$^{-/-}$ and STAT2$^{-/-}$ mice with HMPV strain TN/94-49 and found that the virus grew to significantly higher titer in STAT2$^{-/-}$ mice compared to STAT1$^{-/-}$ or WT mice (**Figure 4-1A**). We subsequently inoculated STAT1$^{-/-}$ and STAT2$^{-/-}$ mice with HMPV (strains C1-718 and TN/94-49, respectively) and found that HMPV could be serially passaged in these strains.

With each passage, weight loss increased (data not shown). Additionally, over subsequent passages of C1-718 in STAT1$^{-/-}$ mice, cytokines measured from lung homogenates transitioned from a type 2 to type 1 phenotype (**Figure 4-1B**). Over serial passage of TN/94-49 in STAT2$^{-/-}$ mice, type 1 cytokines and chemoattractants increased (**Figure 4-1C**). These data show that serial passage of HMPV is restricted by STAT1 or STAT2 *in vivo*, indicating that either or both of these proteins or the IFN signaling pathway in general is a barrier to mouse adaptation by HMPV.

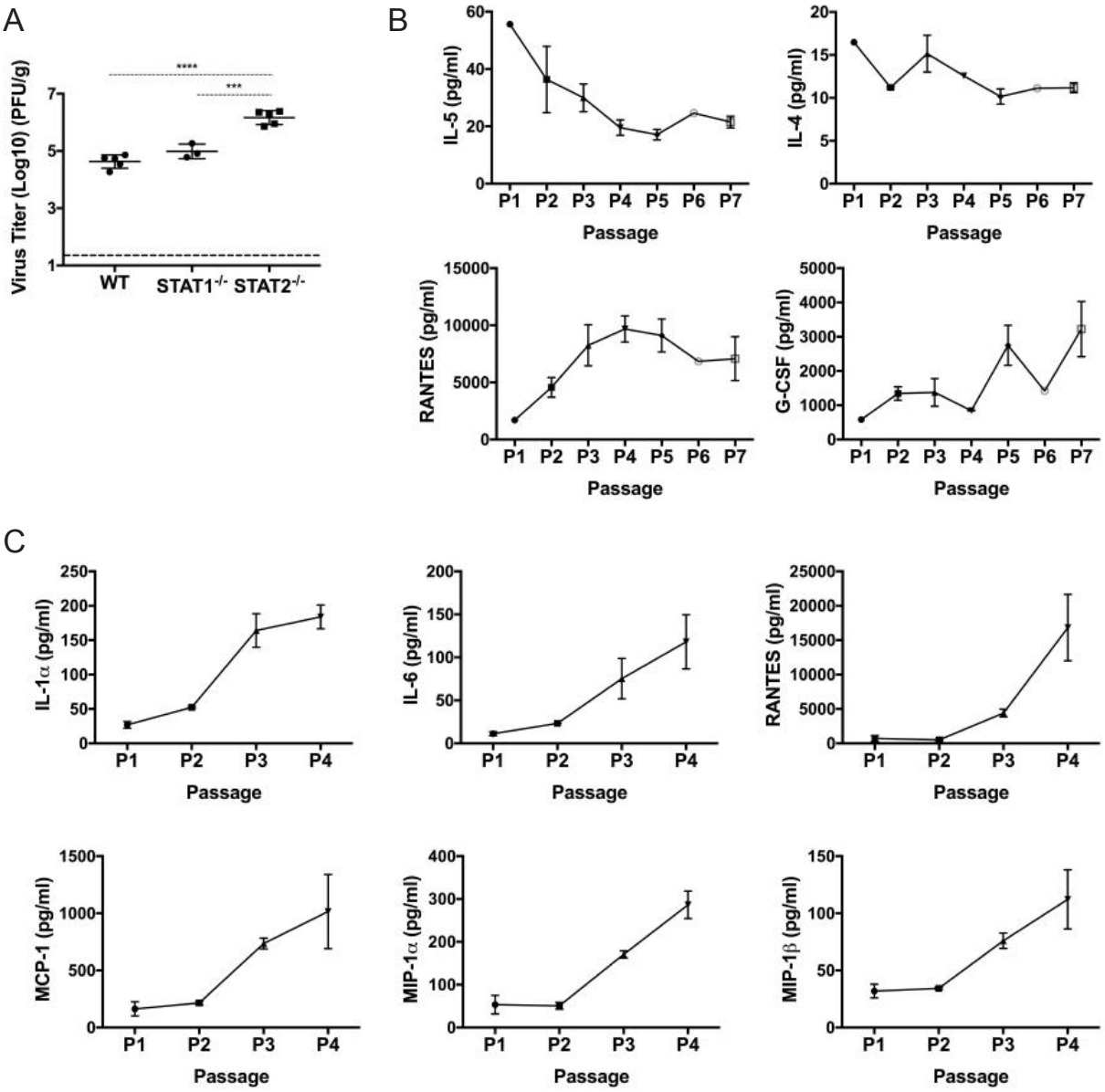

Figure 4-1. Serial passage of HMPV in STAT1$^{-/-}$ and STAT2$^{-/-}$ mice. (**A**) Mice were infected with HMPV TN/94-49 and euthanized at day 5 of infection. Lung virus titers were determined by plaque assay. (**B**) HMPV C1-718 was serially passaged in STAT1$^{-/-}$ mice, and cytokines were measured in lung homogenate at each passage at day 5 post-inoculation. (**C**) HMPV TN/94-49 was serially passaged in STAT2$^{-/-}$ mice, and cytokines were measured from lung homogenate at each passage at day 5. ***p<0.001, ****p<0.0001, One-way ANOVA with Tukey post-hoc test. N=2-5/group.

HMPV infection prohibits nuclear translocation of STAT1 and STAT2 in human cells

Since we found that STAT1 and STAT2 appeared to be important in restricting HMPV infection of mice, we next explored how HMPV infection affects STAT1 and STAT2 in humans. Previously, it had been shown by us and others that HMPV can specifically inhibit STAT1 phosphorylation and expression (65, 69). We used a human bronchoepithelial cell line, BEAS2b, to perform imaging studies of STAT1 and STAT2 in the presence or absence of HMPV. After infection with HMPV for 24 hours, BEAS2b cells were treated with IFN to induce phosphorylation and nuclear translocation of STAT1 and STAT2. After treatment with IFN, STAT1 and STAT2 translocated to the nucleus in mock-infected cells, whereas nuclear import was inhibited in HMPV-infected cells (**Figure 4-2**). These data indicate that HMPV infection inhibits nuclear translocation of the STAT1/2 heterodimer *in vitro*, indicating that antagonism of STAT1/2 may be a key step to promote HMPV infection.

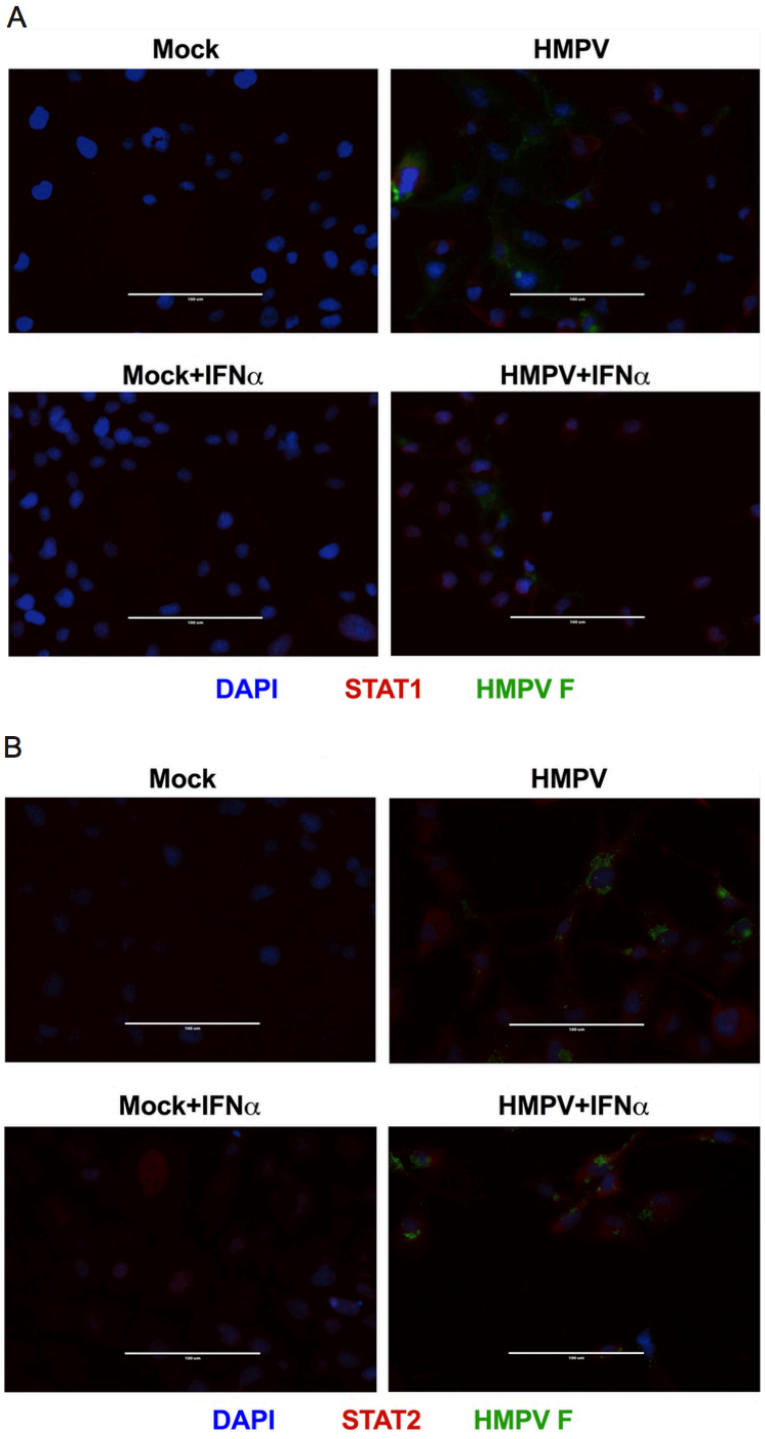

Figure 4-2. Nuclear localization of STAT1 and STAT2 is inhibited by HMPV. Human BEAS2b cells were infected with HMPV or mock for 20 hours, and treated with IFN for 40 min. After IFN treatment, cells were fixed and stained for immunofluorescence. (**A**) HMPV infection inhibits nuclear translocation of STAT1. (**B**) STAT2 nuclear localization is impaired during HMPV infection.

HMPV antagonizes STAT1 and STAT2 in primate but not murine cells

We were interested in the fact that HMPV grew to significantly higher titer in STAT2$^{-/-}$ mice than in either WT or STAT1$^{-/-}$ mice and that STAT1$^{-/-}$ and STAT2$^{-/-}$ mice were permissive for serial HMPV passage. We hypothesized that HMPV inhibits STAT1 and STAT2 in primate cells but fails to inhibit these in murine cells. To test this hypothesis, we infected both primate and murine cell lines with HMPV and measured expression as well as phosphorylation of STAT1 and STAT2 after IFN treatment. We found that HMPV infection of VeroE6 cells (primate cells that cannot produce IFN) led to reduced phosphorylation of both STAT1 and STAT2 and decreased expression of STAT1. In contrast, when murine cell lines CMT64/61 (C57BL/6 lung adenocarcinoma) and NIH/3T3 (murine fibroblast, deficient in some steps of IFN signaling (315)) were infected with HMPV, STAT1 and STAT2 expression and phosphorylation increased (**Figure 3-3**). These data indicate that HMPV is able to antagonize STAT1 and STAT2 in human/primate cells but fails to achieve this inhibition when introduced to murine cells.

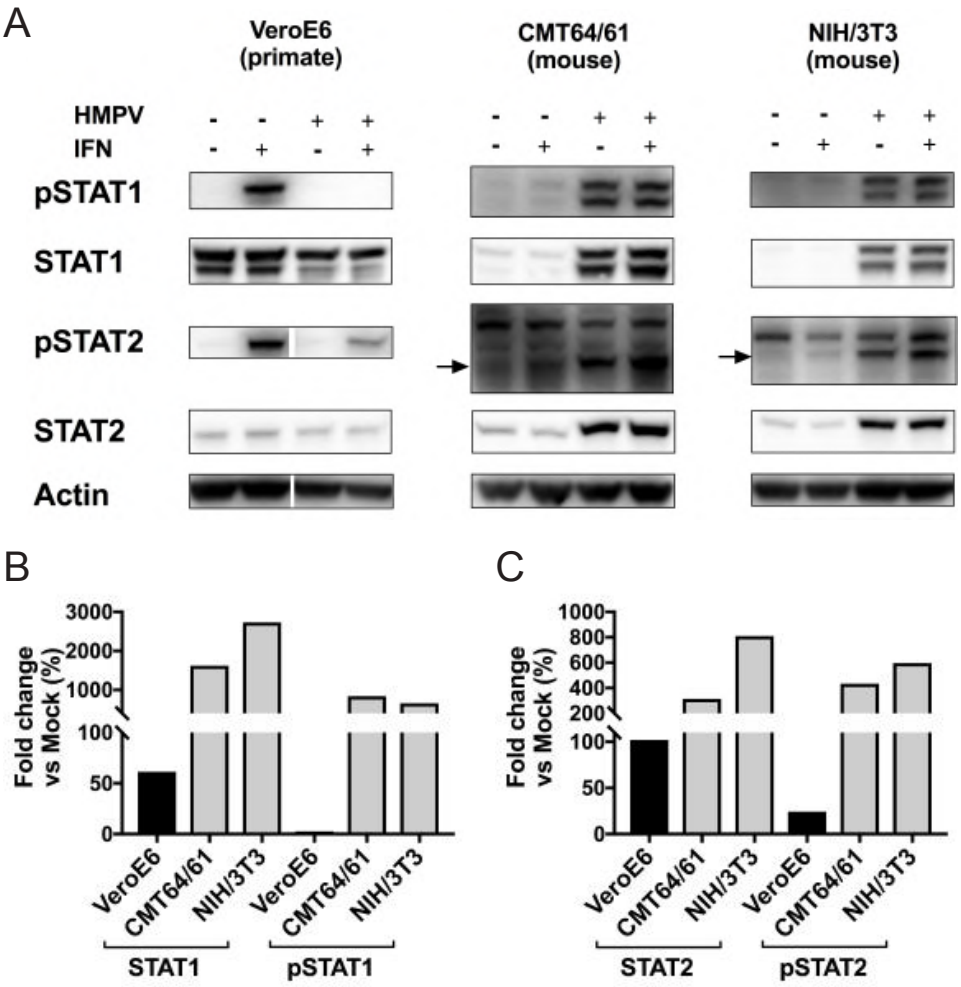

Figure 4-3. HMPV reduces STAT1 and STAT2 activation in primate cells, but not murine cells. (**A**) VeroE6 (primate), CMT64/61 (murine), and NIH3T3 (murine) cells were infected with HMPV for 24 hours, then treated with IFN for 30 minutes before cells were lysed for western blotting against total and phosphorylated STAT1 and STAT2. (**B**) Quantification of STAT1 and pSTAT1 signals compared to mock-infected wells. (**C**) Quantification of STAT2 and pSTAT2 compared to mock-infected wells.

HMPV inhibition of STAT1 or STAT2 occurs independently of the other

Studies of hPIV2 and hPIV5 showed that degradation of STAT2 or STAT1, respectively, required the expression of both STAT1 and STAT2 (316). To understand whether HMPV inhibition of STAT1 and STAT2 is dependent on expression of both proteins, we infected U3A and U6A cells with HMPV. These cells are derived from a

human fibrosarcoma cell line and are specifically deficient in STAT1 and STAT2, respectively (317). We found that HMPV infection of STAT2-deficient U6A cells led to reduced expression and phosphorylation of STAT1 in a dose-dependent manner with increasing MOI (**Figure 4-4A,B**). HMPV infection of STAT1-deficient U3A cells also antagonized STAT2 expression and phosphorylation but only at an MOI of 3 (**Figure 4-4A,B**). At MOI=1, HMPV did not inhibit STAT2 phosphorylation, and STAT2 expression was slightly increased compared to mock-infected cells. These data indicate that HMPV has the capacity to target STAT1 and STAT2 independently of each other; however, antagonism of STAT1 by HMPV appears to be a more efficient process than STAT2 inhibition.

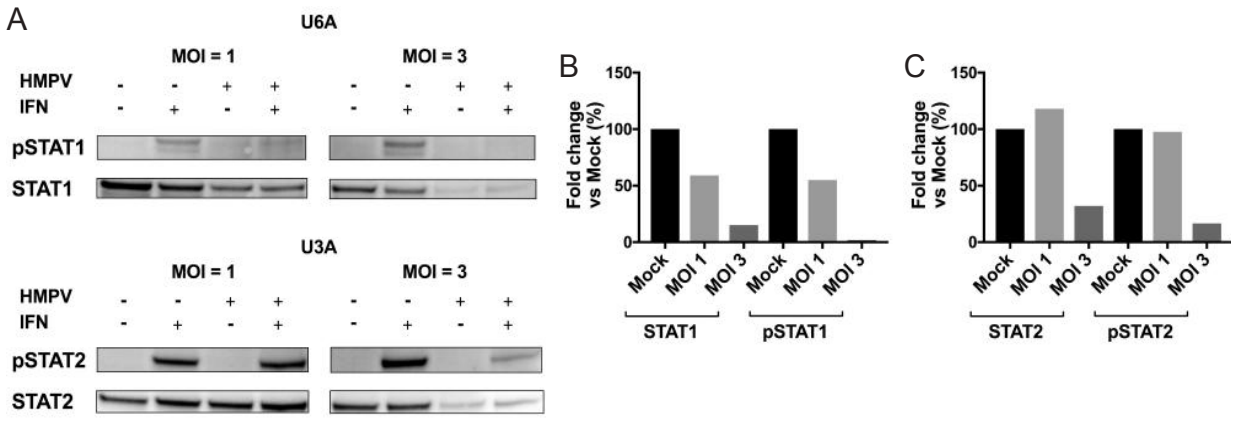

Figure 4-4. HMPV does not require STAT1 or STAT2 to inhibit expression and phosphorylation of the other. STAT1-deficient U3A and STAT2-deficient U6A cells were infected with HMPV for 20 hours at an MOI of 1 and 3, treated with IFN for 40 minutes, and lysed for western blotting. (**A**) Expression and phosphorylation of STAT1 and STAT2 in U6A and U3A cells. (**B**) Quantification of STAT1/pSTAT1 protein levels in U6A cells. (**C**) Quantification of STAT2/pSTAT2 levels in U3A cells.

Expression of hSTAT2 but not mSTAT2 promotes STAT1/2 inhibition by HMPV

So far, our data indicate that HMPV antagonizes STAT1/2 in human cells but not mouse cells. However, we have not shown whether this phenotype is specifically due to differences in the human and murine forms of STAT2, or whether HMPV fails to inhibit some other step in the innate immune response in murine cells.

To better understand the specific role of human and mouse STAT2 during HMPV infection, U6A (human) and NIH/3T3 (murine) cells were transfected with either human or murine STAT2 and infected with HMPV. After HMPV infection, cells were treated with IFN and processed for western blotting.

Expression and phosphorylation of STAT2 were inhibited in both human and murine cell lines that expressed mSTAT2 (**Figure 4-5**). Interestingly, we found that even though STAT2 was not required for STAT1 inhibition, the presence of mSTAT2 in human U6A cells inhibited both inhibition and degradation of STAT1 (**Figure 4-5A,C**). In contrast, transfection of hSTAT2 into NIH/3T3 cells promoted degradation and inhibition of STAT1 and STAT2 by HMPV (**Figure 4-5B,D**), though these effects were not complete, which may have been due to limited overlap between cells that successfully expressed the STAT2 plasmids and those that were infected. Overall, these indicate that species differences in STAT2 control degradation of both STAT proteins by HMPV.

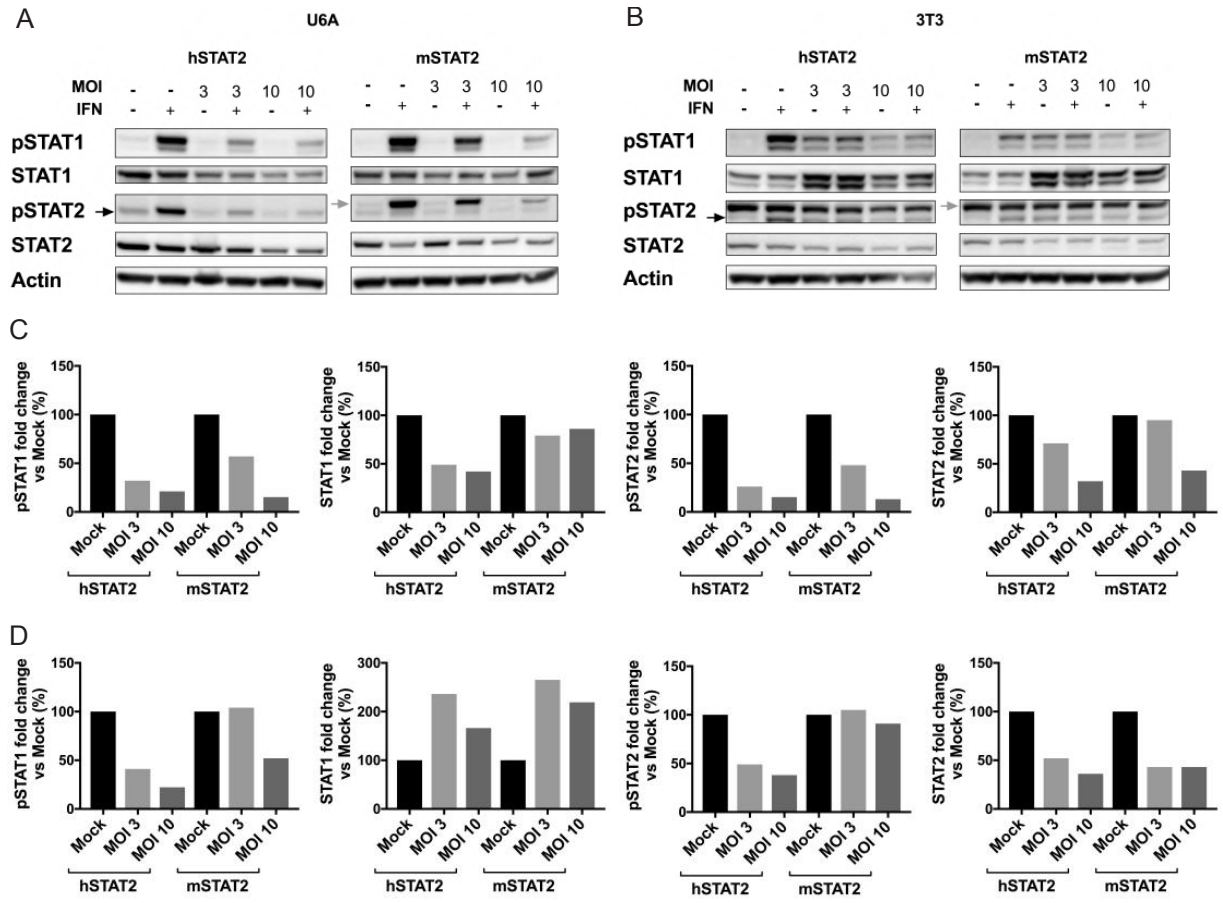

Figure 4-5. Expression of human STAT2 promotes STAT1 and STAT2 inhibition, while murine STAT2 inhibits STAT degradation. U6A and NIH/3T3 cells were transfected with hSTAT2 and mSTAT2, then infected with HMPV. Cells were treated with IFN 16 hours after infection for 40 min before cell lysis. (**A**) STAT1 and STAT2 expression and phosphorylation in U6A cells in the presence of human or murine STAT2. (**B**) STAT1 and STAT2 in NIH/3T3 cells after transfection of human and murine STAT2. (**C**) Quantification of band intensity as a measure of fold change in U6A cells from (A). (**D**) Fold change of STAT1 and STAT2 in NIH/3T3 cells from (B).

Discussion

Here, we show that HMPV promotes infection in primate cells by inhibiting phosphorylation and expression of STAT1 and STAT2, while the virus fails to inhibit either STAT in murine cells. STAT inhibition occurs in an hSTAT2-dependent manner, as transfection of mSTAT2 into human cells prevents STAT1 and STAT2 antagonism.

Furthermore, HMPV can be serially passaged in both STAT1- and STAT2-deficient mice and appears to become more virulent, whereas serial passage in WT mice is not possible. These passaging data suggest that STAT1/2 in mice represents a significant barrier to mouse adaptation of HMPV.

A relatively high MOI of HMPV (3 or more, depending on the cell line) to inhibit STAT2, whereas inhibition of STAT1 occurred at an MOI of 1. The different MOIs suggest that STAT1 inhibition by HMPV is more efficient than STAT2 inhibition. HMPV proteins could have a higher affinity for STAT1 compared to STAT2, or perhaps STAT2 inhibition is achieved with a viral protein that is transcribed at a lower abundance.

One limitation of this work is that both transfection and infection have limited efficiencies, which will vary based on cell lines, cell confluency, and transfection and infection protocols. Previously, the state of STAT1 and pSTAT1 in either infected or non-infected cells was assessed by flow cytometry, using fluorescent labeling of HMPV proteins and STAT1/pSTAT1 (69). A similar method could be used to assess the levels of STAT2 and pSTAT2 in HMPV-infected Vero or BEAS2b cells, and the level of STAT2 in murine cells. However, the only pSTAT2 antibody that currently exists for flow cytometry does not recognize murine pSTAT2.

A combination of transfection and infection, as in Figure 4-5, means it is possible that only a fraction of cells both expressed the transfected STAT2 protein and were infected. To circumvent this, stably transfected cells that express either human or murine STAT2 could be engineered, and then infected with HMPV to assess the state of both STATs.

Transfection efficiency of hSTAT2 and mSTAT2 may have been different and may have varied between the U6A cells and the NIH/3T3 cells. However, we controlled for this internally by comparing the levels of STAT2 in infected wells with the level and phosphorylation of STAT2 from mock-infected wells that were transfected with the same plasmid. It would be interesting to titrate the transfection so that both human and murine STAT2 are expressed at the same level in mock-infected cells, as it is possible that HMPV's capacity to target either could be limited by the amount of transfected protein in a cell.

Previous work in the lab showed that the SH protein from HMPV is responsible for suppression of STAT1. In an attempt to determine whether SH also inhibited STAT2, we transiently transfected 293T cells with SH plasmid, but found no detectable decrease in STAT2 (data not shown). However, this does not rule out SH as a possible STAT2 antagonist. It is possible that due to transfection efficiency, not enough virus protein was synthesized to affect STAT2, especially since transfection itself upregulates STAT signaling.

It is possible that SH is also responsible for differences in STAT2, but that SH may preferentially target STAT1, especially in circumstances of low abundance. To determine whether SH antagonizes STAT2, cells could be stably transfected with HMPV proteins to analyze the STAT2 phenotype.

We attempted to assess an interaction between SH or G and STAT1 or STAT2 via co-immunoprecipitation; however, an interaction was not found (data not shown). It is possible that an interaction exists, but that this is transient or not stable. Stabilization of protein interactions using *in vivo* crosslinking with protein stabilizers may allow

transient interactions to remain stable enough for analysis. Additionally, earlier time points should be measured in case interactions happen earlier than the 24-hour time point that we used. If STAT1/2 are degraded rapidly, proteasome inhibitors could allow these proteins to remain long enough for Co-IP. Additionally, use of a proteasome inhibitor would reveal whether degradation occurs in a proteasome-dependent manner.

It is possible that inhibition of STAT1 and STAT2 by HMPV occurs in an indirect manner. For example, others have reported that HMPV infection downregulates Tyk2 and Jak1 expression (76), though it was not shown what HMPV protein is responsible and whether this occurs in a direct manner. Murine and human Tyk2 and Jak1 have 80% and 95% amino acid homology, respectively (NCBI Homologene). It is unknown how HMPV infection of murine cells affects Tyk2 and Jak1. However, we found that transfection of mSTAT2 into human cells reduced the virus' capacity to target both STAT1 and STAT2, which suggests that mSTAT2 might need to directly interact with the protein antagonized by HMPV to guard it from inhibition.

Mock-infected human and murine cells phosphorylate transfected mSTAT2 and hSTAT2 (Figure 4-5). Therefore, the upstream mediators of STAT2 phosphorylation, Tyk2 and Jak1, can interact with both human and murine forms of STAT2, although it is possible that phosphorylation efficiency could be reduced in cross-species protein interactions.

In future work, it will be important to determine which domain of STAT2 is targeted by HMPV and whether these or other domains of STAT2 are responsible for the virus host-species restriction. Previous work in hPIV2 and hPIV5 determined that the N-terminus containing the coiled-coil domains of hSTAT2 was required for virus

degradation (119). STAT2 has 7 domains (318). The coiled-coil domain of STAT2 that is essential in hPIV2 and hPIV5 is essential for interaction with IRF9. Additionally, STAT2 contains a DNA-binding domain and nuclear localization signal, a Src homology 2 domain that is necessary for STAT dimerization, a tyrosine phosphorylation site, and a c-terminal transcriptional activation domain (TAD) (318). HMPV, or an HMPV-recruited intermediate, could interact with any of these to cause protein degradation; mSTAT2 is highly divergent in the c-terminal TAD, so this region could contribute to the host specificity of HMPV.

It will be important to determine how human and murine STAT2 affect replication of HMPV in either human or murine cells. We know that HMPV replicates in mice (278) and *in vitro* in CMT64/61 cells (unpublished data), indicating that murine STAT2 does not eliminate HMPV's capacity to replicate in mice or murine cell lines. However, the presence of hSTAT2 may enhance replication in murine cells, while the presence of mSTAT2 in human cells may restrict HMPV replication. Additionally, to assess whether human STAT2 enhances *in vivo* infection of mice, huSTAT2 mice, which have been engineered to express human STAT2, will be infected, and virus titer and the immune response to HMPV will be compared (huSTAT2 mice were courtesy of Adolfo Garcia-Sastre (124)).

Serial passage of HMPV in $STAT1^{-/-}$ and $STAT2^{-/-}$ mice has been completed to P13 (data not shown). While we have found that this P13 lung homogenate is capable of infecting WT mice, the virus did not replicate to high enough titer to productively infect a subsequent mouse. Alternative strategies to achieve the transition from infection in STAT-deficient mice into WT mice have been attempted. These have included sucrose

purification of lung homogenate in order to concentrate the virus, *in vitro* passage in murine cells, chemical inhibition of STAT1 with fludarabine (319), and siRNA and morpholino knockdown of STAT2 to titrate STAT2 levels in WT mice. Thus far, these have not been successful, though it is possible that with more optimization, one of these strategies will aid serial passage in WT mice. Additionally, DBA/2 mice will be infected with the lung homogenate, as previous work in the lab has shown that this line is more permissive for HMPV (278). DBA/2 mice or another more permissive mouse line could be an intermediate in the transition from $STAT1^{-/-}$ and $STAT2^{-/-}$ passaged virus to a fully mouse adapted virus for WT mice.

RNA from P13 lung homogenate has been extracted and will be sequenced in order to determine which mutations have arisen during the 13 passages. By comparing these sequences with the original parent HMPV, we will be able to determine other mutations that enhance HMPV replication in mice.

Overall, these data indicate that HMPV targets expression and phosphorylation of both STAT1 and STAT2 in a host-specific manner. Future studies to determine the specific HMPV and STAT interactions involved in STAT inhibition will reveal a mechanism for how this virus achieves productive infection in humans. While all mouse models of human diseases have limitations, these data highlight how the innate immune response to HMPV in mice is likely to be profoundly different than it is during natural infection of humans.

Materials and Methods

Cells

The following cell lines were used: BEAS2b (ATCC CRL-9609), 293T (ATCC CRL-3216), Vero E6 (ATCC CCL-81), NIH/3T3 (ATCC CRL-1658), U3A (ECACC). CMT64/61 (ECACC) and U6A (ECACC) cells were purchased from Sigma. All cell lines were maintained, infected, and transfected in DMEM supplemented with 10% FBS.

Viruses

HMPV clinical strains TN/94-49 and C1-718 (subtypes A2) were grown and titered in LLC-MK2 cells (ATCC CCL-7) as previously described (278).

Plasmids

pUNO1-hSTAT2 and pUNO1-mSTAT2 plasmids were purchased from Invivogen. EGFP/mCherry tagged hSTAT2 and mSTAT2 were generated by Jiuyang Xu by subcloning the h/mSTAT2 sequence from the pUNO1 plasmids into pEGFP-N1/pmCherry-C1 vectors (Clontech). XhoI/KpnI sites were used for hSTAT2, and KpnI/BamHI sites were used for mSTAT2.

Codon optimized constructs in a pcDNA3.1+ plasmid (Invitrogen) for HMPV proteins SH, G, N, M2, M were previously generated in the lab (69) based on the sequence for HMPV TN/94-49. C-terminal Myc-His-tagged proteins were generated by subcloning into pcDNA3.1-myc-His (Invitrogen) using the Kpn1 and EcoRV sites by Jiuyang Xu,

In vitro infection

For cell experiments, cells were inoculated with HMPV strain TN/94-49 at an MOI of 1-10 in a 24-well plate. Mock-infected cells were given media or cell lysate, which had an equivalent effect on STAT1 and STAT2 protein levels and phosphorylation (data not shown). 16-24 hours post-infection, cells were treated with 1000 U/ml human IFNα (Alpha 2a) (PBL) for human and primate cells, or 1000 U/ml murine IFNβ (PBL) for mouse cells for 30-40 minutes. After treatment, media was aspirated from the tissue culture dish and cells were lysed in RIPA buffer (ThermoFisher) for western blotting or fixed in 4% paraformaldehyde for immunofluorescence.

Transfection

Transfections were performed using Lipofectamine 2000 (Life Technologies) following the manufacturer's protocol with some exceptions: for each well in 24-well plates, 2.5 μl Lipofectamine 2000 was diluted into 37.5 μl Opti-MEM (not supplemented) and was mixed with 1 μg plasmid in 37.5 μl Opti-MEM for a total volume of ~75 μl. This was incubated for 15 min before being added to wells. 50% of media was replaced after 6 hours. 16-24 hours post-transfection, cells were treated with IFNα/β as above, and lysed for western blotting.

Western blotting

Cells were lysed in ice-cold RIPA buffer (Thermo Scientific) that contained protease and phosphatase inhibitors (Halt, Thermo Scientific). Samples were centrifuged at 14,000xg for 15 minutes to pellet debris, and supernatant was used for

protein analysis. Total protein from cell lysate was quantified by BCA assay (Thermo Scientific) and protein was normalized between samples. Samples were diluted in 4x LDS sample buffer (Invitrogen) and 10X Sample Reducing Agent (Invitrogen) and boiled for 8 minutes at 95°C. Proteins were separated on a 4-12% Bis-Tris polyacrylamide gel before transfer to a PVDF membrane. Membranes were blocked in 5% BSA in Tris-buffered saline with 0.1% Tween-20 (TBS-T) or 5% nonfat dry milk boiled in TBS-T. Primary antibodies against STAT1 (Cell Signaling Technologies (CST), D1K9Y), pSTAT1 (CST, 58D6), STAT2 (CST, D9J7L), pSTAT2 (for human, CST D3P2P; for mouse (polyclonal), EMD Millipore), actin (Hrp conjugated, Abcam), and GFP (Invitrogen, A-11122) were used in a 1:1000 dilution (or a 1:10,000 dilution for actin) overnight with rocking at 4°C. After TBS-T wash, HRP-conjugated secondary antibodies against rabbit or mouse were added in 5% BSA-TBS-T or 5% milk-TBST for 1 hour. Blots were washed with TBS-T and put in TBS until imaging. Western blots were developed using West Femto (Thermo Scientific) and imaged on a ChemiDoc XRS+ (BioRad). Band quantification was performed using Image Lab v5.2 (BioRad).

Immunofluorescence

After infection and IFN treatment, cell supernatant was removed from BEAS2b cells and cells were fixed with 4% PFA. Cells were permeabilized with 100% methanol at -20°C. Cells were blocked with 5% goat serum and 0.3% Triton-X100 in PBS. Primary and secondary antibodies were diluted in 1% BSA and 0.3% Triton-X100 in PBS. DAPI (5ug/ml) was added to distinguish nuclei. Antibodies used were STAT1 (CST, D1K9Y) STAT2 (CST, D9J7L), HMPV anti-Fusion protein 54G10 (320),

secondary Alexa Fluor 488-conjugated anti-human and Alexa Fluor 568-conjugated anti-rabbit (Invitrogen).

Co-Immunoprecipitation

293T cells were seeded in a 100mm tissue culture dish and transfected when 50-70% confluent with hSTAT2-eGFP, HMPV SH, HMPV G, or eGFP, either in combination or alone using Lipofectamine 2000 (Life Technologies) as above. 16 hours post-transfection, cells were harvested, lysed, and Co-IP was performed using the Pierce Co-IP kit (Thermo Scientific) following manufacturer's protocol. 30-50 μg of capture antibodies (anti-GFP (Invitrogen, A-11122) or anti-His (Invitrogen, His.H8)) were bound to each column. Capture step was performed overnight at 4°C with continuous rotation.

Mice

C57BL/6 mice were obtained from Jackson Laboratories. $STAT1^{-/-}$ and $STAT2^{-/-}$ mice were from Dr. Christian Schindler (Columbia University) and Dr. David Levy (New York University), courtesy of Dr. John Alcorn. 6-14-week-old mice of both sexes were used for all experiments. All mice were bred and maintained in specific pathogen free conditions in accordance with the Institutional Animal Care and Use Committee of University of Pittsburgh.

Serial passage

For all animal experiments, mice were anesthetized with ketamine-xylazine and intranasally infected with $1x10^6$ PFU HMPV, or lung homogenate from a previously infected mouse, in a 100-uL volume. For serial passage, mice were euthanized at day 5 post-inoculation. Lungs were harvested and homogenized in 1-2 ml 0% Opti-MEM in a glass dounce homogenizer as previously described (278). Lung homogenates were clarified by centrifugation at 1200 RPM (300xg) for 10 minutes. Clarified lung homogenate was aliquoted into cryovials and snap-frozen in an ethanol-dry ice bath before storage at -80°C. For serial passage, clarified lung homogenate was pooled from 2-3 mice before inoculation into recipient mice.

Virus titration

Virus titers were measured by plaque assay in LLC-MK2 cells (previously described (278)).

Multiplex Cytokine Analysis

Lung homogenate from the whole lung was used for cytokine analysis by Bio-plex Mouse Cytokine 23-plex Assay (BioRad, Hercules, CA) according to manufacturer's instructions. The following cytokines and chemokines were measured: IL-1α, IL-1β, IL-2, IL-3, IL-4, IL-5, IL-6, IL-9, IL-10, IL-12p40, IL-12p70, IL-13, IL-17A, Eotaxin, G-CSF, GM-CSF, IFNγ, CXCL1, MCP-1, MIP-1α, MIP-1β, RANTES, TNFα.

Statistical Analysis

Data were analyzed using Prism version 6.0 or 7.0 (GraphPad Software). A two-tailed Student's T test was used to analyze comparisons between two groups. For comparisons between multiple groups, a one-way ANOVA was performed using a Bonferroni posttest. Error bars on graphs represent SD unless otherwise noted.

CHAPTER V

Summary and Future Directions

Thesis Summary

The work I have presented here represents a diverse exploration into the interactions of the innate and adaptive immune systems with respiratory viruses during infection. I have discovered that despite their suppressive role in infection, regulatory T cells (Tregs) balance types 1 and 2 immunity to allow for proper antiviral response and control immune cell migration. I have also found that T cell impairment occurs even in the absence of PD-L1, the principal ligand for the inhibitory receptor PD-1, which may represent a preference for T cell impairment in the lung. Lastly, I established that human metapneumovirus (HMPV) is restricted in host species tropism due to divergent sequences of the innate immune mediator STAT2. While each chapter in this dissertation explored a unique aspect of host-pathogen interaction, some important themes emerge, both with host and virus.

Many, and perhaps all, respiratory virus infections cause T cell impairment (**Figure 5-1**) (131-139). This phenomenon has been described numerous times in mouse models of human infection as well as infections by murine viruses in mice (136). Additionally, there is convincing evidence that this occurs in naturally infected humans (138, 233). T cell impairment may be programmed as a universal response to respiratory virus infections. It is striking that respiratory virus infections drive a phenotype of dysfunctional T cells observed with few other acute infections. Instead, the

state of T cells during T cell impairment mimics the exhausted phenotype that T cells adopt during chronic infection or cancer (202-204). T cell exhaustion is considered detrimental for chronic disease; in contrast, T cell impairment might represent the best possible immune strategy against a type of infection where immune-mediated pathology is common and may be irreversible. In chapters II and III, I explored two potential drivers of T cell impairment: Tregs and the inhibitory ligand PD-L1.

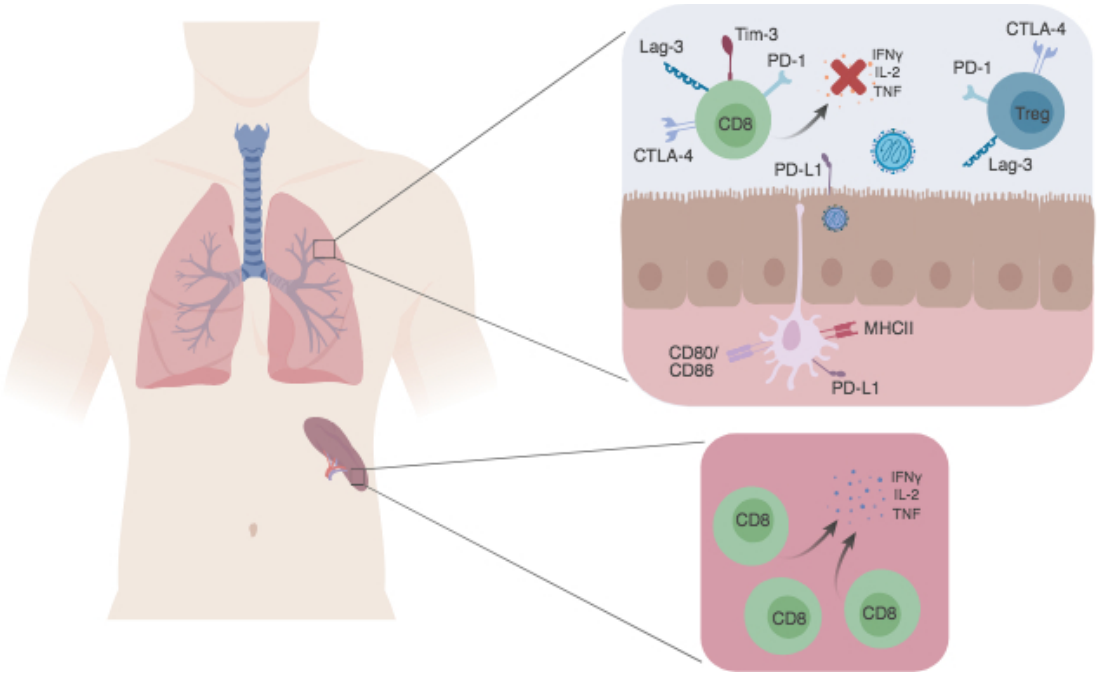

Figure 5-1. T cell impairment in respiratory virus infection. Image created with BioRender. Adapted from Rogers & Williams 2018, *PLOS Pathog.* (Under review)

In chapter II, I sought to understand how Tregs influence the adaptive immune response to respiratory virus infections. My goals in this project were twofold: first, to understand the contribution of Tregs to the immune response to HMPV, as this had never been described previously. Second, I wished to gain an understanding of what role Tregs play at different stages of the immune response to respiratory virus infections

in general, with the goal of establishing a more universal picture of the importance of Tregs in lung infections.

When I depleted Tregs before and during HMPV infection, $CD8^+$ T cells became more functional and virus titer was decreased. Although $CD8^+$ T cells were more functional in the absence of Tregs, I found that the magnitude of HMPV-specific $CD8^+$ T cells was reduced compared to that in control mice. To understand this, I depleted Tregs early in infection and found that DC and $CD8^+$ T cell migration were impaired. Moreover, when I measured markers of type 2 immunity in infected, Treg-depleted mice, I found that type 2 cytokines, T_H2 $CD4^+$ T cells, and ILC2s were significantly increased in mice that were depleted of Tregs before infection. In contrast, delayed Treg depletion led to increased type 1 cytokines and T_H1 cells.

With this project, I was able to show that Tregs have an essential, previously unappreciated role in control of immune cell migration during respiratory virus infection. I also found that Tregs controlled the balance of types 1 and 2 immunity to respiratory virus infection and demonstrated for the first time that Tregs could specifically control the balance of types 1 and 2 innate lymphoid cells.

Chapters II and III are linked by two important features: both Tregs and inhibitory receptors suppress $CD8^+$ T cell responses, and some of the actions of inhibitory receptors may be through their expression on, and activation of, Tregs. Chapter III addresses unanswered questions about the role of the ligand PD-L1 in respiratory virus infection. This project initially began with the observation that both antibody blockade of PD-L1 and genetic absence of PD-1 restored $CD8^+$ T cell function in respiratory virus infection. We reasoned that a mouse deficient in PD-L1 would also demonstrate

improved $CD8^+$ T cell function in respiratory virus infection, as this had been previously shown for LCMV chronic infection (286). Therefore, we were surprised to find that not only were $CD8^+$ T cells from PD-$L1^{-/-}$ impaired following both HMPV and influenza infection, but that PD-$L1^{-/-}$ mice also demonstrated delayed virus clearance. Impairment of $CD8^+$ T cells was seen previously in the lab using a different strain of PD-$L1^{-/-}$ mice (unpublished observation), so it seems clear that the inability to restore $CD8^+$ T cell function is not simply due to the strain having unintentional defects in function due to some other mutation. Additionally, I saw that PD-L2 did not compensate for a lack of PD-L1, but that other inhibitory receptors were upregulated upregulated on $CD8^+$ T cells from PD-$L1^{-/-}$ mice at baseline and during HMPV infection.

After generation of reciprocal bone marrow chimeras between WT and PD-$L1^{-/-}$ mice, I found no obvious differences in $CD8^+$ T cell function or virus titer. Interestingly, both WT and PD-$L1^{-/-}$ mice that received PD-$L1^{-/-}$ bone marrow had higher expression of inhibitory receptors, similar to that observed in PD-$L1^{-/-}$ mice in earlier experiments. The fact that the WT/PD-$L1^{-/-}$ chimeras with PD-$L1^{-/-}$ hematopoietic cells had higher inhibitory receptor expression on $CD8^+$ T cells, while the reciprocal chimeras did not, indicates that PD-L1 on hematopoietic cells may control homeostasis of inhibitory receptors and T cell impairment.

Despite evidence that PD-L1 has a compartment-specific role in T cell exhaustion (286), I was unable to determine whether PD-L1 expression by a particular compartment or cell drives T cell impairment in respiratory virus infection. Epithelial and dendritic cells from respiratory virus-infected mice both upregulate PD-L1 (231-235, 237), likely due to the increased levels of proinflammatory cytokines in the lung during

infection. Thus, it is possible that multiple cell types interact with PD-1^{+} CD8^{+} T cells to drive impairment. It may also be that genetic absence of PD-L1 drives immune skewing in a way that does not occur in PD-1$^{-/-}$ mice, or that interactions of PD-L1 and its second receptor, B7-1 are important in immune system development.

There are multiple similarities between T cell impairment and T cell exhaustion, such as inhibitory receptor expression, transcriptome profile, and loss of multiple effector functions in T cells. However, in other aspects these processes are fundamentally different—most importantly in differences in the time required for cells to become exhausted or impaired. The difference in phenotype of PD-L1$^{-/-}$ mice that was seen here in T cell impairment compared to that seen in T cell exhaustion (286) may be one other important feature that differentiates these distinct immune programs.

Chapter IV focused on host species specificity of HMPV. Mouse adaptation of viruses generates a new tool for the field that helps further the understanding of the virus and host factors that are important for pathogenesis both in the natural host of the virus as well as in the mouse. Murine adaptation of respiratory viruses has only been successfully completed for influenza, SARS, and MERS viruses (310, 311, 321). Mouse adaptation of RSV was previously attempted but was unsuccessful (personal communication, Dr. Marty Moore, Emory University). It is reasonable to assume that unsuccessful attempts in other respiratory viruses have been made. Previously, our lab had attempted mouse passage of HMPV in B6 mice, but was unsuccessful.

I hypothesized that mice deficient in innate immunity might allow for serial passage of HMPV, as mice with deficiencies in innate immunity allow HMPV to replicate to higher titer (54). I infected STAT1$^{-/-}$ and STAT2$^{-/-}$ mice with HMPV and found that

both strains of knockout mice were permissive for serial mouse-to-mouse passage of HMPV. Attempts to transition the mouse-passaged virus into WT mice and develop a completely murine-adapted HMPV are ongoing.

I became intrigued over the course of these serial-passage studies about the role that STAT2 might play in HMPV infection and pathogenesis. Other labs had previously shown that STAT2 controlled host species permissiveness of hPIV2 and hPIV5, RSV, dengue, and Zika viruses (82, 119, 122, 123). I infected both primate and murine cells with HMPV and saw inhibition of STAT2 only in primate cells. Furthermore, when mSTAT2 was transfected into human cells, both STAT2 and STAT1 were resistant to HMPV. In contrast, when I transfected murine cells with hSTAT2 and infected them with HMPV, HMPV gained the ability to target both STAT2 and STAT1.

This work highlights an essential role of one host protein and its capacity to confer susceptibility or resistance to HMPV infection depending on human or murine form. Though a mouse-adapted virus has not yet been generated, STAT2 has been identified as an essential determinant of HMPV host species specificity (**Figure 5-2**), and therefore represents a barrier that most likely will need to be overcome to generate a fully mouse-adapted HMPV.

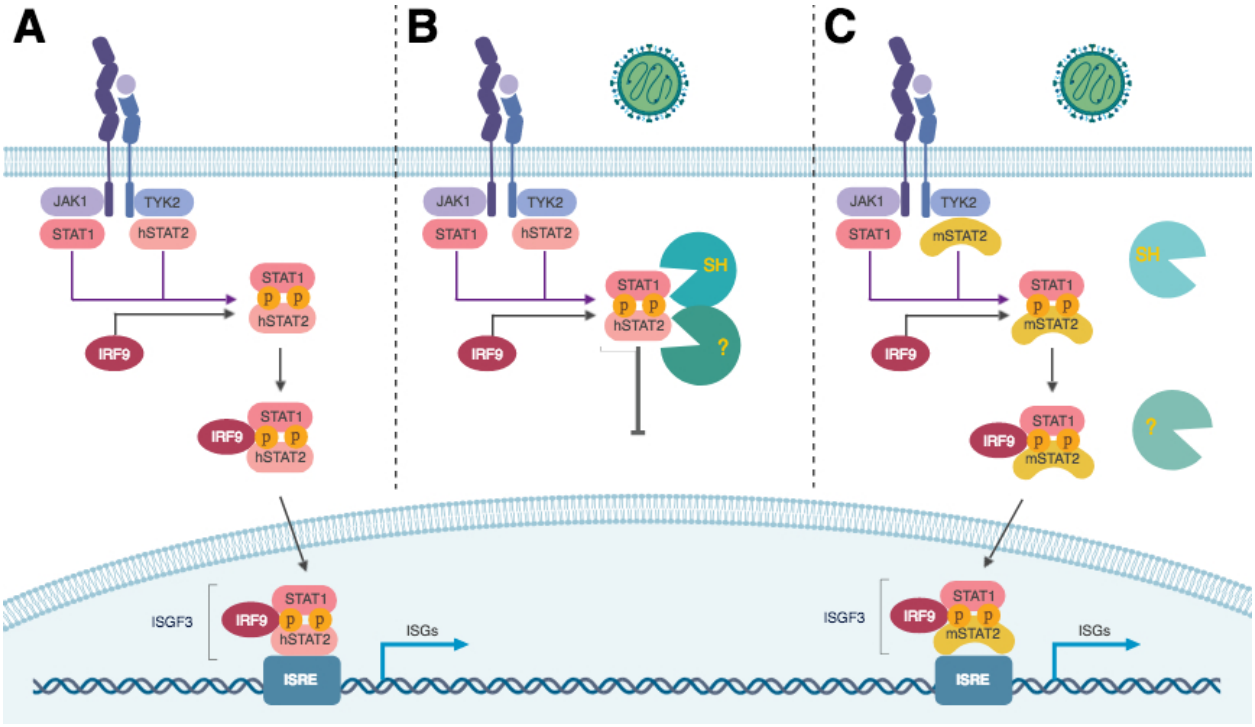

Figure 5-2. HMPV inhibition of STAT1/2. (**A**) Canonical Type I Interferon signaling is mediated by STAT1 and STAT2. (**B**) HMPV, through the SH protein and unknown mechanisms, antagonizes and degrades STAT1 and STAT2 in human cells. (**C**) Murine STAT2 confers resistance of both STAT1 and STAT2 to degradation by HMPV. Image created with BioRender.

Viruses are obligate intracellular parasites that must rely on, co-opt, and inhibit host cell machinery to achieve productive infection. To understand host-pathogen interactions in virus infections, a thorough understanding of both innate and adaptive immune responses to a virus is essential. In my dissertation work, I have made strides towards revealing host factors of both the innate and adaptive immune systems that play a role in infection by HMPV and other respiratory viruses. I discovered a novel role of Tregs in controlling immune skewing and immune cell migration during respiratory virus infection. Additionally, I found that Tregs have different functions early and late in the immune response to infection. I also revealed that PD-L1 may play a differential role

in T cell impairment and T cell exhaustion. Finally, I report for the first time that HMPV inhibits STAT2, and host species restriction of HMPV is at least partially mediated by species differences in the STAT2 protein. While I have answered some questions here, these data bring to light new questions and opportunities to better elucidate the host immune response to respiratory virus infection.

Future Directions

The findings from this thesis present new avenues to further evaluate the importance of Tregs, inhibitory receptors, and STAT2 in respiratory virus infections, in both the laboratory setting as well as in patients. With regard to immunoregulation, some of the most intriguing of these potential studies are: how does PD-1 affect Treg function in respiratory virus infection? Do polymorphisms of inhibitory receptors affect outcomes to respiratory virus infections in patients? Can Tregs or inhibitory receptors be manipulated during infection or vaccination? Additionally, how does HMPV antagonize STAT2, and can this be harnessed to create a fully mouse-adapted form of the virus? I explore these questions below.

Cell-specific roles of PD-1/PD-L1

Treg-specific role of PD-1 in T cell impairment

In Chapter II of my studies I found that Tregs highly upregulate PD-1 during HMPV infection. I also found that antibody blockade of PD-L1 after Treg depletion could not enhance $CD8^+$ T cell function further than Treg depletion alone. Others have found

that PD-1 is important for induction and maintenance of Tregs. However, the role of PD-1 on Tregs in respiratory virus and T cell impairment is unclear.

One method to understand the requirement and function of PD-1 on Tregs is to perform adoptive transfers of PD-$1^{-/-}$ Tregs into WT mice, or into Treg-depleted $FoxP3^{DTR}$ mice, and assess the function of the Tregs as well as the immune response to respiratory virus infection. However, this is somewhat convoluted, and Treg function itself could have been altered due to genetic deficiency of PD-1. Instead, PD-$1^{fl/fl}$ mice were recently developed by Arlene Sharpe's lab, and one strain of these, PD-$1^{fl/fl}$-$CD8^{cre}$, are currently breeding in our lab's colony. The PD-$1^{fl/fl}$ mice could be crossed to a FoxP3 inducible Cre mouse (322) in order to specifically delete PD-1 from Tregs at various time points before and during respiratory virus infection.

Cell-specific role of PD-L1

I was disappointed to find no obvious phenotype for T cell impairment and $CD8^+$ T cell function in PD-$L1^{-/-}$ mice or with reciprocal bone marrow chimeras between PD-$L1^{-/-}$ and WT mice. The fact that T cell impairment and T cell exhaustion appear to differ in their requirement for PD-L1 (286) is worth further investigation. However, bone marrow chimeras or experiments like adoptive transfers of PD-L1-deficient cells are limited in specificity for assessing specific cell types. Instead, to study PD-L1 expression only on certain cells, PD-$L1^{fl/fl}$ mice, which were recently reported (323), could be used. These mice could be crossed with a variety of mice that express Cre recombinase in specific cells or tissues, such as $CD11c^+$ cells (324) or club cells (325).

These experiments may lead to the conclusion that PD-1^{+} CD8^{+} T cells receive PD-L1 signals from multiple cell types in T cell impairment, or that other inhibitory receptor pathways make up for a lack of PD-L1 on any cell type in lung infections. This would be one more piece of evidence regarding the differences between T cell impairment and exhaustion. Perhaps the lung environment has been developmentally programmed to suppress CD8^{+} T cell function over the course of evolution, when long-term lung defects due to immunopathology from clearing respiratory infections would decrease fitness. The immune response to respiratory virus infections may be as a bell curve, where an overactive immune response or a failure to respond to infection could be fatal. Instead, by programming the pulmonary immune response in favor of dampening the immune response at the cost of slightly delayed virus clearance, the majority of people (and mice or other animals that are susceptible to respiratory virus infections) could recover without consequence.

Human polymorphisms in PD-1/PD-L1 and their role in respiratory virus infection

To date, no humans have been identified with gene deletions of PD-1. Based on studies of PD-1$^{-/-}$ mice, we would expect that this is due to a lack of obvious disease phenotype in PD-1-deficient humans, rather than to embryonic lethality of a PD-1 deletion. In contrast, mutations in the inhibitory receptor CTLA-4 cause an autosomal dominant autoimmune syndrome in humans (326). These CTLA-4-deficient patients also had immune-mediated interstitial lung disease, and interestingly, recurrent respiratory tract infections. CTLA-4 has a crucial role in Treg function (327), and it is

intriguing to imagine that these patients could have defects in immune priming of respiratory virus infection, as I have shown in my work, leading to recurrent infections.

PD-1 polymorphisms have been associated with increased susceptibility to autoimmune diseases (328-330) and decreased susceptibility to some cancers (331). PD-L1 polymorphisms have also been associated with cancer risk, graft rejection, and autoimmunity (332-334). Limited data exist on the association between infections and PD-1 polymorphisms; some found an association between one PD-1 polymorphism and increased risk of hepatitis B infection (335), whereas others found no association (336).

No polymorphisms in PD-1 or PD-L1 have been reported to be associated with respiratory virus infections, but this may be due to the very recent discovery of PD-1-mediated T cell impairment during acute respiratory viral infection (138). These might be challenging genetic association studies because respiratory virus infections are ubiquitous. Nonetheless, polymorphisms in PD-1 or PD-L1 could be associated with poor outcomes of respiratory virus infection. Most pediatric patients hospitalized with HMPV or RSV are otherwise healthy with no underlying conditions (5, 13). Patients hospitalized for severe lower respiratory infection and those who are treated as outpatients for mild disease could have sequencing of PD-1 and PD-L1 (and potentially inhibitory receptors such as CTLA-4), and polymorphisms compared between groups.

Manipulation of Tregs or inhibitory receptors during respiratory virus infection and vaccination

One essential goal of research of respiratory virus pathogenesis and immunity is to move toward the development of treatments and vaccines. It is possible that

strategies for manipulating Tregs or inhibitory receptors could be one day used as treatments or vaccination approaches.

Specific Treg manipulation has not been well studied for clinical use, and therefore the side effects and potential harm or benefit to patients is unclear (though considering the abundant expression of PD-1, CTLA-4, and other inhibitory receptors on activated Tregs, checkpoint inhibitors likely work at least in part by disruption of Treg function). One potential obstacle facing the development of Treg-specific therapies is that while some surface markers are highly enriched on Tregs, no surface marker identified so far is completely unique to these cells. Therapies that affect Tregs more than other cell populations (e.g., anti-GARP (337) or anti-CD25) could be sufficient, but specific Treg targeting might require a drug that could penetrate both the cell and nucleus to interact with FoxP3.

Considering the tissue protective effects of Tregs in respiratory virus infection, a therapeutic strategy could be to stimulate Tregs or inhibitory receptors during respiratory viral infection to lessen immunopathology. Although inhibitory receptor agonists have not been tested in respiratory virus infection, administering soluble PD-L1 or another inhibitory receptor ligand could potentially reduce immunopathology and preserve lung function during infection. Additionally, enhanced Treg function during respiratory virus infection might be protective against future asthma, based on studies in RSV (184-186).

On the other hand, Treg inhibition could offer a target for vaccination improvement. Studies of chronic infections and one study of IAV infection found that Treg blockade during vaccination can enhance the immune response to subsequent

viral challenge (338-340). Vaccination combined with manipulation of inhibitory receptors is another possibility. Since deficits in $CD8^+$ T cell function in a vaccination model is associated with high PD-1 expression (238), small molecule inhibitors or other strategies to reduce PD-1 signaling during vaccination may be a useful strategy, and has shown promise in antibody blockade of some mouse vaccination studies of chronic infection or cancer (239-241). Whether Treg or inhibitory receptor inhibition could cause similar improvements in antiviral response after respiratory virus vaccination in patients remains to be determined, and is worth investigating in mouse models and humans.

Finally, there is a growing use of immunomodulatory treatments such as checkpoint inhibitors for cancer immunotherapy. An uncommon but severe and occasionally fatal adverse effect of checkpoint inhibition is pneumonitis (341). This side effect suggests that patients who are on checkpoint inhibitor treatment could have exacerbated disease severity if they become infected with a respiratory virus. However, there is not yet any published data on the how these patients respond to respiratory virus infection. A deeper understanding of the effect of community-acquired respiratory virus infection during checkpoint inhibitor therapy is important, considering the increasing use of these therapies.

Mouse adaptation of HMPV

My project on the role of STAT2 as a host determinant of HMPV originally started with the goal of generated a mouse-adapted form of the virus. Considering that mice are the primary *in vivo* model for studying HMPV, and that mice are only semi-permissive

for the virus, a mouse-adapted strain would allow for greater understanding of the pathogenesis of HMPV and of the virus and host factors that contribute to virulence.

So far, I have passaged HMPV to P13 in STAT1$^{-/-}$ and STAT2$^{-/-}$ mice. The P13 viruses caused nearly 30% weight loss in mice, whereas irradiated lung homogenate did not cause weight loss. This indicates that HMPV is becoming more virulent in STAT knockout mice over subsequent passages. For influenza, SARS, and MERS virus infections, 10-30 passages were required for mouse adaptation (310, 311, 321). However, passaging of these viruses occurred in WT mice.

The limiting step in complete mouse adaptation of HMPV is the transition from the partially adapted P13 STAT viruses into WT mice. While sequencing of the passaged viruses will likely reveal some virus mutations that were essential for increased virulence in mice, virulence in knockout mice is not sufficient, as I and others have already shown that HMPV specifically antagonizes STAT1 and STAT2 in the course of infecting human cells.

One potential model to consider for the mouse passaged virus is a mouse that was engineered to express the human form of STAT2 (124), which we recently received. While this would not generate a virus that is 100% mouse-adapted, others have used this same mouse to study mouse-adapted Zika virus (124), which is highly virulent in huSTAT2 mice. Another example of a “nearly mouse-adapted virus” is MERS-CoV, where mouse adaptation required use of a human DPP4 knock-in mouse, as DPP4, the natural MERS-CoV receptor in humans, is not sufficiently conserved in mice (311)

However, it may still be possible to develop a completely adapted HMPV. When I challenged WT C57BL/6 mice with lung homogenate from STAT-knockout mice, virus replicated but not to a high enough titer to infect a subsequent mouse. A mouse that is naturally more permissive for HMPV replication may overcome this barrier. For example, our lab has found that DBA/2 mice support higher viral replication than B6 mice and were permissive for all HMPV subtypes (278, 320). Thus, DBA/2 mice could allow for complete adaptation and could represent an intermediate step before passage into B6 mice, which are favored in the field because of the numerous immunological tools available for this strain.

Other ideas to promote mouse adaptation include partially knocking down STAT1 or STAT2 in WT mice, and then gradually titrating the STAT levels to apply selective pressure on the virus to mutate and inhibit STAT1 and STAT2. I previously attempted chemical inhibition of STAT1 and also tried siRNA and morpholino knockdown of STAT2 in murine cells and mice. However, I found poor knockdown of either STAT1 or STAT2 using these methods, which could be attributed to the long half-life of both proteins. Inhibition of STAT1 and STAT2 using these methods might not eliminate the STAT proteins currently present in a cell, but these could prevent the translation of new STAT1 and STAT2 in response to infection. Alternatives to STAT titration would be to generate bone marrow chimeras of WT and STAT1/2 mice so that either somatic or hematopoietic cells expressed STAT1/2, or to add STAT expression back to $STAT1^{-/-}$ and $STAT2^{-/-}$ mice using an adenovirus expression vector, which has been shown to be titratable in other models (342). Another strategy to try might be transitioning the virus

back and forth between WT mice and murine cells in vitro to propagate a high enough titer to infect subsequent WT mice.

While there are numerous potential strategies for generating a virulent strain of HMPV in WT mice, I believe that with perseverance, development of a fully mouse-adapted virus is possible. After generating the fully mouse-adapted HMPV, it will be important to determine which virus mutations were essential for this transition. By swapping segments of the mouse adapted HMPV genome and the parent strain, we will be able to determine which residues from which virus protein were responsible for adaptation, and why. For example, I hypothesize that HMPV will need to mutate in order to inhibit murine STAT2. Other mutations could involve engineering a polymerase that is more efficient in mouse cells, as in mouse adapted influenza (343). HMPV uses $\alpha v\beta 1$ integrin as a receptor (27, 344), which is expressed in the murine lung (NCBI Protein). However, other HMPV proteins such as the G protein, which has a putative role in attachment (26, 28), may need to mutate to enhance replication and virulence in mice.

Interactions of HMPV and STAT1/2

My work here and previous work by our lab on STAT1 inhibition by HMPV utilized the TN/94-49 subtype A2 virus (69). HMPV has 4 subtypes that all circulate in humans (5, 6, 24, 25). Previous work in HMPV had found that the phosphoprotein from HMPV subtype B1 was able to inhibit the pattern recognition receptor RIG-I, while this did not occur with the A1 subtype (47). Thus, it will be important to test other HMPV subtypes and different clinical isolates for their ability to antagonize STAT1 and STAT2.

Though I found that HMPV specifically antagonizes STAT2 in human and primate cells, I was not able to identify which HMPV protein mediates this. Previous work in the lab suggested that STAT1 expression and phosphorylation is inhibited by the HMPV SH protein (69). However, the mechanism and the residues of SH and STAT1 required were not determined.

I attempted to determine which HMPV protein antagonizes STAT2 using transient cell transfection. However, I did not see any decrease in STAT2 expression or phosphorylation. Since I needed to use a higher MOI to see STAT2 antagonism with HMPV infection, I hypothesize that transfection efficiency was not high enough to inhibit STAT2. To understand which HMPV protein antagonizes STAT2, cells that have been stably transfected with different HMPV proteins could be used. Stably transfected cells were previously used in the lab to determine that SH is responsible for STAT1 inhibition and could be assessed for their capacity to inhibit STAT2. However, it is possible that multiple HMPV proteins are required for STAT2 inhibition. If there is no STAT2 inhibition in cells stably transfected with single HMPV genes, transfection with a combination of HMPV genes could be used. I would propose using SH, G, P, and M2-2 first, as all have been reported to have some role in antagonizing innate immunity (47, 51, 55, 66-71).

All STAT proteins share similar domains: a coiled-coil region at the N terminus, a DNA binding domain in the middle, SH2 domains (required for STAT1/2 heterodimer formation) and phosphorylation sites towards the C terminus, and transcriptional activation domains at the C-terminus (345). Considering that STAT1 and STAT2 share similar structures, I would hypothesize that SH antagonizes both STAT1 and STAT2,

and furthermore, I hypothesize that inhibition of either protein by an HMPV protein occurs in homologous domains.

After determining which HMPV protein is involved, the interacting residues of the HMPV protein, STAT1, and STAT2 must be determined. For STAT1 and STAT2, I would transfect plasmids with truncated versions of each protein into U3A and U6A cells, respectively, as these are deficient in either STAT1 or STAT2. Previous work in hPIV2 and hPIV5 found that the N-terminal coiled-coil domain of STAT2 was essential for inhibition by the parainfluenza virus V protein (119). However, hPIV requires expression of both STAT1 and STAT2 for STAT2 inhibition (316), which indicates that inhibition of STAT2 by these viruses occurs via a different mechanism than inhibition of either STAT1 or STAT2 by HMPV, and therefore a different domain may be involved.

For determining which HMPV protein domain is required for STAT1 and STAT2 inhibition, plasmids with truncated versions of SH (or whichever HMPV protein was identified for STAT2 using stable transfection) would be constructed and stably expressed in cell lines. If in earlier work it was determined that multiple HMPV strains could antagonize STAT1 and STAT2, this would indicate that a conserved protein domain or amino acid residue is responsible, which would narrow the search—especially if SH is responsible, as this protein is not highly conserved between HMPV strains (346). Once the appropriate domain is determined, targeted point mutations in this domain could enable identification of specific amino acid residues responsible for antagonism of STAT1 and STAT2. Then, HMPV could be reverse engineered with these mutations to confirm the loss of STAT1 and STAT2 antagonism in human cells. Considering that HMPV fails to antagonize mSTAT2, domain substitutions between

hSTAT2 and mSTAT2 could also be constructed to determine which residues of mSTAT2 confer resistance to HMPV.

It is intriguing that STAT1 and STAT2 can be degraded by HMPV in the absence of each other, yet expression of the murine form of STAT2 in human cells inhibits both STAT2 and STAT1 degradation. This indicates that STAT1 and STAT2 do not need to form a heterodimer before HMPV inhibition. However, it is possible that a heterodimer of STAT1 and mSTAT2 could protect both proteins from HMPV. Degradation of STAT1 and mSTAT2 did occur at an MOI of 10, suggesting that HMPV can degrade mSTAT2 but with very low efficiency.

Finally, it will be important to determine whether HMPV and STAT1/2 interact in a direct manner, in a protein complex, or indirectly via an intermediate. To determine whether HMPV and STAT2 interacted either directly or in a complex, I previously attempted to perform co-immunoprecipitation of STAT2 and HMPV proteins, and while Coomassie stain showed that other proteins had been pulled down with STAT2 (as would be expected based on STAT2's multiple interactions with other cellular proteins (347)), I did not see that either SH or G pulled STAT2 down. However, this does not preclude an interaction between STAT2 and SH or another HMPV protein. It is possible that this interaction is transient, or that STAT2 degradation occurs quickly after HMPV protein binding. An interaction could be assessed using proteasome inhibitors or protein cross-linkers to stabilize interactions (90, 120, 123, 348, 349).

It is possible that HMPV does not interact directly or in complex with STAT1 and STAT2. In this case, I would pull down SH or whichever HMPV protein inhibits STAT2, and send protein bands for mass spectrometry to identify them, an approach that has

been previously used to identify STAT1-protein interactions (350). To then identify which proteins were indeed intermediates in HMPV inhibition of STAT1/2, I would knockdown the particular protein before HMPV infection and assess whether STAT1/2 were inhibited.

Conclusions and Significance

My thesis work provides insight into the roles of adaptive and innate immunity in a common serious infectious disease with few treatments or vaccines, and lays the groundwork for future studies on HMPV pathogenesis, T cell impairment, and immunoregulation of respiratory virus infection. I discovered a role for Tregs in promoting cell migration during different stages of the immune response to respiratory virus infections. I identified that T cell impairment is a unique process that is highly resistant to reversal. Finally, I have developed a partially mouse adapted strain of HMPV and identified factors that restrict HMPV to human and primate cells. Furthermore, in my studies I have developed assays for assessing Treg function, cell migration, and HMPV antagonism of innate immunity.

The future directions I have described here will develop a completely murine adapted HMPV virus, determine the mechanism of how HMPV interacts with STAT proteins to promote infection, and determine how species differences in STAT2 confer resistance to HMPV infection. These studies will also further understanding of the roles of PD-1 and its ligands on specific cell types in T cell impairment. This future work will also establish whether polymorphisms in PD-1 or other inhibitory receptors are protective or detrimental to severe respiratory virus infections in order to better

understand T cell impairment in human disease. Lastly, I have presented potential strategies for manipulation of immunoregulatory cells and molecules for therapy and vaccination against respiratory virus infections.

The work I have presented here represents a step towards the thorough elucidation of T cell regulation, innate immunity, and host species restriction of respiratory virus infection, and enhances understanding of lung infection and lung immunobiology in the goal of developing treatments and vaccines against a class of infections that is in need of novel strategies and therapeutics.

References

1. Troeger C, Forouzanfar M, Rao PC, Khalil I, Brown A, et al. Estimates of the global, regional, and national morbidity, mortality, and aetiologies of lower respiratory tract infections in 195 countries: a systematic analysis for the Global Burden of Disease Study 2015. *The Lancet Infectious Diseases* 17: 1133-61
2. Dieleman JL, Baral R, Birger M, Bui AL, Bulchis A, et al. 2016. US Spending on Personal Health Care and Public Health, 1996-2013. *Jama* 316: 2627-46
3. Herold S, Becker C, Ridge KM, Budinger GR. 2015. Influenza virus-induced lung injury: pathogenesis and implications for treatment. *Eur Respir J* 45: 1463-78
4. van den Hoogen BG, de Jong JC, Groen J, Kuiken T, de Groot R, et al. 2001. A newly discovered human pneumovirus isolated from young children with respiratory tract disease. *Nat Med* 7: 719-24
5. Williams JV, Harris PA, Tollefson SJ, Halburnt-Rush LL, Pingsterhaus JM, et al. 2004. Human metapneumovirus and lower respiratory tract disease in otherwise healthy infants and children. *N Engl J Med* 350: 443-50
6. Williams JV, Wang CK, Yang CF, Tollefson SJ, House FS, et al. 2006. The role of human metapneumovirus in upper respiratory tract infections in children: a 20-year experience. *J Infect Dis* 193: 387-95
7. Boivin G, Abed Y, Pelletier G, Ruel L, Moisan D, et al. 2002. Virological Features and Clinical Manifestations Associated with Human Metapneumovirus: A New Paramyxovirus Responsible for Acute Respiratory-Tract Infections in All Age Groups. *Journal of Infectious Diseases* 186: 1330-34
8. Boivin G, De Serres G, Hamelin ME, Cote S, Argouin M, et al. 2007. An outbreak of severe respiratory tract infection due to human metapneumovirus in a long-term care facility. *Clin Infect Dis* 44: 1152-8
9. van den Hoogen BG, Osterhaus DM, Fouchier RA. 2004. Clinical impact and diagnosis of human metapneumovirus infection. *Pediatr Infect Dis J* 23: S25-32
10. Dunn SR, Ryder AB, Tollefson SJ, Xu M, Saville BR, Williams JV. 2013. Seroepidemiologies of human metapneumovirus and respiratory syncytial virus in young children, determined with a new recombinant fusion protein enzyme-linked immunosorbent assay. *Clin Vaccine Immunol* 20: 1654-6
11. Jain S, Williams DJ, Arnold SR, Ampofo K, Bramley AM, et al. 2015. Community-acquired pneumonia requiring hospitalization among U.S. children. *N Engl J Med* 372: 835-45
12. Williams JV, Edwards KM, Weinberg GA, Griffin MR, Hall CB, et al. 2010. Population-based incidence of human metapneumovirus infection among hospitalized children. *J Infect Dis* 201: 1890-8
13. Edwards KM, Zhu Y, Griffin MR, Weinberg GA, Hall CB, et al. 2013. Burden of human metapneumovirus infection in young children. *N Engl J Med* 368: 633-43

14. van den Hoogen BG, van Doornum GJ, Fockens JC, Cornelissen JJ, Beyer WE, et al. 2003. Prevalence and clinical symptoms of human metapneumovirus infection in hospitalized patients. *J Infect Dis* 188: 1571-7
15. Walsh EE, Peterson DR, Falsey AR. 2008. Human metapneumovirus infections in adults: another piece of the puzzle. *Arch Intern Med* 168: 2489-96
16. Williams JV, Martino R, Rabella N, Otegui M, Parody R, et al. 2005. A prospective study comparing human metapneumovirus with other respiratory viruses in adults with hematologic malignancies and respiratory tract infections. *J Infect Dis* 192: 1061-5
17. Williams JV, Tollefson SJ, Heymann PW, Carper HT, Patrie J, Crowe JE. 2005. Human metapneumovirus infection in children hospitalized for wheezing. *J Allergy Clin Immunol* 115: 1311-2
18. Garcia-Garcia ML, Calvo C, Casas I, Bracamonte T, Rellan A, et al. 2007. Human metapneumovirus bronchiolitis in infancy is an important risk factor for asthma at age 5. *Pediatr Pulmonol* 42: 458-64
19. Lu G, Gonzalez R, Guo L, Wu C, Wu J, et al. 2011. Large-scale seroprevalence analysis of human metapneumovirus and human respiratory syncytial virus infections in Beijing, China. *Virology Journal* 8: 62
20. Lüsebrink J, Wiese C, Thiel A, Tillmann R-L, Ditt V, et al. 2010. High Seroprevalence of Neutralizing Capacity against Human Metapneumovirus in All Age Groups Studied in Bonn, Germany. *Clinical and Vaccine Immunology : CVI* 17: 481-84
21. Scheuerman O, Barkai G, Mandelboim M, Mishali H, Chodick G, Levy I. 2016. Human metapneumovirus (hMPV) infection in immunocompromised children. *J Clin Virol* 83: 12-6
22. Widmer K, Zhu Y, Williams JV, Griffin MR, Edwards KM, Talbot HK. 2012. Rates of Hospitalizations for Respiratory Syncytial Virus, Human Metapneumovirus, and Influenza Virus in Older Adults. *Journal of Infectious Diseases* 206: 56-62
23. Afonso CL, Amarasinghe GK, Bányai K, Bào Y, Basler CF, et al. 2016. TAXONOMY OF THE ORDER MONONEGAVIRALES: UPDATE 2016. *Archives of virology* 161: 2351-60
24. Aberle JH, Aberle SW, Redlberger-Fritz M, Sandhofer MJ, Popow-Kraupp T. 2010. Human metapneumovirus subgroup changes and seasonality during epidemics. *Pediatr Infect Dis J* 29: 1016-8
25. van den Hoogen BG, Herfst S, Sprong L, Cane PA, Forleo-Neto E, et al. 2004. Antigenic and genetic variability of human metapneumoviruses. *Emerg Infect Dis* 10: 658-66
26. van den Hoogen BG, Bestebroer TM, Osterhaus AD, Fouchier RA. 2002. Analysis of the genomic sequence of a human metapneumovirus. *Virology* 295: 119-32
27. Cox RG, Livesay SB, Johnson M, Ohi MD, Williams JV. 2012. The human metapneumovirus fusion protein mediates entry via an interaction with RGD-binding integrins. *J Virol* 86: 12148-60
28. Thammawat S, Sadlon TA, Hallsworth PG, Gordon DL. 2008. Role of cellular glycosaminoglycans and charged regions of viral G protein in human metapneumovirus infection. *J Virol* 82: 11767-74

29. Leyrat C, Renner M, Harlos K, Huiskonen JT, Grimes JM. 2014. Structure and self-assembly of the calcium binding matrix protein of human metapneumovirus. *Structure* 22: 136-48
30. Buchholz UJ, Biacchesi S, Pham QN, Tran KC, Yang L, et al. 2005. Deletion of M2 gene open reading frames 1 and 2 of human metapneumovirus: effects on RNA synthesis, attenuation, and immunogenicity. *J Virol* 79: 6588-97
31. Derdowski A, Peters TR, Glover N, Qian R, Utley TJ, et al. 2008. Human metapneumovirus nucleoprotein and phosphoprotein interact and provide the minimal requirements for inclusion body formation. *The Journal of general virology* 89: 2698-708
32. Cifuentes-Muñoz N, Branttie J, Slaughter KB, Dutch RE. 2017. Human Metapneumovirus Induces Formation of Inclusion Bodies for Efficient Genome Replication and Transcription. *Journal of Virology* 91: e01282-17
33. DiMaio D. 2012. Viruses, Masters at Downsizing. *Cell Host & Microbe* 11: 560-61
34. Wen SC, Williams JV. 2015. New Approaches for Immunization and Therapy against Human Metapneumovirus. *Clinical and Vaccine Immunology : CVI* 22: 858-66
35. Schildgen V, van den Hoogen B, Fouchier R, Tripp RA, Alvarez R, et al. 2011. Human Metapneumovirus: Lessons Learned over the First Decade. *Clinical Microbiology Reviews* 24: 734-54
36. Rima B, Collins P, Easton A, Fouchier R, Kurath G, et al. 2017. ICTV Virus Taxonomy Profile: Pneumoviridae. *Journal of General Virology* 98: 2912-13
37. Paules C, Subbarao K. 2017. Influenza. *The Lancet* 390: 697-708
38. Epstein SL. 2006. Prior H1N1 Influenza Infection and Susceptibility of Cleveland Family Study Participants during the H2N2 Pandemic of 1957: An Experiment of Nature. *The Journal of Infectious Diseases* 193: 49-53
39. Couch RB. 1996. Orthomyxoviruses. In *Medical Microbiology*, ed. th, S Baron. Galveston (TX): University of Texas Medical Branch at Galveston
The University of Texas Medical Branch at Galveston.
40. Gamblin SJ, Skehel JJ. 2010. Influenza Hemagglutinin and Neuraminidase Membrane Glycoproteins. *The Journal of Biological Chemistry* 285: 28403-09
41. La Gruta NL, Turner SJ. 2014. T cell mediated immunity to influenza: mechanisms of viral control. *Trends in Immunology* 35: 396-402
42. McMichael AJ, Gotch FM, Noble GR, Beare PAS. 1983. Cytotoxic T-Cell Immunity to Influenza. *New England Journal of Medicine* 309: 13-17
43. Dupuis S, Jouanguy E, Al-Hajjar S, Fieschi C, Al-Mohsen IZ, et al. 2003. Impaired response to interferon-α/β and lethal viral disease in human STAT1 deficiency. *Nature Genetics* 33: 388
44. Durbin JE, Hackenmiller R, Simon MC, Levy DE. 1996. Targeted disruption of the mouse Stat1 gene results in compromised innate immunity to viral disease. *Cell* 84: 443-50
45. Kato H, Takeuchi O, Sato S, Yoneyama M, Yamamoto M, et al. 2006. Differential roles of MDA5 and RIG-I helicases in the recognition of RNA viruses. *Nature* 441: 101-5

46. Pichlmair A, Schulz O, Tan CP, Näslund TI, Liljeström P, et al. 2006. RIG-I-Mediated Antiviral Responses to Single-Stranded RNA Bearing 5'-Phosphates. *Science* 314: 997-1001
47. Goutagny N, Jiang Z, Tian J, Parroche P, Schickli J, et al. 2010. Cell Type-Specific Recognition of Human Metapneumoviruses (HMPVs) by Retinoic Acid-Inducible Gene I (RIG-I) and TLR7 and Viral Interference of RIG-I Ligand Recognition by HMPV-B1 Phosphoprotein. *The Journal of Immunology* 184: 1168-79
48. Liao S, Bao X, Liu T, Lai S, Li K, et al. 2008. Role of retinoic acid inducible gene-I in human metapneumovirus-induced cellular signalling. *Journal of General Virology* 89: 1978-86
49. Baños-Lara MDR, Ghosh A, Guerrero-Plata A. 2013. Critical Role of MDA5 in the Interferon Response Induced by Human Metapneumovirus Infection in Dendritic Cells and In Vivo. *Journal of Virology* 87: 1242-51
50. Takeuchi O, Akira S. 2009. Innate immunity to virus infection. *Immunol Rev* 227: 75-86
51. Ren J, Liu G, Go J, Kolli D, Zhang G, Bao X. 2014. Human Metapneumovirus M2-2 Protein Inhibits Innate Immune Response in Monocyte-Derived Dendritic Cells. *PLOS ONE* 9: e91865
52. McNab F, Mayer-Barber K, Sher A, Wack A, O'Garra A. 2015. Type I interferons in infectious disease. *Nat Rev Immunol* 15: 87-103
53. Kotenko SV, Durbin JE. 2017. Contribution of type III interferons to antiviral immunity: location, location, location. *J Biol Chem* 292: 7295-303
54. Hastings AK, Erickson JJ, Schuster JE, Boyd KL, Tollefson SJ, et al. 2015. Role of type I interferon signaling in human metapneumovirus pathogenesis and control of viral replication. *J Virol* 89: 4405-20
55. Baños-Lara MDR, Harvey L, Mendoza A, Simms D, Chouljenko VN, et al. 2015. Impact and Regulation of Lambda Interferon Response in Human Metapneumovirus Infection. *Journal of Virology* 89: 730-42
56. Lehtonen A, Matikainen S, Julkunen I. 1997. Interferons up-regulate STAT1, STAT2, and IRF family transcription factor gene expression in human peripheral blood mononuclear cells and macrophages. *J Immunol* 159: 794-803
57. Schneider WM, Chevillotte MD, Rice CM. 2014. Interferon-Stimulated Genes: A Complex Web of Host Defenses. *Annual review of immunology* 32: 513-45
58. Wang IM, Lin H, Goldman SJ, Kobayashi M. 2004. STAT-1 is activated by IL-4 and IL-13 in multiple cell types. *Mol Immunol* 41: 873-84
59. Garcia-Sastre A. 2017. Ten Strategies of Interferon Evasion by Viruses. *Cell Host Microbe* 22: 176-84
60. Audsley MD, Moseley GW. 2013. Paramyxovirus evasion of innate immunity: Diverse strategies for common targets. *World J Virol* 2: 57-70
61. Andrejeva J, Childs KS, Young DF, Carlos TS, Stock N, et al. 2004. The V proteins of paramyxoviruses bind the IFN-inducible RNA helicase, mda-5, and inhibit its activation of the IFN-β promoter. *Proceedings of the National Academy of Sciences of the United States of America* 101: 17264-69

62. Childs K, Randall R, Goodbourn S. 2012. Paramyxovirus V proteins interact with the RNA Helicase LGP2 to inhibit RIG-I-dependent interferon induction. *J Virol* 86: 3411-21
63. Parisien JP, Bamming D, Komuro A, Ramachandran A, Rodriguez JJ, et al. 2009. A shared interface mediates paramyxovirus interference with antiviral RNA helicases MDA5 and LGP2. *J Virol* 83: 7252-60
64. Ding B, Zhang L, Li Z, Zhong Y, Tang Q, et al. 2017. The Matrix Protein of Human Parainfluenza Virus Type 3 Induces Mitophagy that Suppresses Interferon Responses. *Cell Host & Microbe* 21: 538-47.e4
65. Dinwiddie DL, Harrod KS. 2008. Human metapneumovirus inhibits IFN-alpha signaling through inhibition of STAT1 phosphorylation. *Am J Respir Cell Mol Biol* 38: 661-70
66. Bao X, Liu T, Shan Y, Li K, Garofalo RP, Casola A. 2008. Human Metapneumovirus Glycoprotein G Inhibits Innate Immune Responses. *PLOS Pathogens* 4: e1000077
67. Bao X, Kolli D, Ren J, Liu T, Garofalo RP, Casola A. 2013. Human Metapneumovirus Glycoprotein G Disrupts Mitochondrial Signaling in Airway Epithelial Cells. *PLOS ONE* 8: e62568
68. Cheemarla NR, Guerrero-Plata A. 2017. Human Metapneumovirus Attachment Protein Contributes to Neutrophil Recruitment into the Airways of Infected Mice. *Viruses* 9: 310
69. Hastings AK, Amato KR, Wen SC, Peterson LS, Williams JV. 2016. Human metapneumovirus small hydrophobic (SH) protein downregulates type I IFN pathway signaling by affecting STAT1 expression and phosphorylation. *Virology* 494: 248-56
70. Kolli D, Bao X, Liu T, Hong C, Wang T, et al. 2011. Human Metapneumovirus Glycoprotein G Inhibits TLR4-Dependent Signaling in Monocyte-Derived Dendritic Cells. *The Journal of Immunology* 187: 47-54
71. Ren J, Wang Q, Kolli D, Prusak DJ, Tseng C-TK, et al. 2012. Human Metapneumovirus M2-2 Protein Inhibits Innate Cellular Signaling by Targeting MAVS. *Journal of Virology* 86: 13049-61
72. Biacchesi S, Skiadopoulos MH, Yang L, Lamirande EW, Tran KC, et al. 2004. Recombinant Human Metapneumovirus Lacking the Small Hydrophobic SH and/or Attachment G Glycoprotein: Deletion of G Yields a Promising Vaccine Candidate. *Journal of Virology* 78: 12877-87
73. Tedcastle AB, Fenwick F, Robinson MJ, Toms GL. 2014. Immunogenicity in mice of human metapneumovirus with a truncated SH glycoprotein. *J Med Virol* 86: 547-57
74. Monsalvo AC, Batalle JP, Lopez MF, Krause JC, Klemenc J, et al. 2011. Severe pandemic 2009 H1N1 influenza disease due to pathogenic immune complexes. *Nature medicine* 17: 195-99
75. Kurt-Jones EA, Popova L, Kwinn L, Haynes LM, Jones LP, et al. 2000. Pattern recognition receptors TLR4 and CD14 mediate response to respiratory syncytial virus. *Nat Immunol* 1: 398-401

76. Ren J, Kolli D, Liu T, Xu R, Garofalo RP, et al. 2011. Human Metapneumovirus Inhibits IFN-β Signaling by Downregulating Jak1 and Tyk2 Cellular Levels. *PLOS ONE* 6: e24496
77. Mitzel DN, Jaramillo RJ, Stout-Delgado H, Senft AP, Harrod KS. 2014. Human metapneumovirus inhibits the IL-6-induced JAK/STAT3 signalling cascade in airway epithelium. *Journal of General Virology* 95: 26-37
78. Le Nouen C, Hillyer P, Brock LG, Winter CC, Rabin RL, et al. 2014. Human metapneumovirus SH and G glycoproteins inhibit macropinocytosis-mediated entry into human dendritic cells and reduce CD4+ T cell activation. *J Virol* 88: 6453-69
79. Barik S. 2013. Respiratory Syncytial Virus Mechanisms to Interfere with Type 1 Interferons. In *Challenges and Opportunities for Respiratory Syncytial Virus Vaccines*, ed. LJ Anderson, BS Graham, pp. 173-91. Berlin, Heidelberg: Springer Berlin Heidelberg
80. Chowdhury FZ, Farrar JD. 2013. STAT2: A shape-shifting anti-viral super STAT. *JAK-STAT* 2: e23633
81. Park C, Lecomte MJ, Schindler C. 1999. Murine Stat2 is uncharacteristically divergent. *Nucleic Acids Res* 27: 4191-9
82. Lo MS, Brazas RM, Holtzman MJ. 2005. Respiratory syncytial virus nonstructural proteins NS1 and NS2 mediate inhibition of Stat2 expression and alpha/beta interferon responsiveness. *J Virol* 79: 9315-9
83. Ramaswamy M, Shi L, Varga SM, Barik S, Behlke MA, Look DC. 2006. Respiratory syncytial virus nonstructural protein 2 specifically inhibits type I interferon signal transduction. *Virology* 344: 328-39
84. Elliott J, Lynch OT, Suessmuth Y, Qian P, Boyd CR, et al. 2007. Respiratory syncytial virus NS1 protein degrades STAT2 by using the Elongin-Cullin E3 ligase. *J Virol* 81: 3428-36
85. Swedan S, Musiyenko A, Barik S. 2009. Respiratory syncytial virus nonstructural proteins decrease levels of multiple members of the cellular interferon pathways. *J Virol* 83: 9682-93
86. Swedan S, Andrews J, Majumdar T, Musiyenko A, Barik S. 2011. Multiple functional domains and complexes of the two nonstructural proteins of human respiratory syncytial virus contribute to interferon suppression and cellular location. *J Virol* 85: 10090-100
87. Zheng J, Yang P, Tang Y, Pan Z, Zhao D. 2015. Respiratory Syncytial Virus Nonstructural Proteins Upregulate SOCS1 and SOCS3 in the Different Manner from Endogenous IFN Signaling. *J Immunol Res* 2015: 738547
88. Croker BA, Kiu H, Nicholson SE. 2008. SOCS Regulation of the JAK/STAT Signalling Pathway. *Seminars in cell & developmental biology* 19: 414-22
89. Schomacker H, Hebner RM, Boonyaratanakornkit J, Surman S, Amaro-Carambot E, et al. 2012. The C proteins of human parainfluenza virus type 1 block IFN signaling by binding and retaining Stat1 in perinuclear aggregates at the late endosome. *PLoS One* 7: e28382
90. Andrejeva J, Young DF, Goodbourn S, Randall RE. 2002. Degradation of STAT1 and STAT2 by the V Proteins of Simian Virus 5 and Human Parainfluenza Virus

Type 2, Respectively: Consequences for Virus Replication in the Presence of Alpha/Beta and Gamma Interferons. *Journal of Virology* 76: 2159-67
91. Parisien JP, Lau JF, Rodriguez JJ, Sullivan BM, Moscona A, et al. 2001. The V protein of human parainfluenza virus 2 antagonizes type I interferon responses by destabilizing signal transducer and activator of transcription 2. *Virology* 283: 230-9
92. Didcock L, Young DF, Goodbourn S, Randall RE. 1999. The V Protein of Simian Virus 5 Inhibits Interferon Signalling by Targeting STAT1 for Proteasome-Mediated Degradation. *Journal of Virology* 73: 9928-33
93. Kraus TA, Garza L, Horvath CM. 2008. Enabled interferon signaling evasion in an immune-competent transgenic mouse model of parainfluenza virus 5 infection. *Virology* 371: 196-205
94. Gotoh B, Takeuchi K, Komatsu T, Yokoo J. 2003. The STAT2 activation process is a crucial target of Sendai virus C protein for the blockade of alpha interferon signaling. *J Virol* 77: 3360-70
95. Gotoh B, Takeuchi K, Komatsu T, Yokoo J, Kimura Y, et al. 1999. Knockout of the Sendai virus C gene eliminates the viral ability to prevent the interferon-alpha/beta-mediated responses. *FEBS Lett* 459: 205-10
96. Kato A, Cortese-Grogan C, Moyer SA, Sugahara F, Sakaguchi T, et al. 2004. Characterization of the amino acid residues of sendai virus C protein that are critically involved in its interferon antagonism and RNA synthesis down-regulation. *J Virol* 78: 7443-54
97. Garcin D, Curran J, Kolakofsky D. 2000. Sendai virus C proteins must interact directly with cellular components to interfere with interferon action. *J Virol* 74: 8823-30
98. Garcin D, Marq JB, Goodbourn S, Kolakofsky D. 2003. The amino-terminal extensions of the longer Sendai virus C proteins modulate pY701-Stat1 and bulk Stat1 levels independently of interferon signaling. *J Virol* 77: 2321-9
99. Garcin D, Marq JB, Iseni F, Martin S, Kolakofsky D. 2004. A short peptide at the amino terminus of the Sendai virus C protein acts as an independent element that induces STAT1 instability. *J Virol* 78: 8799-811
100. Garcin D, Marq JB, Strahle L, le Mercier P, Kolakofsky D. 2002. All four Sendai Virus C proteins bind Stat1, but only the larger forms also induce its mono-ubiquitination and degradation. *Virology* 295: 256-65
101. Rodriguez JJ, Wang LF, Horvath CM. 2003. Hendra virus V protein inhibits interferon signaling by preventing STAT1 and STAT2 nuclear accumulation. *J Virol* 77: 11842-5
102. Hagmaier K, Stock N, Goodbourn S, Wang LF, Randall R. 2006. A single amino acid substitution in the V protein of Nipah virus alters its ability to block interferon signalling in cells from different species. *J Gen Virol* 87: 3649-53
103. Rodriguez JJ, Cruz CD, Horvath CM. 2004. Identification of the nuclear export signal and STAT-binding domains of the Nipah virus V protein reveals mechanisms underlying interferon evasion. *J Virol* 78: 5358-67
104. Rodriguez JJ, Parisien JP, Horvath CM. 2002. Nipah virus V protein evades alpha and gamma interferons by preventing STAT1 and STAT2 activation and nuclear accumulation. *J Virol* 76: 11476-83

105. Ciancanelli MJ, Volchkova VA, Shaw ML, Volchkov VE, Basler CF. 2009. Nipah virus sequesters inactive STAT1 in the nucleus via a P gene-encoded mechanism. *J Virol* 83: 7828-41
106. Shaw ML, Garcia-Sastre A, Palese P, Basler CF. 2004. Nipah virus V and W proteins have a common STAT1-binding domain yet inhibit STAT1 activation from the cytoplasmic and nuclear compartments, respectively. *J Virol* 78: 5633-41
107. Caignard G, Guerbois M, Labernardiere JL, Jacob Y, Jones LM, et al. 2007. Measles virus V protein blocks Jak1-mediated phosphorylation of STAT1 to escape IFN-alpha/beta signaling. *Virology* 368: 351-62
108. Takeuchi K, Kadota SI, Takeda M, Miyajima N, Nagata K. 2003. Measles virus V protein blocks interferon (IFN)-alpha/beta but not IFN-gamma signaling by inhibiting STAT1 and STAT2 phosphorylation. *FEBS Lett* 545: 177-82
109. Ramachandran A, Parisien JP, Horvath CM. 2008. STAT2 is a primary target for measles virus V protein-mediated alpha/beta interferon signaling inhibition. *J Virol* 82: 8330-8
110. Palosaari H, Parisien JP, Rodriguez JJ, Ulane CM, Horvath CM. 2003. STAT protein interference and suppression of cytokine signal transduction by measles virus V protein. *J Virol* 77: 7635-44
111. Caignard G, Bourai M, Jacob Y, Tangy F, Vidalain PO. 2009. Inhibition of IFN-alpha/beta signaling by two discrete peptides within measles virus V protein that specifically bind STAT1 and STAT2. *Virology* 383: 112-20
112. Takayama I, Sato H, Watanabe A, Omi-Furutani M, Sugai A, et al. 2012. The nucleocapsid protein of measles virus blocks host interferon response. *Virology* 424: 45-55
113. Nishio M, Garcin D, Simonet V, Kolakofsky D. 2002. The carboxyl segment of the mumps virus V protein associates with Stat proteins in vitro via a tryptophan-rich motif. *Virology* 300: 92-9
114. Kubota T, Yokosawa N, Yokota S, Fujii N, Tashiro M, Kato A. 2005. Mumps virus V protein antagonizes interferon without the complete degradation of STAT1. *J Virol* 79: 4451-9
115. Kubota T, Yokosawa N, Yokota S, Fujii N. 2001. C terminal CYS-RICH region of mumps virus structural V protein correlates with block of interferon alpha and gamma signal transduction pathway through decrease of STAT 1-alpha. *Biochem Biophys Res Commun* 283: 255-9
116. Yokosawa N, Yokota S, Kubota T, Fujii N. 2002. C-terminal region of STAT-1alpha is not necessary for its ubiquitination and degradation caused by mumps virus V protein. *J Virol* 76: 12683-90
117. Didcock L, Young DF, Goodbourn S, Randall RE. 1999. Sendai virus and simian virus 5 block activation of interferon-responsive genes: importance for virus pathogenesis. *J Virol* 73: 3125-33
118. Young DF, Chatziandreou N, He B, Goodbourn S, Lamb RA, Randall RE. 2001. Single amino acid substitution in the V protein of simian virus 5 differentiates its ability to block interferon signaling in human and murine cells. *J Virol* 75: 3363-70

119. Parisien JP, Lau JF, Horvath CM. 2002. STAT2 acts as a host range determinant for species-specific paramyxovirus interferon antagonism and simian virus 5 replication. *J Virol* 76: 6435-41
120. Ashour J, Laurent-Rolle M, Shi PY, Garcia-Sastre A. 2009. NS5 of dengue virus mediates STAT2 binding and degradation. *J Virol* 83: 5408-18
121. Mazzon M, Jones M, Davidson A, Chain B, Jacobs M. 2009. Dengue virus NS5 inhibits interferon-alpha signaling by blocking signal transducer and activator of transcription 2 phosphorylation. *J Infect Dis* 200: 1261-70
122. Ashour J, Morrison J, Laurent-Rolle M, Belicha-Villanueva A, Plumlee CR, et al. 2010. Mouse STAT2 restricts early dengue virus replication. *Cell Host Microbe* 8: 410-21
123. Grant A, Ponia Sanket S, Tripathi S, Balasubramaniam V, Miorin L, et al. 2016. Zika Virus Targets Human STAT2 to Inhibit Type I Interferon Signaling. *Cell Host & Microbe* 19: 882-90
124. Gorman MJ, Caine EA, Zaitsev K, Begley MC, Weger-Lucarelli J, et al. 2018. An Immunocompetent Mouse Model of Zika Virus Infection. *Cell Host & Microbe* 23: 672-85.e6
125. Kolli D, Bataki EL, Spetch L, Guerrero-Plata A, Jewell AM, et al. 2008. T lymphocytes contribute to antiviral immunity and pathogenesis in experimental human metapneumovirus infection. *J Virol* 82: 8560-9
126. Erickson JJ, Rogers MC, Hastings AK, Tollefson SJ, Williams JV. 2014. Programmed Death-1 Impairs Secondary Effector Lung CD8+ T Cells during Respiratory Virus Reinfection. *J Immunol* 193: 5108-17
127. Alvarez R, Harrod KS, Shieh WJ, Zaki S, Tripp RA. 2004. Human metapneumovirus persists in BALB/c mice despite the presence of neutralizing antibodies. *J Virol* 78: 14003-11
128. Wen SC, Schuster JE, Gilchuk P, Boyd KL, Joyce S, Williams JV. 2015. Lung CD8+ T Cell Impairment Occurs during Human Metapneumovirus Infection despite Virus-Like Particle Induction of Functional CD8+ T Cells. *J Virol* 89: 8713-26
129. Bauer TT, Ewig S, Rodloff AC, Müller EE. 2006. Acute Respiratory Distress Syndrome and Pneumonia: A Comprehensive Review of Clinical Data. *Clinical Infectious Diseases* 43: 748-56
130. Englund J, Feuchtinger T, Ljungman P. 2011. Viral infections in immunocompromised patients. *Biol Blood Marrow Transplant* 17: S2-5
131. Chang J, Braciale TJ. 2002. Respiratory syncytial virus infection suppresses lung CD8+ T-cell effector activity and peripheral CD8+ T-cell memory in the respiratory tract. *Nat Med* 8: 54-60
132. Chang J, Srikiatkhachorn A, Braciale TJ. 2001. Visualization and characterization of respiratory syncytial virus F-specific CD8(+) T cells during experimental virus infection. *J Immunol* 167: 4254-60
133. Vallbracht S, Unsold H, Ehl S. 2006. Functional impairment of cytotoxic T cells in the lung airways following respiratory virus infections. *Eur J Immunol* 36: 1434-42
134. Lukens MV, Claassen EA, de Graaff PM, van Dijk ME, Hoogerhout P, et al. 2006. Characterization of the CD8+ T cell responses directed against respiratory

syncytial virus during primary and secondary infection in C57BL/6 mice. *Virology* 352: 157-68
135. Gray PM, Arimilli S, Palmer EM, Parks GD, Alexander-Miller MA. 2005. Altered function in CD8+ T cells following paramyxovirus infection of the respiratory tract. *J Virol* 79: 3339-49
136. Claassen EA, van der Kant PA, Rychnavska ZS, van Bleek GM, Easton AJ, van der Most RG. 2005. Activation and inactivation of antiviral CD8 T cell responses during murine pneumovirus infection. *J Immunol* 175: 6597-604
137. DiNapoli JM, Murphy BR, Collins PL, Bukreyev A. 2008. Impairment of the CD8+ T cell response in lungs following infection with human respiratory syncytial virus is specific to the anatomical site rather than the virus, antigen, or route of infection. *Virol J* 5: 105
138. Erickson JJ, Gilchuk P, Hastings AK, Tollefson SJ, Johnson M, et al. 2012. Viral acute lower respiratory infections impair CD8+ T cells through PD-1. *J Clin Invest* 122: 2967-82
139. Erickson JJ, Rogers MC, Hastings AK, Tollefson SJ, Williams JV. 2014. Programmed death-1 impairs secondary effector lung CD8(+) T cells during respiratory virus reinfection. *J Immunol* 193: 5108-17
140. Rudensky AY. 2011. Regulatory T cells and Foxp3. *Immunol Rev* 241: 260-8
141. Brunkow ME, Jeffery EW, Hjerrild KA, Paeper B, Clark LB, et al. 2001. Disruption of a new forkhead/winged-helix protein, scurfin, results in the fatal lymphoproliferative disorder of the scurfy mouse. *Nat Genet* 27: 68-73
142. Kmieciak M, Gowda M, Graham L, Godder K, Bear HD, et al. 2009. Human T cells express CD25 and Foxp3 upon activation and exhibit effector/memory phenotypes without any regulatory/suppressor function. *Journal of Translational Medicine* 7: 89-89
143. Abbas AK, Benoist C, Bluestone JA, Campbell DJ, Ghosh S, et al. 2013. Regulatory T cells: recommendations to simplify the nomenclature. *Nat Immunol* 14: 307-8
144. Kretschmer K, Apostolou I, Hawiger D, Khazaie K, Nussenzweig MC, von Boehmer H. 2005. Inducing and expanding regulatory T cell populations by foreign antigen. *Nat Immunol* 6: 1219-27
145. Schmitt EG, Williams CB. 2013. Generation and function of induced regulatory T cells. *Front Immunol* 4: 152
146. Yadav M, Stephan S, Bluestone JA. 2013. Peripherally induced tregs - role in immune homeostasis and autoimmunity. *Front Immunol* 4: 232
147. Horwitz DA, Zheng SG, Wang J, Gray JD. 2008. Critical role of IL-2 and TGF-beta in generation, function and stabilization of Foxp3+CD4+ Treg. *Eur J Immunol* 38: 912-5
148. Selvaraj RK, Geiger TL. 2007. A kinetic and dynamic analysis of Foxp3 induced in T cells by TGF-beta. *J Immunol* 179: 11 p following 1390
149. Polansky JK, Kretschmer K, Freyer J, Floess S, Garbe A, et al. 2008. DNA methylation controls Foxp3 gene expression. *Eur J Immunol* 38: 1654-63
150. Floess S, Freyer J, Siewert C, Baron U, Olek S, et al. 2007. Epigenetic control of the foxp3 locus in regulatory T cells. *PLoS Biol* 5: e38

151. Chen Q, Kim YC, Laurence A, Punkosdy GA, Shevach EM. 2011. IL-2 Controls the Stability of Foxp3 expression in TGF-β-induced Foxp3(+) T cells in vivo. *Journal of immunology (Baltimore, Md. : 1950)* 186: 6329-37
152. Ohkura N, Hamaguchi M, Morikawa H, Sugimura K, Tanaka A, et al. 2012. T cell receptor stimulation-induced epigenetic changes and Foxp3 expression are independent and complementary events required for Treg cell development. *Immunity* 37: 785-99
153. Miyao T, Floess S, Setoguchi R, Luche H, Fehling HJ, et al. 2012. Plasticity of Foxp3(+) T cells reflects promiscuous Foxp3 expression in conventional T cells but not reprogramming of regulatory T cells. *Immunity* 36: 262-75
154. Chinen T, Kannan AK, Levine AG, Fan X, Klein U, et al. 2016. An essential role for IL-2 receptor in regulatory T cell function. *Nature immunology* 17: 1322-33
155. Josefowicz SZ, Lu LF, Rudensky AY. 2012. Regulatory T cells: mechanisms of differentiation and function. *Annu Rev Immunol* 30: 531-64
156. Vignali DA, Collison LW, Workman CJ. 2008. How regulatory T cells work. *Nat Rev Immunol* 8: 523-32
157. Nakamura K, Kitani A, Strober W. 2001. Cell contact-dependent immunosuppression by CD4(+)CD25(+) regulatory T cells is mediated by cell surface-bound transforming growth factor beta. *J Exp Med* 194: 629-44
158. Oida T, Zhang X, Goto M, Hachimura S, Totsuka M, et al. 2003. CD4+CD25- T cells that express latency-associated peptide on the surface suppress CD4+CD45RBhigh-induced colitis by a TGF-beta-dependent mechanism. *J Immunol* 170: 2516-22
159. Francisco LM, Salinas VH, Brown KE, Vanguri VK, Freeman GJ, et al. 2009. PD-L1 regulates the development, maintenance, and function of induced regulatory T cells. *J Exp Med* 206: 3015-29
160. Sakaguchi S, Sakaguchi N, Asano M, Itoh M, Toda M. 1995. Immunologic self-tolerance maintained by activated T cells expressing IL-2 receptor alpha-chains (CD25). Breakdown of a single mechanism of self-tolerance causes various autoimmune diseases. *J Immunol* 155: 1151-64
161. Kohm AP, McMahon JS, Podojil JR, Begolka WS, DeGutes M, et al. 2006. Cutting Edge: Anti-CD25 monoclonal antibody injection results in the functional inactivation, not depletion, of CD4+CD25+ T regulatory cells. *J Immunol* 176: 3301-5
162. McNeill A, Spittle E, Backstrom BT. 2007. Partial depletion of CD69low-expressing natural regulatory T cells with the anti-CD25 monoclonal antibody PC61. *Scand J Immunol* 65: 63-9
163. Corthay A. 2009. How do regulatory T cells work? *Scand J Immunol* 70: 326-36
164. Fontenot JD, Rasmussen JP, Williams LM, Dooley JL, Farr AG, Rudensky AY. 2005. Regulatory T cell lineage specification by the forkhead transcription factor foxp3. *Immunity* 22: 329-41
165. Fulton RB, Meyerholz DK, Varga SM. 2010. Foxp3+ CD4 regulatory T cells limit pulmonary immunopathology by modulating the CD8 T cell response during respiratory syncytial virus infection. *J Immunol* 185: 2382-92
166. Hori S, Nomura T, Sakaguchi S. 2003. Control of regulatory T cell development by the transcription factor Foxp3. *Science* 299: 1057-61

167. Kim JM, Rasmussen JP, Rudensky AY. 2007. Regulatory T cells prevent catastrophic autoimmunity throughout the lifespan of mice. *Nat Immunol* 8: 191-97
168. Lahl K, Loddenkemper C, Drouin C, Freyer J, Arnason J, et al. 2007. Selective depletion of Foxp3+ regulatory T cells induces a scurfy-like disease. *J Exp Med* 204: 57-63
169. Ziegler SF. 2007. FOXP3: not just for regulatory T cells anymore. *Eur J Immunol* 37: 21-3
170. Christiaansen AF, Boggiatto PM, Varga SM. 2014. Limitations of Foxp3(+) Treg depletion following viral infection in DEREG mice. *J Immunol Methods* 406: 58-65
171. Raiden S, Pandolfi J, Payaslian F, Anderson M, Rivarola N, et al. 2014. Depletion of circulating regulatory T cells during severe respiratory syncytial virus infection in young children. *Am J Respir Crit Care Med* 189: 865-8
172. Lee DC, Harker JA, Tregoning JS, Atabani SF, Johansson C, et al. 2010. CD25+ natural regulatory T cells are critical in limiting innate and adaptive immunity and resolving disease following respiratory syncytial virus infection. *J Virol* 84: 8790-8
173. Ruckwardt TJ, Bonaparte KL, Nason MC, Graham BS. 2009. Regulatory T cells promote early influx of CD8+ T cells in the lungs of respiratory syncytial virus-infected mice and diminish immunodominance disparities. *J Virol* 83: 3019-28
174. Couper KN, Blount DG, Riley EM. 2008. IL-10: the master regulator of immunity to infection. *J Immunol* 180: 5771-7
175. Weiss KA, Christiaansen AF, Fulton RB, Meyerholz DK, Varga SM. 2011. Multiple CD4+ T cell subsets produce immunomodulatory IL-10 during respiratory syncytial virus infection. *J Immunol* 187: 3145-54
176. Loebbermann J, Schnoeller C, Thornton H, Durant L, Sweeney NP, et al. 2012. IL-10 regulates viral lung immunopathology during acute respiratory syncytial virus infection in mice. *PLoS One* 7: e32371
177. Loebbermann J, Thornton H, Durant L, Sparwasser T, Webster KE, et al. 2012. Regulatory T cells expressing granzyme B play a critical role in controlling lung inflammation during acute viral infection. *Mucosal Immunol* 5: 161-72
178. Liu J, Ruckwardt TJ, Chen M, Johnson TR, Graham BS. 2009. Characterization of respiratory syncytial virus M- and M2-specific CD4 T cells in a murine model. *J Virol* 83: 4934-41
179. Liu J, Ruckwardt TJ, Chen M, Nicewonger JD, Johnson TR, Graham BS. 2010. Epitope-specific regulatory CD4 T cells reduce virus-induced illness while preserving CD8 T-cell effector function at the site of infection. *J Virol* 84: 10501-9
180. Suvas S, Kumaraguru U, Pack CD, Lee S, Rouse BT. 2003. CD4+CD25+ T cells regulate virus-specific primary and memory CD8+ T cell responses. *J Exp Med* 198: 889-901
181. Durant LR, Makris S, Voorburg CM, Loebbermann J, Johansson C, Openshaw PJ. 2013. Regulatory T cells prevent Th2 immune responses and pulmonary eosinophilia during respiratory syncytial virus infection in mice. *J Virol* 87: 10946-54
182. Jartti T, Gern JE. 2017. Role of viral infections in the development and exacerbation of asthma in children. *J Allergy Clin Immunol* 140: 895-906

183. Fahy JV. 2015. Type 2 inflammation in asthma — present in most, absent in many. *Nature reviews. Immunology* 15: 57-65
184. Krishnamoorthy N, Khare A, Oriss TB, Raundhal M, Morse C, et al. 2012. Early infection with respiratory syncytial virus impairs regulatory T cell function and increases susceptibility to allergic asthma. *Nat Med* 18: 1525-30
185. Wang J, Kong L, Luo Q, Li B, Wu J, et al. 2014. Dual effects of respiratory syncytial virus infections on airway inflammation by regulation of Th17/Treg responses in ovalbumin-challenged mice. *Inflammation* 37: 1984-2005
186. Liu J, Cao S, Peppers G, Kim SH, Graham BS. 2014. Clonotype-specific avidity influences the dynamics and hierarchy of virus-specific regulatory and effector CD4(+) T-cell responses. *Eur J Immunol* 44: 1058-68
187. Zheng Y, Chaudhry A, Kas A, deRoos P, Kim JM, et al. 2009. Regulatory T-cell suppressor program co-opts transcription factor IRF4 to control T(H)2 responses. *Nature* 458: 351-6
188. Tian L, Altin JA, Makaroff LE, Franckaert D, Cook MC, et al. 2011. Foxp3(+) regulatory T cells exert asymmetric control over murine helper responses by inducing Th2 cell apoptosis. *Blood* 118: 1845-53
189. Josefowicz SZ, Niec RE, Kim HY, Treuting P, Chinen T, et al. 2012. Extrathymically generated regulatory T cells control mucosal TH2 inflammation. *Nature* 482: 395-9
190. Schulze B, Piehler D, Eschke M, von Buttlar H, Kohler G, et al. 2014. CD4(+) FoxP3(+) regulatory T cells suppress fatal T helper 2 cell immunity during pulmonary fungal infection. *Eur J Immunol* 44: 3596-604
191. Wiesner DL, Smith KD, Kotov DI, Nielsen JN, Bohjanen PR, Nielsen K. 2016. Regulatory T Cell Induction and Retention in the Lungs Drives Suppression of Detrimental Type 2 Th Cells During Pulmonary Cryptococcal Infection. *J Immunol* 196: 365-74
192. Betts RJ, Prabhu N, Ho AW, Lew FC, Hutchinson PE, et al. 2012. Influenza A virus infection results in a robust, antigen-responsive, and widely disseminated Foxp3+ regulatory T cell response. *J Virol* 86: 2817-25
193. Bedoya F, Cheng GS, Leibow A, Zakhary N, Weissler K, et al. 2013. Viral antigen induces differentiation of Foxp3+ natural regulatory T cells in influenza virus-infected mice. *J Immunol* 190: 6115-25
194. Haeryfar SM, DiPaolo RJ, Tscharke DC, Bennink JR, Yewdell JW. 2005. Regulatory T cells suppress CD8+ T cell responses induced by direct priming and cross-priming and moderate immunodominance disparities. *J Immunol* 174: 3344-51
195. Ballesteros-Tato A, Leon B, Lund FE, Randall TD. 2013. CD4+ T helper cells use CD154-CD40 interactions to counteract T reg cell-mediated suppression of CD8+ T cell responses to influenza. *J Exp Med* 210: 1591-601
196. Betts RJ, Ho AW, Kemeny DM. 2011. Partial depletion of natural CD4(+)CD25(+) regulatory T cells with anti-CD25 antibody does not alter the course of acute influenza A virus infection. *PLoS One* 6: e27849
197. Moser EK, Hufford MM, Braciale TJ. 2014. Late engagement of CD86 after influenza virus clearance promotes recovery in a FoxP3+ regulatory T cell dependent manner. *PLoS Pathog* 10: e1004315

198. Arpaia N, Green JA, Moltedo B, Arvey A, Hemmers S, et al. 2015. A Distinct Function of Regulatory T Cells in Tissue Protection. *Cell* 162: 1078-89
199. Singer BD, Mock JR, Aggarwal NR, Garibaldi BT, Sidhaye VK, et al. 2015. Regulatory T cell DNA methyltransferase inhibition accelerates resolution of lung inflammation. *Am J Respir Cell Mol Biol* 52: 641-52
200. Sakthivel P, Gereke M, Breithaupt A, Fuchs D, Gigliotti L, et al. 2014. Attenuation of immune-mediated influenza pneumonia by targeting the inducible co-stimulator (ICOS) molecule on T cells. *PLoS One* 9: e100970
201. Roquilly A, McWilliam HEG, Jacqueline C, Tian Z, Cinotti R, et al. 2017. Local Modulation of Antigen-Presenting Cell Development after Resolution of Pneumonia Induces Long-Term Susceptibility to Secondary Infections. *Immunity* 47: 135-47.e5
202. Dyck L, Mills KHG. 2017. Immune checkpoints and their inhibition in cancer and infectious diseases. *Eur J Immunol* 47: 765-79
203. Wherry EJ. 2011. T cell exhaustion. *Nat Immunol* 12: 492-9
204. Wherry EJ, Kurachi M. 2015. Molecular and cellular insights into T cell exhaustion. *Nat Rev Immunol* 15: 486-99
205. Wherry EJ, Blattman JN, Murali-Krishna K, van der Most R, Ahmed R. 2003. Viral persistence alters CD8 T-cell immunodominance and tissue distribution and results in distinct stages of functional impairment. *J Virol* 77: 4911-27
206. Wilson RAM, Evans TRJ, Fraser AR, Nibbs RJB. 2018. Immune checkpoint inhibitors: new strategies to checkmate cancer. *Clin Exp Immunol* 191: 133-48
207. Freeman GJ, Long AJ, Iwai Y, Bourque K, Chernova T, et al. 2000. Engagement of the PD-1 immunoinhibitory receptor by a novel B7 family member leads to negative regulation of lymphocyte activation. *J Exp Med* 192: 1027-34
208. Latchman Y, Wood CR, Chernova T, Chaudhary D, Borde M, et al. 2001. PD-L2 is a second ligand for PD-1 and inhibits T cell activation. *Nat Immunol* 2: 261-8
209. Chemnitz JM, Parry RV, Nichols KE, June CH, Riley JL. 2004. SHP-1 and SHP-2 associate with immunoreceptor tyrosine-based switch motif of programmed death 1 upon primary human T cell stimulation, but only receptor ligation prevents T cell activation. *J Immunol* 173: 945-54
210. Sheppard KA, Fitz LJ, Lee JM, Benander C, George JA, et al. 2004. PD-1 inhibits T-cell receptor induced phosphorylation of the ZAP70/CD3zeta signalosome and downstream signaling to PKCtheta. *FEBS Lett* 574: 37-41
211. Hui E, Cheung J, Zhu J, Su X, Taylor MJ, et al. 2017. T cell costimulatory receptor CD28 is a primary target for PD-1-mediated inhibition. *Science* 355: 1428-33
212. Patsoukis N, Brown J, Petkova V, Liu F, Li L, Boussiotis VA. 2012. Selective effects of PD-1 on Akt and Ras pathways regulate molecular components of the cell cycle and inhibit T cell proliferation. *Sci Signal* 5: ra46
213. Nurieva R, Thomas S, Nguyen T, Martin-Orozco N, Wang Y, et al. 2006. T-cell tolerance or function is determined by combinatorial costimulatory signals. *Embo j* 25: 2623-33
214. Patsoukis N, Bardhan K, Chatterjee P, Sari D, Liu B, et al. 2015. PD-1 alters T-cell metabolic reprogramming by inhibiting glycolysis and promoting lipolysis and fatty acid oxidation. *Nat Commun* 6: 6692

215. Keir ME, Butte MJ, Freeman GJ, Sharpe AH. 2008. PD-1 and its ligands in tolerance and immunity. *Annu Rev Immunol* 26: 677-704
216. Barber DL, Wherry EJ, Masopust D, Zhu B, Allison JP, et al. 2006. Restoring function in exhausted CD8 T cells during chronic viral infection. *Nature* 439: 682-7
217. Alsaab HO, Sau S, Alzhrani R, Tatiparti K, Bhise K, et al. 2017. PD-1 and PD-L1 Checkpoint Signaling Inhibition for Cancer Immunotherapy: Mechanism, Combinations, and Clinical Outcome. *Front Pharmacol* 8: 561
218. Petrovas C, Casazza JP, Brenchley JM, Price DA, Gostick E, et al. 2006. PD-1 is a regulator of virus-specific CD8+ T cell survival in HIV infection. *J Exp Med* 203: 2281-92
219. Nakamoto N, Kaplan DE, Coleclough J, Li Y, Valiga ME, et al. 2008. Functional restoration of HCV-specific CD8 T cells by PD-1 blockade is defined by PD-1 expression and compartmentalization. *Gastroenterology* 134: 1927-37, 37.e1-2
220. Radziewicz H, Ibegbu CC, Fernandez ML, Workowski KA, Obideen K, et al. 2007. Liver-infiltrating lymphocytes in chronic human hepatitis C virus infection display an exhausted phenotype with high levels of PD-1 and low levels of CD127 expression. *J Virol* 81: 2545-53
221. Boni C, Fisicaro P, Valdatta C, Amadei B, Di Vincenzo P, et al. 2007. Characterization of hepatitis B virus (HBV)-specific T-cell dysfunction in chronic HBV infection. *J Virol* 81: 4215-25
222. Fisicaro P, Valdatta C, Massari M, Loggi E, Biasini E, et al. 2010. Antiviral intrahepatic T-cell responses can be restored by blocking programmed death-1 pathway in chronic hepatitis B. *Gastroenterology* 138: 682-93, 93.e1-4
223. Attanasio J, Wherry EJ. 2016. Costimulatory and Coinhibitory Receptor Pathways in Infectious Disease. *Immunity* 44: 1052-68
224. Rotte A, Jin JY, Lemaire V. 2018. Mechanistic overview of immune checkpoints to support the rational design of their combinations in cancer immunotherapy. *Ann Oncol* 29: 71-83
225. Zelinskyy G, Myers L, Dietze KK, Gibbert K, Roggendorf M, et al. 2011. Virus-specific CD8+ T cells upregulate programmed death-1 expression during acute friend retrovirus infection but are highly cytotoxic and control virus replication. *J Immunol* 187: 3730-7
226. Lafon M, Megret F, Meuth SG, Simon O, Velandia Romero ML, et al. 2008. Detrimental contribution of the immuno-inhibitor B7-H1 to rabies virus encephalitis. *J Immunol* 180: 7506-15
227. Phares TW, Ramakrishna C, Parra GI, Epstein A, Chen L, et al. 2009. Target-dependent B7-H1 regulation contributes to clearance of central nervous system infection and dampens morbidity. *J Immunol* 182: 5430-8
228. McNally B, Ye F, Willette M, Flano E. 2013. Local blockade of epithelial PDL-1 in the airways enhances T cell function and viral clearance during influenza virus infection. *J Virol* 87: 12916-24
229. Erickson JJ, Lu P, Wen S, Hastings AK, Gilchuk P, et al. 2015. Acute Viral Respiratory Infection Rapidly Induces a CD8+ T Cell Exhaustion-like Phenotype. *J Immunol* 195: 4319-30

230. Rutigliano JA, Sharma S, Morris MY, Oguin TH, 3rd, McClaren JL, et al. 2014. Highly pathological influenza A virus infection is associated with augmented expression of PD-1 by functionally compromised virus-specific CD8+ T cells. *J Virol* 88: 1636-51
231. Yao S, Jiang L, Moser EK, Jewett LB, Wright J, et al. 2015. Control of pathogenic effector T-cell activities in situ by PD-L1 expression on respiratory inflammatory dendritic cells during respiratory syncytial virus infection. *Mucosal Immunol* 8: 746-59
232. Stanciu LA, Bellettato CM, Laza-Stanca V, Coyle AJ, Papi A, Johnston SL. 2006. Expression of programmed death-1 ligand (PD-L) 1, PD-L2, B7-H3, and inducible costimulator ligand on human respiratory tract epithelial cells and regulation by respiratory syncytial virus and type 1 and 2 cytokines. *J Infect Dis* 193: 404-12
233. Telcian AG, Laza-Stanca V, Edwards MR, Harker JA, Wang H, et al. 2011. RSV-induced bronchial epithelial cell PD-L1 expression inhibits CD8+ T cell nonspecific antiviral activity. *J Infect Dis* 203: 85-94
234. Kirchberger S, Majdic O, Steinberger P, Bluml S, Pfistershammer K, et al. 2005. Human rhinoviruses inhibit the accessory function of dendritic cells by inducing sialoadhesin and B7-H1 expression. *J Immunol* 175: 1145-52
235. Heinecke L, Proud D, Sanders S, Schleimer RP, Kim J. 2008. Induction of B7-H1 and B7-DC expression on airway epithelial cells by the Toll-like receptor 3 agonist double-stranded RNA and human rhinovirus infection: In vivo and in vitro studies. *J Allergy Clin Immunol* 121: 1155-60
236. Valero-Pacheco N, Arriaga-Pizano L, Ferat-Osorio E, Mora-Velandia LM, Pastelin-Palacios R, et al. 2013. PD-L1 expression induced by the 2009 pandemic influenza A(H1N1) virus impairs the human T cell response. *Clin Dev Immunol* 2013: 989673
237. Erickson JJ, Rogers MC, Tollefson SJ, Boyd KL, Williams JV. 2016. Multiple Inhibitory Pathways Contribute to Lung CD8+ T Cell Impairment and Protect against Immunopathology during Acute Viral Respiratory Infection. *J Immunol* 197: 233-43
238. MacLeod MK, McKee AS, David A, Wang J, Mason R, et al. 2011. Vaccine adjuvants aluminum and monophosphoryl lipid A provide distinct signals to generate protective cytotoxic memory CD8 T cells. *Proc Natl Acad Sci U S A* 108: 7914-9
239. Song MY, Park SH, Nam HJ, Choi DH, Sung YC. 2011. Enhancement of vaccine-induced primary and memory CD8(+) T-cell responses by soluble PD-1. *J Immunother* 34: 297-306
240. Dai B, Xiao L, Bryson PD, Fang J, Wang P. 2012. PD-1/PD-L1 blockade can enhance HIV-1 Gag-specific T cell immunity elicited by dendritic cell-directed lentiviral vaccines. *Mol Ther* 20: 1800-9
241. Hobo W, Novobrantseva TI, Fredrix H, Wong J, Milstein S, et al. 2013. Improving dendritic cell vaccine immunogenicity by silencing PD-1 ligands using siRNA-lipid nanoparticles combined with antigen mRNA electroporation. *Cancer Immunol Immunother* 62: 285-97

242. Duan S, Thomas PG. 2016. Balancing Immune Protection and Immune Pathology by CD8(+) T-Cell Responses to Influenza Infection. *Front Immunol* 7: 25
243. Olson MR, Varga SM. 2008. Pulmonary immunity and immunopathology: lessons from respiratory syncytial virus. *Expert Rev Vaccines* 7: 1239-55
244. Stephen-Victor E, Bosschem I, Haesebrouck F, Bayry J. 2017. The Yin and Yang of regulatory T cells in infectious diseases and avenues to target them. *Cell Microbiol* 19
245. Newton AH, Cardani A, Braciale TJ. 2016. The host immune response in respiratory virus infection: balancing virus clearance and immunopathology. *Semin Immunopathol* 38: 471-82
246. Plitas G, Rudensky AY. 2016. Regulatory T Cells: Differentiation and Function. *Cancer Immunol Res* 4: 721-5
247. Sakaguchi S, Yamaguchi T, Nomura T, Ono M. 2008. Regulatory T cells and immune tolerance. *Cell* 133: 775-87
248. Soerens AG, Da Costa A, Lund JM. 2016. Regulatory T cells are essential to promote proper CD4 T-cell priming upon mucosal infection. *Mucosal Immunol* 9: 1395-406
249. Ruckwardt TJ, Bonaparte KL, Nason MC, Graham BS. 2009. Regulatory T Cells Promote Early Influx of CD8+ T Cells in the Lungs of Respiratory Syncytial Virus-Infected Mice and Diminish Immunodominance Disparities. *Journal of Virology* 83: 3019-28
250. Francisco LM, Sage PT, Sharpe AH. 2010. The PD-1 pathway in tolerance and autoimmunity. *Immunological Reviews* 236: 219-42
251. Thornton AM, Korty PE, Tran DQ, Wohlfert EA, Murray PE, et al. 2010. Expression of Helios, an Ikaros transcription factor family member, differentiates thymic-derived from peripherally induced Foxp3+ T regulatory cells. *J Immunol* 184: 3433-41
252. Weiss JM, Bilate AM, Gobert M, Ding Y, Curotto de Lafaille MA, et al. 2012. Neuropilin 1 is expressed on thymus-derived natural regulatory T cells, but not mucosa-generated induced Foxp3+ T reg cells. *J Exp Med* 209: 1723-42, s1
253. Yadav M, Louvet C, Davini D, Gardner JM, Martinez-Llordella M, et al. 2012. Neuropilin-1 distinguishes natural and inducible regulatory T cells among regulatory T cell subsets in vivo. *J Exp Med* 209: 1713-22, s1-19
254. Lee DCP, Harker JAE, Tregoning JS, Atabani SF, Johansson C, et al. 2010. CD25+ Natural Regulatory T Cells Are Critical in Limiting Innate and Adaptive Immunity and Resolving Disease following Respiratory Syncytial Virus Infection. *Journal of Virology* 84: 8790-98
255. Betts MR, Brenchley JM, Price DA, De Rosa SC, Douek DC, et al. 2003. Sensitive and viable identification of antigen-specific CD8+ T cells by a flow cytometric assay for degranulation. *J Immunol Methods* 281: 65-78
256. Widney DP, Xia YR, Lusis AJ, Smith JB. 2000. The murine chemokine CXCL11 (IFN-inducible T cell alpha chemoattractant) is an IFN-gamma- and lipopolysaccharide-inducible glucocorticoid-attenuated response gene expressed in lung and other tissues during endotoxemia. *J Immunol* 164: 6322-31

257. Ariotti S, Beltman JB, Borsje R, Hoekstra ME, Halford WP, et al. 2015. Subtle CXCR3-Dependent Chemotaxis of CTLs within Infected Tissue Allows Efficient Target Localization. *J Immunol* 195: 5285-95
258. Cole KE, Strick CA, Paradis TJ, Ogborne KT, Loetscher M, et al. 1998. Interferon-inducible T cell alpha chemoattractant (I-TAC): a novel non-ELR CXC chemokine with potent activity on activated T cells through selective high affinity binding to CXCR3. *J Exp Med* 187: 2009-21
259. Kamin-Lewis R, Abdelwahab SF, Trang C, Baker A, DeVico AL, et al. 2001. Perforin-low memory CD8+ cells are the predominant T cells in normal humans that synthesize the beta -chemokine macrophage inflammatory protein-1beta. *Proc Natl Acad Sci U S A* 98: 9283-8
260. Fong AM, Robinson LA, Steeber DA, Tedder TF, Yoshie O, et al. 1998. Fractalkine and CX3CR1 mediate a novel mechanism of leukocyte capture, firm adhesion, and activation under physiologic flow. *J Exp Med* 188: 1413-9
261. Bazan JF, Bacon KB, Hardiman G, Wang W, Soo K, et al. 1997. A new class of membrane-bound chemokine with a CX3C motif. *Nature* 385: 640-4
262. Verbist KC, Cole CJ, Field MB, Klonowski KD. 2011. A role for IL-15 in the migration of effector CD8 T cells to the lung airways following influenza infection. *J Immunol* 186: 174-82
263. Culley FJ, Pennycook AM, Tregoning JS, Dodd JS, Walzl G, et al. 2006. Role of CCL5 (RANTES) in viral lung disease. *J Virol* 80: 8151-7
264. Denis M. 1995. Proinflammatory cytokines in hypersensitivity pneumonitis. *Am J Respir Crit Care Med* 151: 164-9
265. Taub DD, Proost P, Murphy WJ, Anver M, Longo DL, et al. 1995. Monocyte chemotactic protein-1 (MCP-1), -2, and -3 are chemotactic for human T lymphocytes. *J Clin Invest* 95: 1370-6
266. Halim TY, Takei F. 2014. Isolation and characterization of mouse innate lymphoid cells. *Curr Protoc Immunol* 106: 3.25.1-13
267. Monticelli LA, Buck MD, Flamar AL, Saenz SA, Tait Wojno ED, et al. 2016. Arginase 1 is an innate lymphoid-cell-intrinsic metabolic checkpoint controlling type 2 inflammation. *Nat Immunol* 17: 656-65
268. Walker JA, Oliphant CJ, Englezakis A, Yu Y, Clare S, et al. 2015. Bcl11b is essential for group 2 innate lymphoid cell development. *The Journal of Experimental Medicine* 212: 875
269. Ebihara T, Song C, Ryu SH, Plougastel-Douglas B, Yang L, et al. 2015. Runx3 specifies lineage commitment of innate lymphoid cells. *Nat Immunol* 16: 1124-33
270. de Kleer IM, Kool M, de Bruijn MJW, Willart M, van Moorleghem J, et al. 2016. Perinatal Activation of the Interleukin-33 Pathway Promotes Type 2 Immunity in the Developing Lung. *Immunity* 45: 1285-98
271. Szurek E, Cebula A, Wojciech L, Pietrzak M, Rempala G, et al. 2015. Differences in Expression Level of Helios and Neuropilin-1 Do Not Distinguish Thymus-Derived from Extrathymically-Induced CD4+Foxp3+ Regulatory T Cells. *PLoS One* 10: e0141161
272. Krishnamoorthy N, Khare A, Oriss TB, Raundhal M, Morse C, et al. 2012. Early infection with respiratory syncytial virus impairs regulatory T cell function and increases susceptibility to allergic asthma. *Nat Med* 18: 1525-30

273. Oliphant S, Lines JL, Hollifield ML, Garvy BA. 2015. Regulatory T Cells Are Critical for Clearing Influenza A Virus in Neonatal Mice. *Viral Immunol* 28: 580-9
274. Rigas D, Lewis G, Aron JL, Wang B, Banie H, et al. 2017. Type 2 innate lymphoid cell suppression by regulatory T cells attenuates airway hyperreactivity and requires inducible T-cell costimulator-inducible T-cell costimulator ligand interaction. *J Allergy Clin Immunol* 139: 1468-77.e2
275. Krishnamoorthy N, Burkett PR, Dalli J, Abdulnour RE, Colas R, et al. 2015. Cutting edge: maresin-1 engages regulatory T cells to limit type 2 innate lymphoid cell activation and promote resolution of lung inflammation. *J Immunol* 194: 863-7
276. Fahy JV. 2015. Type 2 inflammation in asthma--present in most, absent in many. *Nat Rev Immunol* 15: 57-65
277. Edwards MR, Strong K, Cameron A, Walton RP, Jackson DJ, Johnston SL. 2017. Viral infections in allergy and immunology: How allergic inflammation influences viral infections and illness. *J Allergy Clin Immunol* 140: 909-20
278. Williams JV, Tollefson SJ, Johnson JE, Crowe JE, Jr. 2005. The cotton rat (Sigmodon hispidus) is a permissive small animal model of human metapneumovirus infection, pathogenesis, and protective immunity. *J Virol* 79: 10944-51
279. Shafagati N, Fite K, Patanarut A, Baer A, Pinkham C, et al. 2016. Enhanced detection of respiratory pathogens with nanotrap particles. *Virulence* 7: 756-69
280. Gilchuk P, Spencer CT, Conant SB, Hill T, Gray JJ, et al. 2013. Discovering naturally processed antigenic determinants that confer protective T cell immunity. *J Clin Invest* 123: 1976-87
281. Williams NL, Morris JL, Rush CM, Ketheesan N. 2014. Migration of dendritic cells facilitates systemic dissemination of Burkholderia pseudomallei. *Infect Immun* 82: 4233-40
282. Slight SR, Monin L, Gopal R, Avery L, Davis M, et al. 2013. IL-10 restrains IL-17 to limit lung pathology characteristics following pulmonary infection with Francisella tularensis live vaccine strain. *Am J Pathol* 183: 1397-404
283. Yao S, Jiang L, Moser EK, Jewett LB, Wright J, et al. 2014. Control of pathogenic effector T-cell activities in situ by PD-L1 expression on respiratory inflammatory dendritic cells during respiratory syncytial virus infection. *Mucosal Immunol*
284. Kim J, Myers AC, Chen L, Pardoll DM, Truong-Tran QA, et al. 2005. Constitutive and inducible expression of b7 family of ligands by human airway epithelial cells. *Am J Respir Cell Mol Biol* 33: 280-9
285. Keir ME, Butte MJ, Freeman GJ, Sharpe AH. 2008. PD-1 and Its Ligands in Tolerance and Immunity. *Annual Review of Immunology* 26: 677-704
286. Mueller SN, Vanguri VK, Ha S-J, West EE, Keir ME, et al. 2010. PD-L1 has distinct functions in hematopoietic and nonhematopoietic cells in regulating T cell responses during chronic infection in mice. *The Journal of Clinical Investigation* 120: 2508-15
287. Lin H, Wei S, Hurt EM, Green MD, Zhao L, et al. 2018. Host expression of PD-L1 determines efficacy of PD-L1 pathway blockade–mediated tumor regression. *The Journal of Clinical Investigation* 128: 805-15

288. Tang F, Zheng P. 2018. Tumor cells versus host immune cells: whose PD-L1 contributes to PD-1/PD-L1 blockade mediated cancer immunotherapy? *Cell Biosci* 8: 34
289. Cheng X, Veverka V, Radhakrishnan A, Waters LC, Muskett FW, et al. 2013. Structure and interactions of the human programmed cell death 1 receptor. *J Biol Chem* 288: 11771-85
290. Nishimura H, Nose M, Hiai H, Minato N, Honjo T. 1999. Development of Lupus-like Autoimmune Diseases by Disruption of the PD-1 Gene Encoding an ITIM Motif-Carrying Immunoreceptor. *Immunity* 11: 141-51
291. Dong H, Zhu G, Tamada K, Flies DB, van Deursen JM, Chen L. 2004. B7-H1 determines accumulation and deletion of intrahepatic CD8(+) T lymphocytes. *Immunity* 20: 327-36
292. Latchman YE, Liang SC, Wu Y, Chernova T, Sobel RA, et al. 2004. PD-L1-deficient mice show that PD-L1 on T cells, antigen-presenting cells, and host tissues negatively regulates T cells. *Proceedings of the National Academy of Sciences of the United States of America* 101: 10691-96
293. Juneja VR, McGuire KA, Manguso RT, LaFleur MW, Collins N, et al. 2017. PD-L1 on tumor cells is sufficient for immune evasion in immunogenic tumors and inhibits CD8 T cell cytotoxicity. *J Exp Med* 214: 895-904
294. Khunger M, Rakshit S, Pasupuleti V, Hernandez AV, Mazzone P, et al. 2017. Incidence of Pneumonitis With Use of Programmed Death 1 and Programmed Death-Ligand 1 Inhibitors in Non-Small Cell Lung Cancer: A Systematic Review and Meta-Analysis of Trials. *Chest* 152: 271-81
295. Pillai RN, Behera M, Owonikoko TK, Kamphorst AO, Pakkala S, et al. 2018. Comparison of the toxicity profile of PD-1 versus PD-L1 inhibitors in non-small cell lung cancer: A systematic analysis of the literature. *Cancer* 124: 271-77
296. Butte MJ, Keir ME, Phamduy TB, Sharpe AH, Freeman GJ. 2007. Programmed death-1 ligand 1 interacts specifically with the B7-1 costimulatory molecule to inhibit T cell responses. *Immunity* 27: 111-22
297. Chen L, Flies DB. 2013. Molecular mechanisms of T cell co-stimulation and co-inhibition. *Nature reviews. Immunology* 13: 227-42
298. Park JJ, Omiya R, Matsumura Y, Sakoda Y, Kuramasu A, et al. 2010. B7-H1/CD80 interaction is required for the induction and maintenance of peripheral T-cell tolerance. *Blood* 116: 1291-8
299. McBerry C, Dias A, Shryock N, Lampe K, Gutierrez FRS, et al. 2014. PD-1 modulates steady-state and infection-induced IL-10 production in vivo. *European Journal of Immunology* 44: 469-79
300. Dong H, Zhu G, Tamada K, Chen L. 1999. B7-H1, a third member of the B7 family, co-stimulates T-cell proliferation and interleukin-10 secretion. *Nature Medicine* 5: 1365
301. Tseng S-Y, Otsuji M, Gorski K, Huang X, Slansky JE, et al. 2001. B7-Dc, a New Dendritic Cell Molecule with Potent Costimulatory Properties for T Cells. *The Journal of Experimental Medicine* 193: 839-46
302. Xu-Monette ZY, Zhang M, Li J, Young KH. 2017. PD-1/PD-L1 Blockade: Have We Found the Key to Unleash the Antitumor Immune Response? *Frontiers in Immunology* 8: 1597

303. Wang S-F, Fouquet S, Chapon M, Salmon H, Regnier F, et al. 2011. Early T Cell Signalling Is Reversibly Altered in PD-1+ T Lymphocytes Infiltrating Human Tumors. *PLOS ONE* 6: e17621
304. Monroe JG. 2004. Ligand-independent tonic signaling in B-cell receptor function. *Current Opinion in Immunology* 16: 288-95
305. Guo G, Gong K, Wohlfeld B, Hatanpaa KJ, Zhao D, Habib AA. 2015. Ligand-Independent EGFR Signaling. *Cancer Res* 75: 3436-41
306. Chen J, Jiang CC, Jin L, Zhang XD. 2016. Regulation of PD-L1: a novel role of pro-survival signalling in cancer. *Annals of Oncology* 27: 409-16
307. Lee Y-J, Moon Y-H, Hyung KE, Yoo J-S, Lee MJ, et al. 2013. Macrophage PD-L1 strikes back: PD-1/PD-L1 interaction drives macrophages toward regulatory subsets. *Advances in Bioscience and Biotechnology* Vol.04No.08: 11
308. Rogers MC, Lamens KD, Shafagati N, Johnson M, Oury TD, et al. 2018. CD4⁺ Regulatory T Cells Exert Differential Functions during Early and Late Stages of the Immune Response to Respiratory Viruses. *The Journal of Immunology*
309. Hamelin M-È, Yim K, Kuhn KH, Cragin RP, Boukhvalova M, et al. 2005. Pathogenesis of Human Metapneumovirus Lung Infection in BALB/c Mice and Cotton Rats. *Journal of Virology* 79: 8894-903
310. Roberts A, Deming D, Paddock CD, Cheng A, Yount B, et al. 2007. A Mouse-Adapted SARS-Coronavirus Causes Disease and Mortality in BALB/c Mice. *PLOS Pathogens* 3: e5
311. Li K, Wohlford-Lenane CL, Channappanavar R, Park JE, Earnest JT, et al. 2017. Mouse-adapted MERS coronavirus causes lethal lung disease in human DPP4 knockin mice. *Proc Natl Acad Sci U S A* 114: E3119-e28
312. Ilyushina NA, Khalenkov AM, Seiler JP, Forrest HL, Bovin NV, et al. 2010. Adaptation of Pandemic H1N1 Influenza Viruses in Mice. *Journal of Virology* 84: 8607-16
313. Hirst GK. 1947. STUDIES ON THE MECHANISM OF ADAPTATION OF INFLUENZA VIRUS TO MICE. *The Journal of Experimental Medicine* 86: 357-66
314. Raut S, Hurd J, Blandford G, Heath RB, Cureton RJ. 1975. The pathogenesis of infections of the mouse caused by virulent and avirulent variants of an influenza virus. *J Med Microbiol* 8: 127-36
315. Epstein DA, Czarniecki CW, Jacobsen H, Friedman RM, Panet A. 1981. A mouse cell line, which is unprotected by interferon against lytic virus infection, lacks ribonuclease F activity. *Eur J Biochem* 118: 9-15
316. Parisien J-P, Lau JF, Rodriguez JJ, Ulane CM, Horvath CM. 2002. Selective STAT Protein Degradation Induced by Paramyxoviruses Requires both STAT1 and STAT2 but Is Independent of Alpha/Beta Interferon Signal Transduction. *Journal of Virology* 76: 4190-98
317. Pellegrini S, John J, Shearer M, Kerr IM, Stark GR. 1989. Use of a selectable marker regulated by alpha interferon to obtain mutations in the signaling pathway. *Mol Cell Biol* 9: 4605-12
318. Blaszczyk K, Nowicka H, Kostyrko K, Antonczyk A, Wesoly J, Bluyssen HAR. 2016. The unique role of STAT2 in constitutive and IFN-induced transcription and antiviral responses. *Cytokine & Growth Factor Reviews* 29: 71-81

319. Frank DA, Mahajan S, Ritz J. 1999. Fludarabine-induced immunosuppression is associated with inhibition of STAT1 signaling. *Nat Med* 5: 444-7
320. Schuster JE, Cox RG, Hastings AK, Boyd KL, Wadia J, et al. 2014. A Broadly Neutralizing Human Monoclonal Antibody Exhibits In Vivo Efficacy Against Both Human Metapneumovirus and Respiratory Syncytial Virus. *J Infect Dis*
321. Kamal RP, Katz JM, York IA. 2014. Molecular Determinants of Influenza Virus Pathogenesis in Mice. *Current topics in microbiology and immunology* 385: 243-74
322. Rubtsov YP, Niec R, Josefowicz S, Li L, Darce J, et al. 2010. Stability of the regulatory T cell lineage in vivo. *Science (New York, N.Y.)* 329: 1667-71
323. Schwartz C, Khan AR, Floudas A, Saunders SP, Hams E, et al. 2017. ILC2s regulate adaptive Th2 cell functions via PD-L1 checkpoint control. *The Journal of Experimental Medicine*
324. Caton ML, Smith-Raska MR, Reizis B. 2007. Notch–RBP-J signaling controls the homeostasis of CD8(−) dendritic cells in the spleen. *The Journal of Experimental Medicine* 204: 1653-64
325. Li H, Cho SN, Evans CM, Dickey BF, Jeong J-W, DeMayo FJ. 2008. Cre-Mediated Recombination in Mouse Clara Cells. *Genesis (New York, N.Y. : 2000)* 46: 300-07
326. Schubert D, Bode C, Kenefeck R, Hou TZ, Wing JB, et al. 2014. Autosomal-dominant immune dysregulation syndrome in humans with CTLA4 mutations. *Nature medicine* 20: 1410-16
327. Wing K, Onishi Y, Prieto-Martin P, Yamaguchi T, Miyara M, et al. 2008. CTLA-4 control over Foxp3+ regulatory T cell function. *Science* 322: 271-5
328. Kroner A, Mehling M, Hemmer B, Rieckmann P, Toyka KV, et al. 2005. A PD-1 polymorphism is associated with disease progression in multiple sclerosis. *Ann Neurol* 58: 50-7
329. Pawlak-Adamska E, Nowak O, Karabon L, Pokryszko-Dragan A, Partyka A, et al. 2017. PD-1 gene polymorphic variation is linked with first symptom of disease and severity of relapsing-remitting form of MS. *J Neuroimmunol* 305: 115-27
330. Yang M, Zou Y, Bai Y, Li M. 2015. The programmed cell death 1 gene polymorphisms (PD 1.3 G/A, PD 1.5 C/T and PD 1.9 C/T) and susceptibility to ankylosing spondylitis: a meta-analysis. *J Orthop Sci* 20: 55-63
331. Dong W, Gong M, Shi Z, Xiao J, Zhang J, Peng J. 2016. Programmed Cell Death-1 Polymorphisms Decrease the Cancer Risk: A Meta-Analysis Involving Twelve Case-Control Studies. *PLoS One* 11: e0152448
332. Ma Y, Liu X, Zhu J, Li W, Guo L, et al. 2015. Polymorphisms of co-inhibitory molecules (CTLA-4/PD-1/PD-L1) and the risk of non-small cell lung cancer in a Chinese population. *Int J Clin Exp Med* 8: 16585-91
333. Mitchell AL, Cordell HJ, Soemedi R, Owen K, Skinningsrud B, et al. 2009. Programmed Death Ligand 1 (PD-L1) Gene Variants Contribute to Autoimmune Addison's Disease and Graves' Disease Susceptibility. *The Journal of Clinical Endocrinology & Metabolism* 94: 5139-45
334. Zolfaghari L, Solgi G, Nafar M, Ahmadpour P, Lassanpezeshki M, et al. 2015. *Association of Programmed Cell Death 1 and Programmed Cell Death 1 Ligand*

Gene Polymorphisms With Delayed Graft Function and Acute Rejection in Kidney Allograft Recipients
335. Zhang G, Liu Z, Duan S, Han Q, Li Z, et al. 2010. Association of polymorphisms of programmed cell death–1 gene with chronic hepatitis B virus infection. *Human Immunology* 71: 1209-13
336. Lv F, Gao Y-F, Zhang Z-H, Zhang T-C, Pan F-M, et al. 2011. Polymorphisms in programmed death-1 gene are not associated with chronic HBV infection in Chinese patients. *World Journal of Hepatology* 3: 72-78
337. Wang R, Wan Q, Kozhaya L, Fujii H, Unutmaz D. 2008. Identification of a regulatory T cell specific cell surface molecule that mediates suppressive signals and induces Foxp3 expression. *PLoS One* 3: e2705
338. Wen Z, Wang X, Dong K, Zhang H, Bu Z, et al. 2017. Blockage of regulatory T cells augments induction of protective immune responses by influenza virus-like particles in aged mice. *Microbes Infect* 19: 626-34
339. Moore AC, Gallimore A, Draper SJ, Watkins KR, Gilbert SC, Hill AV. 2005. Anti-CD25 antibody enhancement of vaccine-induced immunogenicity: increased durable cellular immunity with reduced immunodominance. *J Immunol* 175: 7264-73
340. Macatangay BJ, Szajnik ME, Whiteside TL, Riddler SA, Rinaldo CR. 2010. Regulatory T cell suppression of Gag-specific CD8 T cell polyfunctional response after therapeutic vaccination of HIV-1-infected patients on ART. *PLoS One* 5: e9852
341. Topalian SL, Hodi FS, Brahmer JR, Gettinger SN, Smith DC, et al. 2012. Safety, activity, and immune correlates of anti-PD-1 antibody in cancer. *N Engl J Med* 366: 2443-54
342. Ertl H, Xiang Z, Li Y, Zhou D, Zhou X, et al. 2011. Highly Sensitive Method for Titration of Adenovirus Vectors.
343. Song M-S, Pascua PNQ, Lee JH, Baek YH, Lee O-J, et al. 2009. The Polymerase Acidic Protein Gene of Influenza A Virus Contributes to Pathogenicity in a Mouse Model. *Journal of Virology* 83: 12325-35
344. Cseke G, Maginnis MS, Cox RG, Tollefson SJ, Podsiad AB, et al. 2009. Integrin αvβ1 promotes infection by human metapneumovirus. *Proceedings of the National Academy of Sciences of the United States of America* 106: 1566-71
345. Hoey T, Schindler U. 1998. STAT structure and function in signaling. *Current Opinion in Genetics & Development* 8: 582-87
346. Piyaratna R, Tollefson SJ, Williams JV. 2011. Genomic analysis of four human metapneumovirus prototypes. *Virus Res* 160: 200-5
347. Shuai K. 2000. Modulation of STAT signaling by STAT-interacting proteins. *Oncogene* 19: 2638
348. Cheon H, Holvey-Bates EG, Schoggins JW, Forster S, Hertzog P, et al. 2013. IFNβ-dependent increases in STAT1, STAT2, and IRF9 mediate resistance to viruses and DNA damage. *The EMBO Journal* 32: 2751-63
349. Koshelnick Y, Ehart M, Hufnagl P, Heinrich PC, Binder BR. 1997. Urokinase Receptor Is Associated with the Components of the JAK1/STAT1 Signaling Pathway and Leads to Activation of This Pathway upon Receptor Clustering in

the Human Kidney Epithelial Tumor Cell Line TCL-598. *Journal of Biological Chemistry* 272: 28563-67

350. Putz EM, Majoros A, Gotthardt D, Prchal-Murphy M, Zebedin-Brandl EM, et al. 2016. Novel non-canonical role of STAT1 in Natural Killer cell cytotoxicity. *Oncoimmunology* 5: e1186314